Iowa State University
Digital Repository

Retrospective Theses and Dissertations

Iowa State University Capstones, Theses and Dissertations

1982

Triple pulse amperometry: a method of detection of carbohydrates and alcohols for liquid chromatography

Scott Hughes
Iowa State University

Follow this and additional works at: https://lib.dr.iastate.edu/rtd

Part of the Analytical Chemistry Commons

Recommended Citation

Hughes, Scott, "Triple pulse amperometry: a method of detection of carbohydrates and alcohols for liquid chromatography " (1982). *Retrospective Theses and Dissertations*. 7506.
https://lib.dr.iastate.edu/rtd/7506

This Dissertation is brought to you for free and open access by the Iowa State University Capstones, Theses and Dissertations at Iowa State University Digital Repository. It has been accepted for inclusion in Retrospective Theses and Dissertations by an authorized administrator of Iowa State University Digital Repository. For more information, please contact digirep@iastate.edu.

المنارة للاستشارات

www.manaraa.com

INFORMATION TO USERS

This reproduction was made from a copy of a document sent to us for microfilming. While the most advanced technology has been used to photograph and reproduce this document, the quality of the reproduction is heavily dependent upon the quality of the material submitted.

The following explanation of techniques is provided to help clarify markings or notations which may appear on this reproduction.

1. The sign or "target" for pages apparently lacking from the document photographed is "Missing Page(s)". If it was possible to obtain the missing page(s) or section, they are spliced into the film along with adjacent pages. This may have necessitated cutting through an image and duplicating adjacent pages to assure complete continuity.
2. When an image on the film is obliterated with a round black mark, it is an indication of either blurred copy because of movement during exposure, duplicate copy, or copyrighted materials that should not have been filmed. For blurred pages, a good image of the page can be found in the adjacent frame. If copyrighted materials were deleted, a target note will appear listing the pages in the adjacent frame.
3. When a map, drawing or chart, etc., is part of the material being photographed, a definite method of "sectioning" the material has been followed. It is customary to begin filming at the upper left hand corner of a large sheet and to continue from left to right in equal sections with small overlaps. If necessary, sectioning is continued again—beginning below the first row and continuing on until complete.
4. For illustrations that cannot be satisfactorily reproduced by xerographic means, photographic prints can be purchased at additional cost and inserted into your xerographic copy. These prints are available upon request from the Dissertations Customer Services Department.
5. Some pages in any document may have indistinct print. In all cases the best available copy has been filmed.

University
Microfilms
International

300 N. Zeeb Road
Ann Arbor, MI 48106

8224224

Hughes, Scott

TRIPLE PULSE AMPEROMETRY: A METHOD OF DETECTION OF CARBOHYDRATES AND ALCOHOLS FOR LIQUID CHROMATOGRAPHY

Iowa State University PH.D. 1982

University
Microfilms
International 300 N. Zeeb Road, Ann Arbor, MI 48106

PLEASE NOTE:

In all cases this material has been filmed in the best possible way from the available copy. Problems encountered with this document have been identified here with a check mark √.

1. Glossy photographs or pages _____
2. Colored illustrations, paper or print _____
3. Photographs with dark background _____
4. Illustrations are poor copy _____
5. Pages with black marks, not original copy _____
6. Print shows through as there is text on both sides of page _____
7. Indistinct, broken or small print on several pages _____
8. Print exceeds margin requirements _____
9. Tightly bound copy with print lost in spine _____
10. Computer printout pages with indistinct print ✓
11. Page(s) _____ lacking when material received. and not available from school or author.
12. Page(s) 47 seem to be missing in numbering only as text follows.
13. Two pages numbered _____. Text follows.
14. Curling and wrinkled pages _____
15. Other _____

University
Microfilms
International

Triple pulse amperometry: A method of detection of carbohydrates and alcohols for liquid chromatography

by

Scott Hughes

An Abstract of
A Dissertation Submitted to the
Graduate Faculty in Partial Fulfillment of the
Requirements for the Degree of
DOCTOR OF PHILOSOPHY

Approved:

Signature was redacted for privacy.

In Charge of Major Work

Signature was redacted for privacy.

For the Major Department

Signature was redacted for privacy.

For the Graduate College

Iowa State University
Ames, Iowa

1982

TABLE OF CONTENTS

Page

I. INTRODUCTION 1

II. REVIEW OF PERTINENT LITERATURE 6
  A. Adsorption of Organic Compounds 6
    1. Adsorption as a function of concentration 8
    2. Adsorption kinetics 9
    3. Adsorption as a function of potential 9
  B. Oxidation of Adsorbed Organic Compounds 11
  C. Methods for Detection of Carbohydrates 15
    1. Wet chemical methods 16
    2. Chromatographic methods 18
    3. Detectors 22

III. EXPERIMENTIAL 24
  A. Electrodes 24
  B. Potentiostats 27
  C. Timing and Potential Control 27
  D. Data Acquisition 32
    1. Sample-hold amplifier 32
    2. Recorders 33
    3. Computer data acquisition 33
  E. Flow-Injection System 43
  F. High Performance Liquid Chromatograph 49
  G. Chemicals 51

IV. OXIDATION OF ALCOHOLS ON PLATINUM ELECTRODES 52
  A. Cyclic Voltammetry 52
  B. Calibration Curves 59
  C. Effect of the Rotational Velocity of the Electrode 66
  D. Triple Pulse Voltammetry at the RDE 67

E. Triple Pulse Amperometry at the RDE 70
F. Summary 76

V. OXIDATION OF CARBOHYDRATES ON PLATINUM ELECTRODES 78
A. Cyclic Voltammetry 78
B. Cyclic Voltammetry with Interrupted Scan 84
C. Flow-Injection Voltammetry 87
D. Effect of Rotational Velocity 93
E. Triple Pulse Voltammetry at the RDE 97
F. Summary 105

VI. FLOW-INJECTION DETECTION 106
A. Flow-Injection Detection of Alcohols 106
B. Flow-Injection Detection of Carbohydrates 107
C. Summary 119

VII. HIGH PERFORMANCE LIQUID CHROMATOGRAPHY 120
A. Synthetic Samples 122
1. Precision 122
2. Resolution 127
3. Calibration 127
4. Variance of quantitative results 134
B. Detector Temperature 141
C. Analysis of Real Samples 147
D. Summary 162

VIII. SUMMARY 163

IX. SUGGESTIONS FOR FUTURE WORK 167

X. BIBLIOGRAPHY 169

XI. ACKNOWLEDGEMENTS 174

XII. APPENDIX 176

LIST OF FIGURES

		Page
Figure III-1	Platinum wire-tip flow-through detector	25
Figure III-2	Block diagram of instrumentation	28
Figure III-3	Block diagram of timing	30
Figure III-4	Block diagram of computer interface	35
Figure III-5	Timing diagram of computer input handshake	37
Figure III-6	Schematic diagram of computer output interface	40
Figure III-7	CRT display of a chromatogram	44
Figure III-8	Parameter menu from data acquisition program	46
Figure IV-1	Current-potential curves obtained by cyclic voltammetry at the platinum RDE	53
Figure IV-2	Current-voltage curves at a platinum RDE by cyclic voltammetry	57
Figure IV-3	Current-voltage curves at a platinum RDE by cyclic voltammetry	60
Figure IV-4	Calibration curves for methanol by cyclic voltammetry at E = 0.48 V	62
Figure IV-5	Triple pulse potential waveform	68
Figure IV-6	Current-potential curves for ethanol obtained by triple pulse voltammetry at the platinum RDE	71
Figure IV-7	Comparison of stability of response for ethanol at the platinum RDE by TPA and d.c. detection	73

Figure V-1 Current-voltage curves at a platinum RDE by cyclic voltammetry 81

Figure V-2 Effect on I-E curves of decreased limit of negative scan 85

Figure V-3 Current-voltage curves at platinum RDE by cyclic voltammetry with interrupted scan 88

Figure V-4 Current-time and I-E curves for the platinum-disc flow-through electrode following injections of sorbitol and dextrose 91

Figure V-5 Effect of rotational velocity on anodic peaks from cyclic voltammetry at the platinum RDE 94

Figure V-6 Plot of $-I_p$ vs. E3 for sorbitol at a platinum RDE by triple pulse voltammetry 99

Figure V-7 Current-voltage curves for dextrose at a platinum RDE by cyclic voltammetry and triple pulse voltammetry 101

Figure V-8 Current-voltage curves for sorbitol at a platinum RDE by cyclic voltammetry and triple pulse voltammetry 103

Figure VI-1 Comparison of detection peaks for ethanol in flow-injection detection with d.c. and triple pulse amperometric detection 108

Figure VI-2 Calibration curves for ethanol by flow-injection with triple pulse amperometric detection 110

Figure VI-3 Peaks obtained with the flow-injection system for dextrose in 0.10 M NaCH 114

Figure VI-4 Calibration curves for dextrose by flow-injection with triple pulse amperometric detection 116

Figure VII-1 Triple pulse potential waveform used for all HPLC studies 123

Figure VII-2 Peaks obtained with the HPLC system for ten injections of 0.40 mg mg^{-1} dextrose 125

Figure VII-3 Comparison of separation of eight carbohydrates by Hamilton and Dionex HPLC columns 129

Figure VII-4 Peaks from calibration of the HPLC system for glycerol 132

Figure VII-5 Plot of dextrose calibration curve, defined in Table VII-2, showing absolute variances for concentrations determined from the curve 137

Figure VII-6 Plot of relative variance vs. concentration for dextrose calibration curve defined in Table VII-2 139

Figure VII-7 Plot of $\ln(-I_p)$ vs. 1/temperature for injections of 0.12 mg ml^{-1} arabinose 148

Figure VII-8 Chromatographic analysis with Hamilton column 150

Figure VII-9 Chromatographic analysis of human urine 153

Figure VII-10 Chromatographic analysis with Hamilton column 155

Figure VII-11 Chromatographic analysis of wine using Dionex column 159

LIST OF TABLES

		Page
Table III-1	Address and conversion sequence of DAC	42
Table V-1	Carbohydrates studied	79
Table VI-1	Least-squares statistics for plots of $-1/I_p$ vs. $1/C^b$	113
Table VI-2	Comparison of peak currents for compounds tested by flow-injection detection	118
Table VII-1	Comparison of performance of Hamilton and Dionex HPLC columns	128
Table VII-2	Linear regression statistics for dextrose calibration curve	136
Table VII-3	Peak current obtained by HPLC with TPA detection at varied detector temperatures for six carbohydrates	146
Table VII-4	Concentration of carbohydrates in beer varieties	157
Table VII-5	Analytical results of wine analysis	158

I. INTRODUCTION

The combining of two simple compounds, carbon dioxide and water, made possible by a green catalyst and sunlight is a process fundamental to all living organisms. This process is carried out in the leaves of plants and is known as "photosynthesis." The products of this process are oxygen and a carbohydrate. This carbohydrate provides energy for all living matter (1).

Carbohydrates, also known as saccharides, are polyhydroxy ketones or aldehydes and their derivatives. Carbohydrates which consist of a single polyhydroxy ketone or aldehyde unit are called "monosaccharides" or "simple sugars." Dextrose[1], the carbohydrate produced by photosynthesis, is a monosaccharide with empirical formula $C_6H_{12}O_6$.

Dextrose is the monosaccharide from which almost all other carbohydrates are derived. Dextrose can be converted to monosaccharides with carbon lengths from three to eight. Monosaccharides can form oligosaccharides which contain from two to ten monosaccharide units in a chain or polysaccharides which are macromolecules consisting of thousands of monosaccharide units.

Plants produce two basic types of polysaccharides, celluose which forms the superstructure of the plant, and starch which is stored in seeds as an energy source for the next generation of plants. Animals which eat the plants can utilize the starch (and some even the celluose) to form glycogen (animal starch) which is used for energy after breaking it down into monosaccharides. Animals, through many biochemical reactions, also produce proteins from polysaccharides, which make up a large fraction of the animal body.

---

[1] Because of common usage in the electrochemical literature, the name "dextrose" is used throughout this dissertation to represent "glucose."

In plants and animals, small amounts of dextrose are used in the synthesis of other carbohydrates (oligo- and monosaccharides) which play important roles in the operation of the organism. The presence or lack of particular carbohydrates can be indicative of physiological phenomena in addition to serving as a fingerprint for identification of certain species (2,3).

The ability to analyze for individual carbohydrates, therefore, can be an important investigative tool. For example, in the food industry the carbohydrate content of fruits is sometimes used to determine the proper time to harvest, or the presence of a particular sugar in a product can be indicative of its adulteration (4). Recent advances in the area of human health have led to greater recognition of a probable correlation between the presence of individual carbohydrates in the human diet and the occurrence of undesirable physiological conditions including cardiovascular disease and diabetes (5,6).

Recently, the determination of individual carbohydrates in complex mixtures has been facilitated by development of relatively efficient liquid chromatographic columns and these determinations have become quite routine (5,6). Determination of carbohydrates by high performance liquid chromatography (HPLC) is characterized by better resolution than obtained by traditional chemical methods, is less costly than enzymatic methods, and involves no derivatization as is required for gas chromatographic methods. Since carbohydrates exhibit only weak photometric absorbance in the UV-visible region of the electromagnetic spectrum, the measurement of refractive index (RI) has served as the standard method of chromatographic detection. The detection limits for RI detection are not sufficiently low for many applications and an improvement in sensitivity for detection of carbohydrates is desired.

Amperometric detection in HPLC with glassy carbon and carbon paste electrodes has been successfully applied for many easily oxidized or reduced organic compounds; however, these electrodes exhibit no response for carbohydrates.

A surface-catalyzed anodic oxidation of alcohols and carbohydrates is obtained at platinum electrodes; however, the faradaic response at a constant applied potential is transitory, decaying to virtually a zero value within a few seconds. The faradaic response is concluded to result from oxidation of hydrogen atoms produced by the surface-catalyzed dehydrogenation of the adsorbed organic molecules. The hydrocarbon products of the dehydrogenation remain adsorbed on the electrode surface, thereby inhibiting adsorption of unreacted molecules and the resulting anodic current.

This dissertation describes the use of a triple potential waveform which results in the reactivation of the platinum electrode as well as the amperometric detection of carbohydrates and alcohols within the execution of a simple potential waveform. The fouling hydrocarbon products can be oxidatively cleaned from the electrode surface, presumably as CO_2, with simultaneous formation of oxide on the platinum surface, when the electrode potential is stepped to a large positive value corresponding approximately to the anodic breakdown of the aqueous solvent. The surface oxide is subsequently reduced by stepping the potential to a negative value corresponding approximately to the cathodic breakdown of the solvent. Molecules of the organic analyte are again adsorbed and are detected following a subsequent step of the potential to a more positive value, but not so positive as to cause formation of surface oxide. The result is a reproducible state of electrode activity for each measurement which makes possible precise amperometric detection of many organic compounds. The time period for completion of the waveform is 0.5-1.5s which is sufficiently short to permit virtually continuous monitoring of the effluent stream in flow-injection and HPLC systems.

II. REVIEW OF PERTINENT LITERATURE

It is the purpose of this section to inform the reader of the theories and practices which already exist concerning the separation and detection of carbohydrates and alcohols. Since the detection method described in this dissertation involves the adsorption and electrochemical oxidation of the organic analytes on a platinum electrode, the review will begin with this topic.

A. Adsorption of Organic Compounds

The study of the mechanism for adsorption and oxidation of organic compounds on platinum has received a lot of attention in recent years. This resulted mainly due to the projected use of platinum electrodes in fuel cells (7,8). Most of the work has centered on the adsorption and oxidation properties of methanol, formic acid and dextrose (8-21). It is generally agreed that the first step of the oxidation process involves the adsorption of the organic molecules onto the electrode surface. The extent of surface adsorption depends greatly on many factors including concentration, electrode potential and temperature. The precise measurement of the surface coverage by organic molecules is complicated by the fact that at certain potentials hydrogen or oxygen is also adsorbed (22). The difficulty is to distinguish between the electrode current resulting from the oxidation of the adsorbed compound from that for other faradaic reactions such as the oxidation of electroactive substances diffusing from the bulk solution and the formation of adsorbed oxygen. The method of adsorption substitution has been widely used to overcome these difficulties (8-10, 12-16). This method utilizes the fact that organic substances adsorb and desorb from platinum at rates which are slow compared to the cathodic and anodic formation and dissolution of adsorbed hydrogen atoms. In this method, the electrode is allowed to adsorb organic molecules at the potential of interest (E_{ads}) and the potential is then scanned in a negative direction ($\approx$40Vsec^{-1}) to the potential region where adsorbed hydrogen atoms are produced at the unoccupied sites producing a cathodic current for the reaction $H^+ + e^- \rightarrow (H\cdot)_{ads}$. Subtracting the integrated current-potential curve from that for the same electrode in an organic-free electrolyte, yields the decrease in the amount of adsorbed hydrogen due to adsorbed organic molecules. This method is believed to have a relative uncertainty of approximately 10% (8-10).

By utilizing this method, investigators have been able to measure the extent of adsorption of many organic compounds on platinum electrodes as a function of concentration, potential, temperature and time.

1. Adsorption as a function of concentration

Bagotzky and Vassiliev (10) determined adsorption isotherms for methanol, ethylene glycol and formic acid in 1 M H_2SO_4 as a function of concentration of the organic compound from 10^{-5} to 10 M. For all potentials from 0.16 to 0.56 V vs. SCE and all adsorbates tested, they found that the fractional surface coverage (θ) depended linearly upon the logarithm of adsorbate concentration for $0.1 < \theta < 0.85$. This type of behavior is characteristic of the Temkin logarithmic isotherm

$$\theta = a + (1/f)\ln(C)$$

which is predicted to apply for an inhomogenous adsorbing surface with a range of adsorption energies. The inhomogeneity factor (f) in the Temkin isotherm is a function of the difference of the maximum and minimum energies of adsorption for the inhomogeneous surface and temperature, $f = (\Delta H_{max} - \Delta H_{min})/RT$. At different electrode potentials, different temperatures and different values of pH of the solution, they found that the slope of the isotherm

(θ vs. lnC) stayed constant with variations observed in the intercept (a).

2. Adsorption kinetics

Due to the relatively slow rate of organic adsorption compared to hydrogen adsorption on platinum, it is also possible to use the adsorption substitution method to measure the rate of adsorption of organic substances. Bagotzky and Vassiliev (10) maintained the electrode at the adsorption potential for a fixed time, τ, and then rapidly scanned the electrode potential in the negative direction. The adsorption at time τ was calculated from the decrease in hydrogen adsorption. The experiment was shown to be valid for adsorption times from 0.05 to 1200 s. The adsorption of methanol in 1 M H_2SO_4 at concentrations of 10^{-3} to 1 M was studied by these investigators. For each methanol concentration, the surface coverage increased with increasing τ until a maximum coverage was attained which then did not change with time up to 1200 s. The time required to reach maximum coverage for a particular concentration of adsorbant ranged from 10 s for 1 M methanol (θ=1) to greater than 100 s for 10^{-3} M methanol (θ=0.3).

3. Adsorption as a function of potential

Several investigators have studied the potential dependence for the adsorption of organic substances on platinum electrodes (8-16). For some metal electrodes, e.g. mercury, the maximum adsorption of neutral substances occurs at the potential of zero charge (E_{zc})(9). This, however, is not the case with platinum. With metals which are capable of significant adsorption of hydrogen or oxygen, e.g. platinum, the point of maximum adsorption of neutral substances normally occurs at potentials of minimum hydrogen and oxygen adsorption rather than E_{zc}. By means of the adsorption substitution method, investigators found this to be the case for adsorption of methanol and formic acid on platinum (8-13). The plots of θ vs. E were dome-like in shape between the potentials for adsorption of hydrogen and oxygen. In contrast to the behavior of methanol and formic acid, dextrose adsorption was found to decrease with increasing oxygen adsorption but increased as hydrogen was adsorbed onto the electrode (14-16). Ernst et al. (16) suggested that a coverage of up to 50% adsorbed hydrogen significantly enhances the reactivity of the platinum surface for adsorption of dextrose in comparison to platinum without adsorbed hydrogen.

B. OXIDATION OF ADSORBED ORGANIC MOLECULES

The determination of the nature of adsorbed molecules on metal surfaces is a complicated task even for molecules adsorbed from the gas phase (9). The problems become even more troublesome when one studies these phenomena in electrolyte solutions. It is not surprising, therefore, that there exist many differences in the conclusions drawn by various investigators for the oxidation mechanisms of adsorbed substances on platinum electrodes. The many theories for the oxidation mechanisms of methanol, formic acid, and dextrose on platinum have been reviewed recently by Tsang (23) and will not be repeated here. However, the major processes which relate directly to the research presented in this dissertation will be discussed.

Oxidation of adsorbed organic materials on platinum electrodes is characterized by a large anodic current which rapidly decays to a negligible value within a few seconds. Many mechanisms for different organic species have been proposed, but all have in common a dehydrogenation step in which cleavage of C-H and/or O-H bonds of the adsorbed molecules produces hydrogen atoms which are adsorbed on the electrode surface. This adsorbed hydrogen can be rapidly oxidized to produce an anodic signal,

$(H\cdot)_{ads} \rightarrow H^+ + e^-$. The fate of the remaining adsorbed carbonaceous products of the dehydrogenation is not certain. For some organic compounds, further oxidation and/or desorption have been suggested (11,17).

Even for compounds in which desorption of the dehydrogenation products is suspected, the extent of desorption is minimal and the electrode activity is observed to be quickly diminished as the by-products of the anodic dehydrogenation build up on the electrode surface. The result is a rapid decrease of the anodic current. At large positive electrode potentials, corresponding to formation of platinum oxide, $Pt + H_2O \rightarrow PtO + 2H^+ + 2e^-$, the adsorbed byproducts are oxidatively removed from the electrode surface. Under these conditions, for several organic compounds, Breiter (19,20), by means of gas chromatography, detected the evolution of CO_2. Breiter concluded that at large enough positive electrode potentials, CO_2 is the final oxidation product for the many forms of adsorbed organic byproducts produced by the dehydrogenation reaction.

A few investigators have utilized the anodic decomposition and removal of adsorbed organic material to regenerate the electrode surface. Nadebaum and Fahidy (24,25), and Farooque and Fahidy (26) used a rotating, bipolar, wiperblade electrode to achieve "continuous reactivation" of a working electrode. They were interested in an electrode which would have commercial applications for electrochemical production or oxidative destruction of organic compounds. The use of a pulse waveform for reactivation of the electrode was not considered desirable because of the large power requirements which would be necessary on a commercial scale. The electrode developed by Nadebaum and Fahidy consisted of a cylindrical, rotating, platinum working electrode surrounded by three axially located, insulating wiperblades. The wiperblades were connected by three platinum outer electrodes, concentric to the cylindrical working electrode, which formed three electrically isolated compartments through which the surface of the working electrode passed. The outer, counter electrode of each compartment set the potential of the rotating electrode. Farooque and Fahidy used this electrode with two of the compartments controlled at the same potential to oxidize methanol in 0.1 M H_2SO_4 and the third compartment controlled at a large positive potential to oxidize the adsorbed products to CO_2, reactivating the electrode surface. They obtained "steady" currents which were twice that of an electrode operated at one potential. Great care had to be utilized in construction of the cell such that leakage current from one compartment to the other was kept at a minimum.

Marincic et al. (27), Lerner et al. (28), Marincic et al. (29) and Giner et al. (30) investigated the use of the oxidation of dextrose at an implantable platinum electrode for in vivo determinations of dextrose. They obtained reproducible results only by application of successive anodic and cathodic polarizations prior to recording the current-voltage (I-E) curve for a positive sweep of electrode potential. The time required for each determination was approximately 6 min.

Having obtained a reproducible response for the oxidation of dextrose, these researchers investigated the dependence of the oxidation current (I) on the dextrose concentration (C^b). Plots of I vs. C^b were found to be non-linear with the sensitivity decreasing at higher concentrations. Skou (17) also noted a similar response for plots of $\dot{I}$ vs. C^b for dextrose using cyclic voltammetry. Skou reasoned that the current should be proportional to the fractional surface coverage, $I = k\theta$. Using the Langmuir model for adsorption

$$\theta = (KC^b)/(1 + KC^b)$$

Shou derived the following expression

$$I^{-1} = (kKC^b)^{-1} + k^{-1}$$

where $K = \exp(-\Delta H_{ads}/RT)$, and k = proportionality constant. The above equation was tested with dextrose concentrations from 10 to 230 mM. A large deviation from theory occurred at the higher concentrations (a plot of I^{-1} vs. $(C^b)^{-1}$ had a r^2 value of 0.9588). When Shou's data, however, are replotted as I vs. ln C^b, as would be indicated assuming adsorption according to the Tempkin isotherm, a much better agreement is obtained ($r^2 = 0.9902$). This treatment is consistent with the previously mentioned findings of Bagotsky and Vassiliev (10).

C. Methods for Detection of Carbohydrates

A large number of methods exists for the determination of carbohydrates in food and physiological samples. The range in generality and accuracy of the different methods is extensive. Carbohydrate concentration of foods determined by the percentage of water, protein, fat and ash subtracted from 100 is commonly used in tables of food composition (31). Much more specific and accurate chromatographic methods are capable of quantitating many individual carbohydrates in complex physiological matrices (32).

Several of the more widely utilized methods will be reviewed.

1. Wet chemical methods

The determination of carbohydrates by titration with Fehlings solution is a common method. The aldehyde and keto groups of monosaccharides, and most disaccharides, are capable of reducing Cu(II) to Cu(I) in alkaline solution (33,34). Fehlings solution, an alkaline solution of Cu(II) ion complexed with tartrate ion, is deep-blue in color and turns colorless as the Cu(II) is reduced. The method is sensitive and easily performed but has many limitations (35). The removal of all other reducing organic material is necessary prior to analysis and, obviously, this technique does not have the ability to differentiate between various reducing sugars.

Another non-specific method in wide use is a colorimetric method in which the carbohydrates are degraded in strong mineral acid and reacted with a color forming organic reagent. Color forming reagents used include anthrone (9,10-dihydro-9-oxoanthracene), phenol and orcinol. Some reagents form color with only specific classes of carbohydrates and, therefore, are not the choice for a total carbohydrate analysis. These are somewhat useful in the differential analysis of mixtures. Hence, it is necessary to select the proper reagent depending upon the application.

Non-chromatographic methods which can totally differentiate between carbohydrates utilize enzymes. As an example, dextrose can be determined in the presence of maltose, sucrose, mannose, galactose, dextrans and starch by a modified method of Salomon and Johnson (36) "AACC Approved Methods" (37). Dextrose is oxidized by dextrose oxidase forming hydrogen peroxide. O-dianisidine hydrochloride is oxidized by the hydrogen peroxide through the action of horseradish peroxidase, yielding a colored solution with maximum absorbance at 525 mμ.

Even though the enzymatic methods are specific and sensitive, they have severe limitations. A separate analysis is required for the determination of each carbohydrate in a sample with each requiring a different enzyme. This increases the quantity of sample needed, the time for a total assay and the total expense of reagents. In addition, purified enzymes for many carbohydrates are not commercially available.

2. Chromatographic methods

Currently, methods for the determinations of individual carbohydrates in mixtures are nearly always based on prior chromatographic separation. While paper and thin-layer chromatography are used for qualitative determinations (38), gas and liquid chromatographic methods are the methods of choice for most quantitative analysis (5,6,39-59).

Gas chromatography (GC) is well-known for its great sensitivity and high resolution (60) and, therefore, would appear to be suitable for the separation and detection of a complex carbohydrate mixture. Since carbohydrates are relatively non-volatile, volatile derivatives of the carbohydrates must be made prior to GC analysis. Trimethylsilyl (TMS) derivatives are the most popular for general GC analysis of samples containing carbohydrates (39). These derivatives are formed by adding a mixture of hexamethyldisilazane, trimethylchlorosilane and anhydrous pyridine to the dried sugars. Although it has been reported that "virtually quantitative" derivatization occurs rapidly at room temperature (42), it is common practice to heat the mixture to 70° C for 25 min (40,41). Precipitate formation is common and decantation of the liquid sample prior to injection onto the GC column is advised to avoid column contamination (39-42). Non-polar stationary liquid phases are generally used for separating the TMS derivatives with a flame ionization detector (42). Two chromatographic peaks can result from a single sugar since its α- and β-anomers can form separate derivatives which leads to complex chromatograms. Use of different derivatization reagents can reduce this effect for some classes of carbohydrates while also decreasing resolution for others (49).

Use of HPLC for the separation and determination of individual sugars and carbohydrates has the advantage over GC analysis that no sample derivatization is required. Recent advances in column material and detectors have considerably improved resolution and sensitivity (44).

There are primarily two classes of column materials which are used for separation of carbohydrates by HPLC: ion-exchange and silica based materials. For the latter, some workers have used pure silica columns with a small amount of amine compound added to the eluent which then coats the silica by simple adsorption (45,46). More commonly, commercially available (61) chemically modified columns with alkylamine or octadecylamine functional groups are utilized. The mobile phase in the case of the silica columns is usually a mixture of water and acetonitrile with the water content between 10% and 40%. A larger water content decreases retention time without affecting elution order. Anomeric forms of the sugars are not separated. Many different elution mechanisms have been proposed. Retention based on hydrogen bonding between the sugar hydroxyl groups and the amine groups of the stationary phase can satisfactorily explain the observed retention orders, with longer retention times for sugars with a greater number of hydroxyl groups (58). For sugars with the same number of hydroxyl groups, those with all the hydroxyl groups on one side of the carbon chain are retained longer (59). To avoid peak broadening, samples are diluted prior to injection with sufficient acetonitrile to match the solvent ratio in the mixed eluent (44).

Anion exchange columns in the sulfate form have been utilized to achieve excellent resolution in the separation of complex mixtures of carbohydrates (32,51,52,54-56). The weakly acidic hydroxyl groups of the sugar play a part in the separation; however, steric influences are also considered to be important (55). Long analysis times, ranging from 4 hr (56) to 15 hr (51), has hindered the acceptance of this separation material for routine use.

The separation of sugars with cation exchange resins is steadily gaining more acceptance (6,50,53,55,57). Separations on columns prepared from these resins have the advantage that pure water can be used as the eluent and analysis times are under one hour. Several properties contribute to the separation of carbohydrates by the cation-exchange resin. The most important interaction is considered to be the partioning of the carbohydrate between the mobile phase and the stagnant water phase within the resin matrix, with the degree of ionic character of the carbohydrate controlling the extent of interaction. Increased resolution is obtained when the column is operated at elevated temperature, due to the increased diffusion of the analyte between the mobile and stagnant phases (6). Size exclusion also plays a role in the separation, with the larger saccharides having the shorter retention times (57). The degree of cross-linking of the resin can be altered to optimize this effect, with less cross-linking (larger pore size) being used for the separation of oligosaccharides.

3. Detectors

The primary limitation of carbohydrate determinations by HPLC is the low sensitivity of available detectors. Monitoring the change of refractive index (RI) is the standard detection method for detecting carbohydrates in HPLC. RI detectors have a response for all carbohydrates but have a sensitivity below that required for many applications (8,50). They are also very sensitive to temperature and minor fluctuations in solvent composition (49). Johncock and Wagstaffe (45) reported a RI detection limit for dextrose of 1 mg ml^{-1}.

Use of post-column derivatization with orcinol in sulfuric acid followed by photometric detection in the visible region of the spectrum has been used with automated anion-exchange systems (32,51,52,56). The method has good sensitivity but suffers from peak broadening due to the post-column mixing. There are also frequent problems due to the corrosive nature of the reagents (62).

Polarimetric detection of carbohydrates separated by HPLC has been demonstrated by Yeung _et al_. (63) and Kuo and Yeung (50). Using a micropolarimeter with a cell volume of 80 µL and an argon ion laser, they obtained a detection limit for fructose of 1 µg ml^{-1}. The polarity of the response aids in the identification of peaks, however, if anomers are present, their ratio must be known for quantitative determinations.

III. EXPERIMENTAL

A. Electrodes

Current-potential (I-E) curves were obtained by cyclic and triple pulse voltammetry at a platinum rotated-disc electrode (RDE, 0.460 cm^2; Pine Instrument Co., Grove City, PA). The rotator was model PIR (Pine Instrument Co.). A platinum-disc, flow-through detector (0.076 cm^2), for use in the flow-injection system, was constructed in the chemistry shop at Iowa State University after a design by Lindstrom (64) which is similar to the so-called "wall-jet" detector (65,66). The detector body was machined from glass-filled (25%) Teflon (Crown Plastics, Inc., St. Paul, MN).

The detector was modified for use in the HPLC system (Figure III-1). The detector body was unchanged, but the inlet fitting was constructed from PTX, a methylpentene polymer (Mitsui Petrochemical Ind., Ltd., Tokyo, Japan), and the electrode holder was modified to accommodate a platinum wire-tip electrode which replaced the platinum-disc. The wire-tip electrode (0.044 cm^2) was constructed from 22-gauge (0.0644 mm o.d.) platinum wire sealed in a 100-µL disposable glass pipet (67).

Figure III-1. Platinum wire-tip flow-through detector

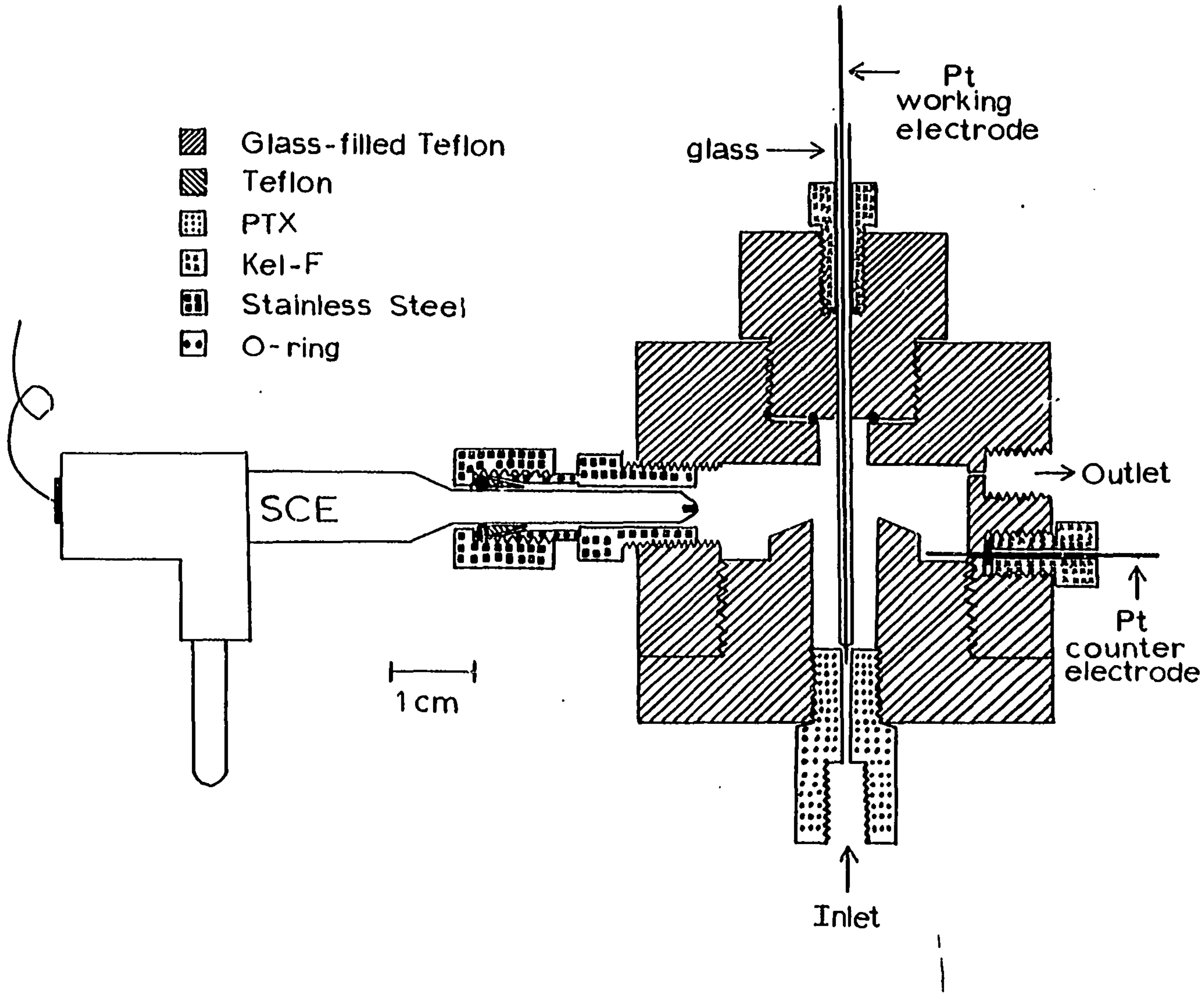

▨ Glass-filled Teflon
▨ Teflon
▦ PTX
▦ Kel-F
▦ Stainless Steel
▦ O-ring
Pt working electrode
glass
Outlet
SCE
Pt counter electrode
1 cm
Inlet

B. Potentiostats

Potentiostatic control was achieved with either of two three-electrode potentiostats. A potentiostat, assembled in this laboratory (68) from operational amplifiers according to the conventional design, was used for the studies of alcohols. A model 173 potentiostat, with a model 176 current-to-voltage converter, (Princeton Applied Research, Princeton, NJ) was used for all other work. The reference electrode was a miniature, saturated calomel electrode (SCE) filled with a saturated solution of KCl. All potentials are reported in V vs. SCE.

C. Timing and Potential Control

A block diagram of the instrument for generating the potential waveform is shown in Figure III-2. Three adjustable voltage signals (E_1, E2 and E3) were connected to the input of the potentiostat through AD 7513 analog switches (Analog Devices Inc., Norwood, MA). The switches were opened and closed at precisely controlled intervals of time by digital pulses produced by a timing circuit designed by Meschi (69). The timing circuit was constructed from five National Semiconductor 555 timing modules in their monostable configurations as shown in Figure III-3. Variable resistors and capacitors connected to each monostable (MS)

Figure III-2. Block diagram of instrumentation

S1-3 Analog Devices 7513 analog switches
E1-3 Adjustable sources of voltage
E_s Linear voltage ramp

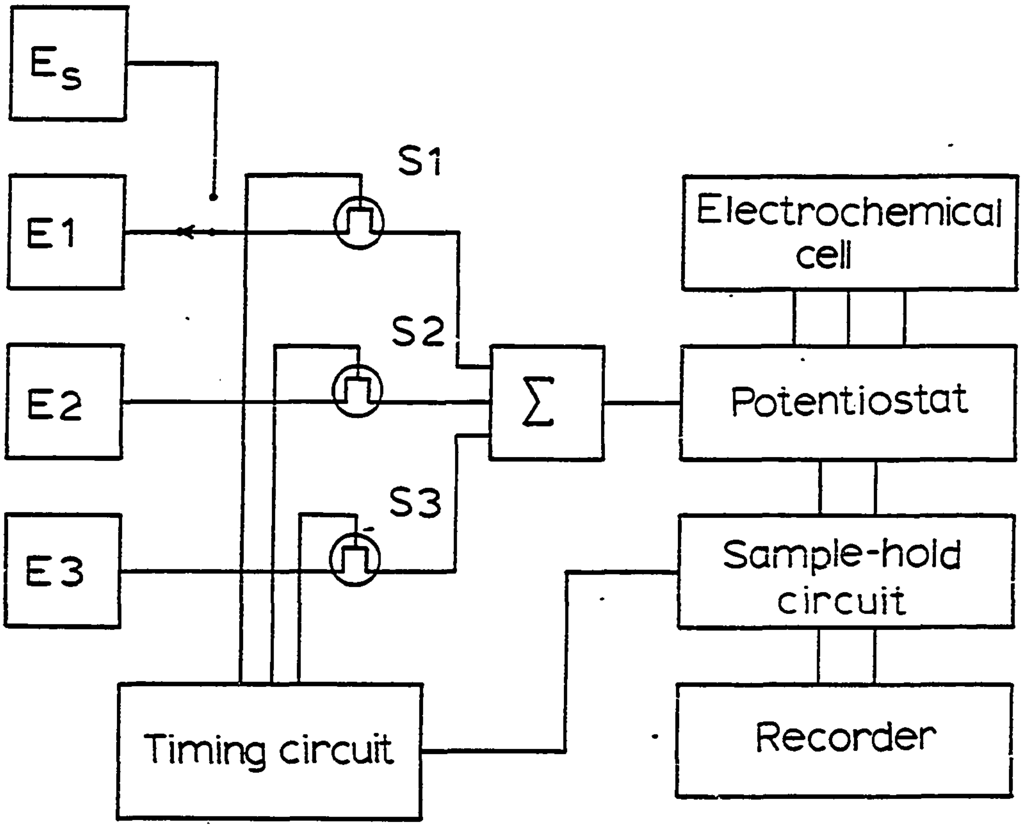
E_s
E1
E2
E3
S1
S2
S3
Σ
Electrochemical cell
Potentiostat
Sample-hold circuit
Recorder
Timing circuit

Figure III-3. Block diagram of timing

MS1-3 National Semiconductor 555 timing modules

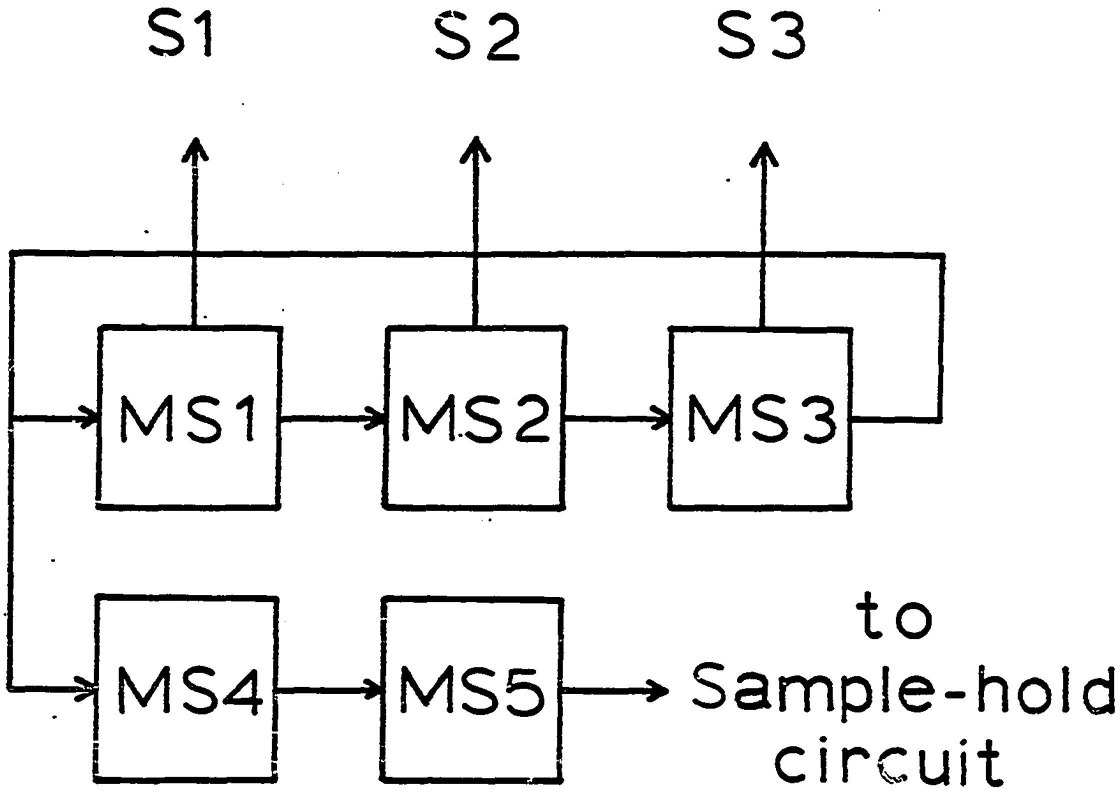
S1
S2
S3
MS1
MS2
MS3
MS4
MS5
to
Sample-hold
circuit

circuit enabled the pulse times to be varied continuously from 0.1 ms to 12 s. The monostable circuits were arranged in two interacting sequences as shown in Figure III-3. The main sequence (MS1-3) was responsible for establishing the potential waveform. Within the sequence, the trigger terminal of each MS was connected to the output of the preceding MS, with MS1 connected to the output of MS3, and triggering occurred with the HI-to-LO transition at the end of a pulse period. The second sequence of monostables (MS4,5) controlled the analog sample-hold circuit for measurement of the faradaic signal during application of the potential E1. MS4 was triggered simultaneously with MS1 and was used to produce a time-delay between the application of E1 and the activation of the sample-hold circuit. The time period for sampling the faradaic current was controlled by MS5.

D. Data Acquisition

1. Sample-hold amplifier

The sample-hold circuit consisted of an AD 582 sample-hold integrated circuit (Analog Devices) in the non-inverting unity gain configuration as specified in the manufacturers instruction sheet. The external hold capacitor was 3 μF.

2. Recorders

Cyclic and triple pulse voltammograms were recorded on a model 2000 X-Y recorder (Houston Instrument Co., Austin, TX). A model SR 204 stripchart recorder (Heath Schlumberger, Benton Harbor, MI) was used to record all flow-injection data and most of the HPLC data.

3. Computer data acquisition

The remaining HPLC data were collected by a computer data acquisition system. The system's hardware consisted of an HP-85 computer (Hewlett-Packard, Corvallis, OR) configured with an HP82903A 16K memory modual, 85-15003 I/O ROM, 85-15005 Advanced Programming ROM, HP82940A GPIO interface (Hewlett-Packard) and a circuit for analog-to-digital, digital-to-analog conversions which was constructed in this laboratory. The HP-85 is an 8-bit microprocessor with 16K memory, a built-in tape drive, CRT and 32-character thermal printer. Usable random access memory was increased to 30K with the addition of the 16K memory module. The "extended" BASIC language used by the HP-85 included a full set of graphics statements which enabled easy conversion of numeric data into chromatograms showing current vs. time displayed on the CRT and copied by the printer. With addition of the I/O ROM and GPIO interface, transfer of digital information into and out of the computer can be accomplished by the use of BASIC statements.

Since the GPIO interface handles only digital signals, an additional interface was necessary for input and output of analog data. A block diagram of the input section of the interface is shown in Figure III-4. The analog-to-digital (A/D) conversion was accomplished with an AD 574 converter (Analog Devices). The AD 574 is a 12-bit A/D converter operating on the principle of successive approximation. It was operated in the bipolar ±5 V mode which gave a resolution of 2.4 mV. The analog input was brought to the A/D converter through an AD 582 sample-hold amplifier controlled by the status line of the A/D converter. Data input was initiated in one of two ways, either by a positive pulse to FlgB of the GPIO interface from MS5 of the timing module (interrupt mode) or at the end of a software-controlled time interval of one of the HP-85's internal timers (time mode). The computer then signaled for the start of conversion with a negative pulse to the Read/Convert ($R/\overline{C}$) line of the A/D converter (see Figure III-5). Converted data were input through ports A and B of the GPIO interface (in a 16-bit parallel input configuration).

Analog output was used to display stored chromatographic data on the X-Y recorder, producing figures of

Figure III-4. Block diagram of computer input interface

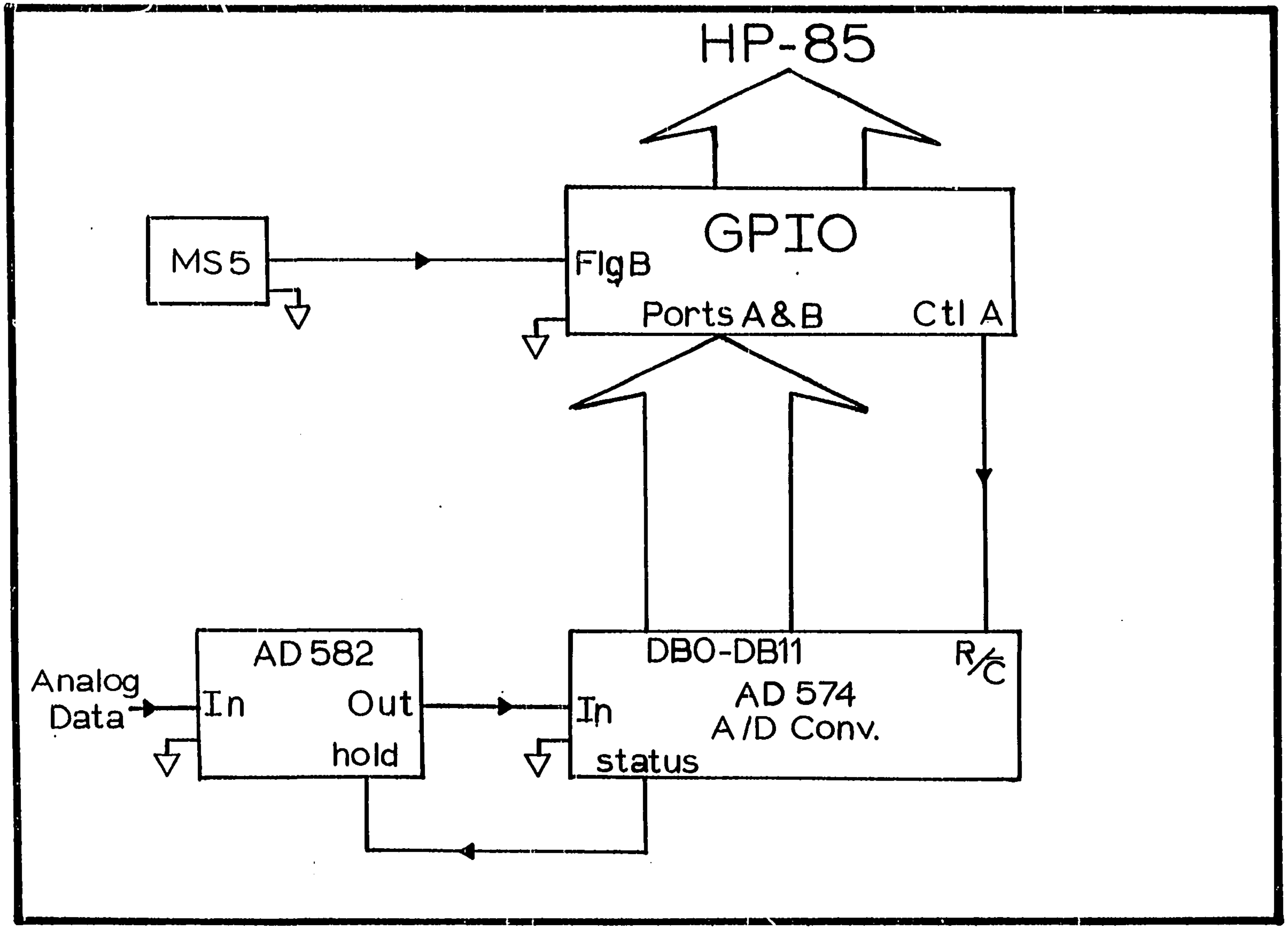
HP-85
MS5
GPIO
FlgB
Ports A&B
Ctl A
Analog
Data
AD 582
In
Out
hold
DB0-DB11
R/C
AD 574
A/D Conv.
In
status

Figure III-5. Timing diagram of computer input handshake

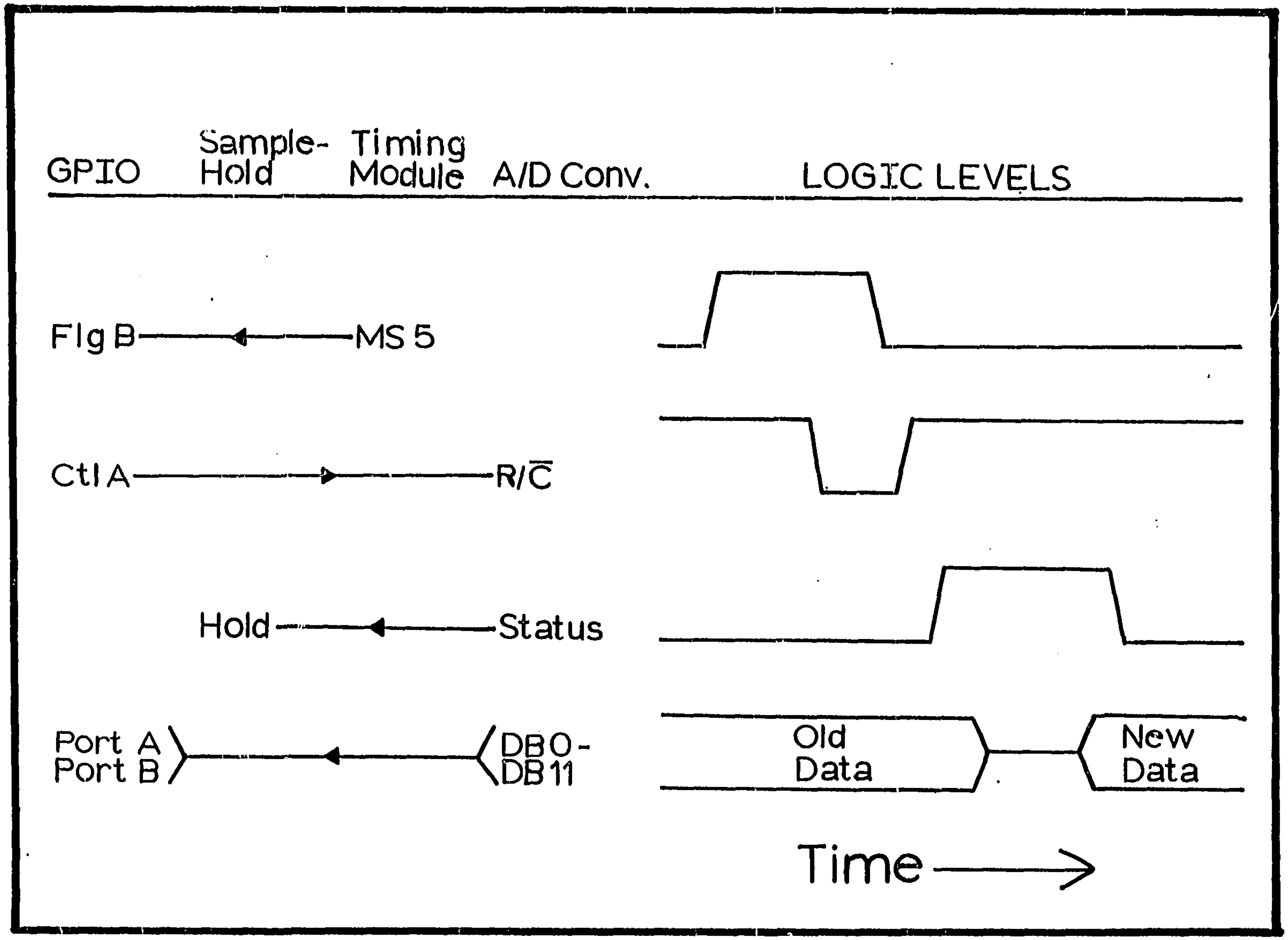
GPIO
Sample-Hold
Timing Module
A/D Conv.
LOGIC LEVELS
Flg B
MS 5
Ctl A
R/C̄
Hold
Status
Port A
Port B
DB0-
DB11
Old Data
New Data
Time

reproduction quality. The digital-to-analog conversion (DAC) was accomplished with an AD 7542 converter (Analog Devices) in the bipolar mode as specified by the manufacturers instruction sheet (Figure III-6). The AD 7542 is a 12-bit converter; however, these had to be input to the AD 7542 as 3, 4-bit nibbles with an address code to specify the low, middle and high nibble. This was accomplished by using the 4 least significant bits of port C of the GPIO interface (C1-3) for the data nibbles and the two most significant bits (C6,7) for the address, as shown in Table III-1. Loading of each nibble and the final conversion was initiated by a pulse from the Ctl 0 line of the GPIO.

Software for the data acquisition system provides a running average of data points to eliminate high frequency fluctuations, determination of the beginning, maximum and end of chromatographic peaks, retention time measurements, calculation of peak heights and peak areas as well as graphical representation of the current-time response (see Appendix). The beginning of a peak is defined by a combination of the signal being greater than a preset threshold value, above the baseline, 5 successive times in addition to the peak maximum being greater than a preset minimum (Ip reject). The peak maximum is defined as the first data

Figure III-6. Schematic diagram of computer output interface

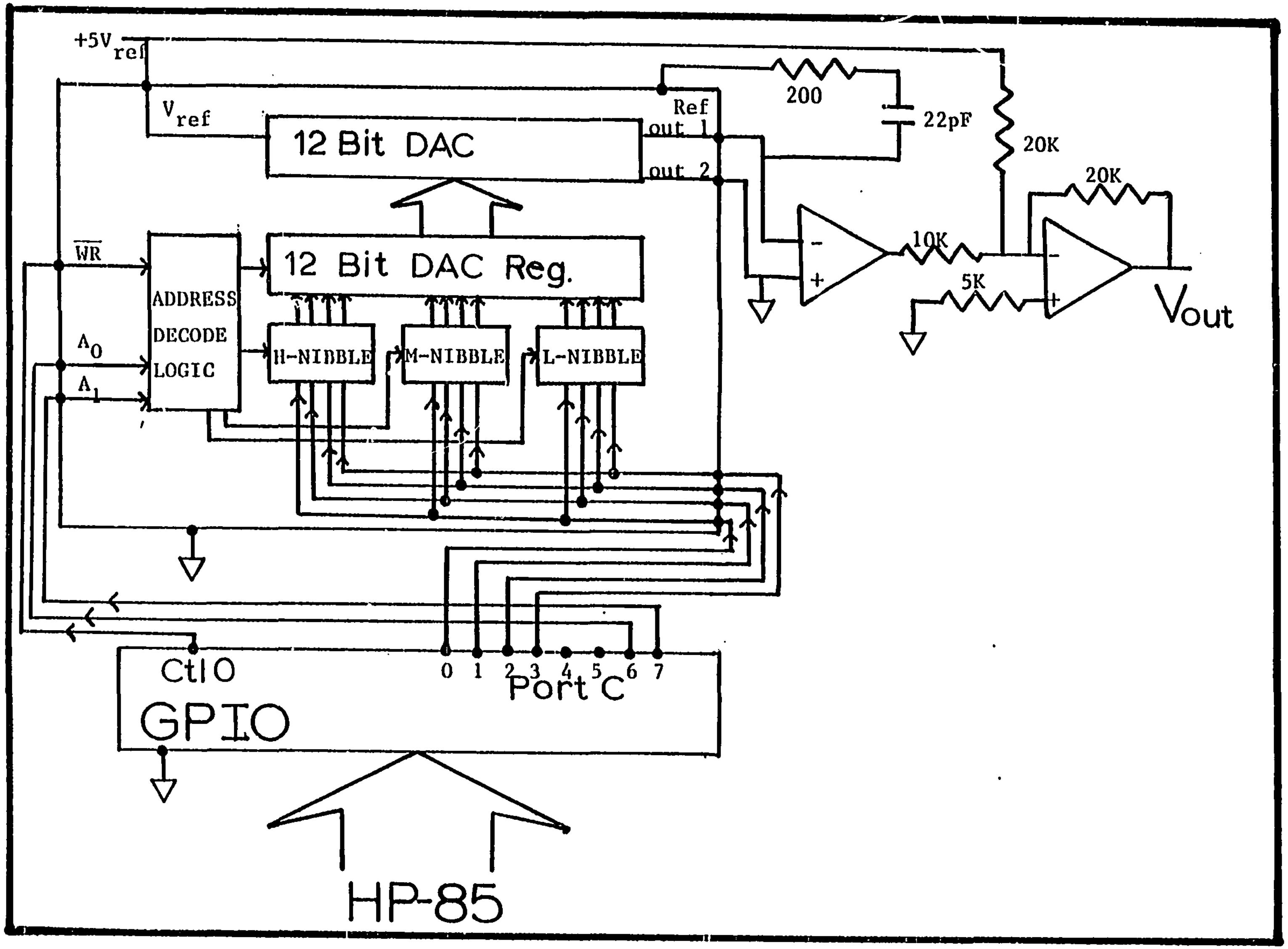
+5V
ref
V
ref
12 Bit DAC
Ref
out 1
out 2
200
22pF
20K
20K
10K
5K
Vout
12 Bit DAC Reg.
WR
ADDRESS
DECODE
LOGIC
A0
A1
H-NIBBLE
M-NIBBLE
L-NIBBLE
Ctl0
GPIO
0 1 2 3 4 5 6 7
Port C
HP-85

Table III-1. Address and conversion sequence of DAC

DAC	A1	A0	$\overline{WR}$	
GPIO	C6	C7	Ctl 0	RESPONSE
	0	0	↑	Load low nibble
	0	1	↑	Load middle nibble
	1	0	↑	load high nibble
	1	1	↑	Load 12-bit DAC register with data in low, middle and high nibble data registers and convert

point in a group in which the next 5 successive data points are less than the preceding one. The peak end is defined as the first data point which is less than the threshold value mentioned previously in which the next 5 data points are also less than the threshold value or the first data point in a group in which the next 5 successive data points are greater than the preceding one, indicating a valley between two fused peaks. The baseline is determined either by averaging data points for a preset time period (the delay time) at the beginning of the chromatogram, or as the line defined by linear regression analysis of the data points collected during the delay time.

Chromatograms are graphically represented as current vs. time on the CRT in real time with the points of peak beginning and ends being indicated by vertical dashes directly below the chromatogram as well as the retention times printed above each peak (Figure III-7). After the end of a run, the peak heights and areas are calculated and printed. At this time, the data can be replotted with the option of changing the scales on the current and time axes.

All variable parameters can be specified by the user before the start of the chromatogram from a menu-driven routine. The menu with the default values is shown in Figure III-8.

E, Flow-Injection System

The flow-injection apparatus was assembled according to the conventional design (69). Flow of the electrolyte solution was maintained by a Milton Roy model CK mini-Pump (Laboratory Data Control, Riviera Beach, FL) with dual pistons operating 180° out of phase. A model 709 pulse dampener (Laboratory Data Control) connected to a 40-ft stainless-steel tube provided sufficient back-pressure to eliminate pulsations in the flow rate. The stainless-

Figure III-7. CRT display of a chromatogram

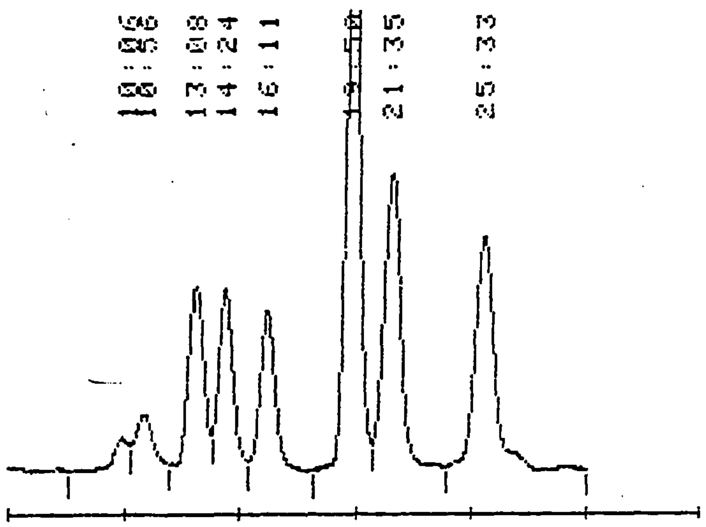
10:06
10:56
13:08
14:24
16:11
19:50
21:35
25:33

Figure III-8. Parameter menu from data acquisition program

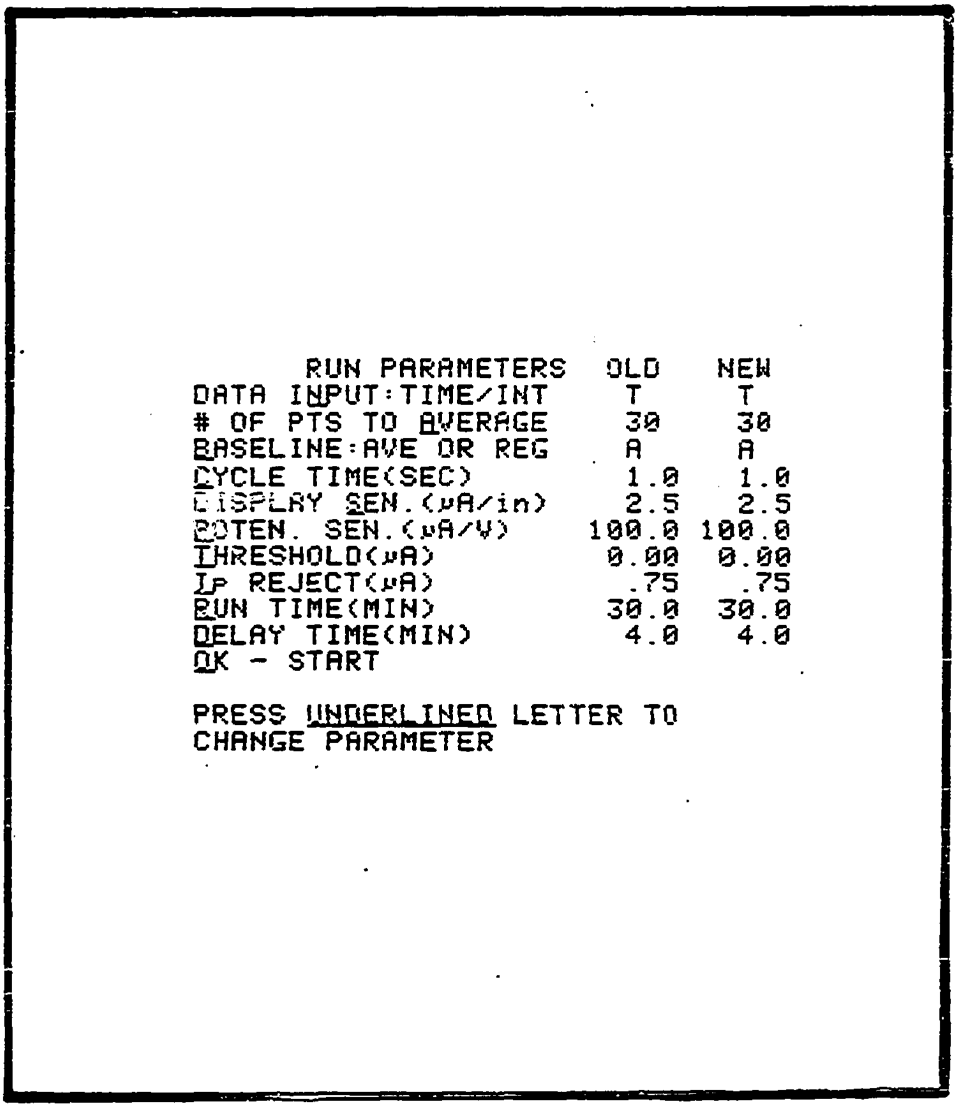

```
      RUN PARAMETERS  OLD   NEW
DATA INPUT:TIME/INT    T     T
# OF PTS TO AVERAGE    30    30
BASELINE:AVE OR REG    A     A
CYCLE TIME(SEC)         1.0   1.0
DISPLAY SEN.(μA/in)     2.5   2.5
POTEN. SEN.(μA/V)    100.0 100.0
THRESHOLD(μA)         0.00  0.00
Ip REJECT(μA)          .75   .75
RUN TIME(MIN)         30.0  30.0
DELAY TIME(MIN)        4.0   4.0
OK - START

PRESS UNDERLINED LETTER TO
CHANGE PARAMETER
```

steel tubing connecting the electrolyte reservoir and the pump was 0.11-in. i.d. x 1/8-in. o.d., and all other tubing was stainless-steel with dimensions 0.016-in. i.d. x 1/16-in. o.d.; stainless-steel compression fittings were used for all connections. The sample injection valve was a Rheodyne model 2125 (Larry Bell and Associates, Minneapolis, MN) with a sample loop having a volume of either 220 µL or 100 µL. An adjustable needle valve constructed from Kel-F (chemistry shop) was connected in the flow system after the detector to generate sufficient back-pressure (∿15 psi) to eliminate bubble formation in the detector. Flow rates were calibrated by measurement of the volume delivered to a 10-ml buret during a measured period of time.

F. High Performance Liquid Chromatograph

Separation of carbohydrates and alcohols was achieved with Ca(II)-loaded, cation-exchange columns. Two columns were tested and compared: a commercially available column, Hamilton HC-75 (Rainin Instrument Co., Woburn, MA), which had been optimized for mono- and disaccharides and sugar alcohols, and a prototype cation-exchange column, in the Ca(II) form, supplied by Dionex Corporation (Sunnyvale, CA). During operation of the HPLC the column was maintained at 85° C by circulating water through a water jacket (chemistry shop) surrounding the column. The flow of aqueous eluent through the column was maintained at 0.5 ml min^{-1} by a Milton Roy model CK miniPump (Laboratory Data Control). A model 709 pulse dampener (Laboratory Data Control) was used to reduce pulsations in the eluent flow. The sample injection valve was a Rheodyne model 7125 (Larry Bell and Associates) with a sample loop of 100 µL.

Detection of carbohydrates by triple pulse amperometry (TPA) is most sensitive at high pH. Hence, a stream of 6.1 M NaOH pumped at 0.01 ml min^{-1} by a Gilson Minipulse-2 peristaltic pump (Middleton, WI) equipped with 0.25 mm i.d. polyvinylchloride manifold tubing (Rainin Instrument Co.) was mixed with the effluent stream in a tee of low dead volume (Unimetrics, Inc., Anaheim CA). The mixing tee was maintained at 60° C (except for the temperature study) by circulating thermostated water through a water jacket (chemistry shop). The net concentration of NaOH in the detector was 0.1 M. All tubing was stainless-steel with compression fittings used for all connections. An adjustable needle valve constructed from Kel-F (chemistry shop) was connected in the flow system after the detector to generate sufficient back-pressure (∿15 psi) to eliminate bubble formation in the detector.

G. Chemicals

All chemicals were reagent grade. All water had been distilled, demineralized and passed through a 12-in. long x 1.5-in. i.d. column of activated carbon. All water used as eluent for the HPLC system was also passed through a 0.45-μm membrane. Dissolved oxygen was removed from all electrolyte and eluent solutions by saturation with nitrogen.

IV. OXIDATION OF ALCOHOLS ON PLATINUM ELECTRODES

Simple alcohols were the first compounds investigated in the development of triple pulse amperometry (TPA). These compounds were selected for the initial work because of their rather elementary structures and because of the extensive literature which has accumulated regarding their electrochemical oxidation on platinum electrodes. Preliminary characterization of the anodic response of simple alcohols was achieved with linear scan; cyclic voltammetry at a platinum RDE. The effects of variations in the rate of potential scan, analyte concentration and the rotational velocity of the electrode were investigated. Experimental conditions for detection of ethanol by TPA were optimized to yield the highest analytical sensitivity and precision.

A. Cyclic Voltammetry

The anodic response for methanol, ethanol, ethylene glycol and formic acid at a platinum RDE in 0.1 M H_2SO_4 was characterized with linear scan cyclic voltammetry. Representative I-E curves for these compounds are shown in Figure IV-1. Although each curve shown for the four compounds exhibits a unique response, the basic features of the four cyclic voltamograms are the same. There is

Figure IV-1. Current-potential curves obtained by cyclic voltammetry at the platinum RDE

$\omega = 41.9$ rad s^{-1}

$\phi = 3.0$ V min^{-1}

Curves

A - 6.5 mM methanol

B - 6.0 mM ethanol

C - 4.0 mM ethylene glycol

D - 2.6 mM formic acid

(----) residual curve

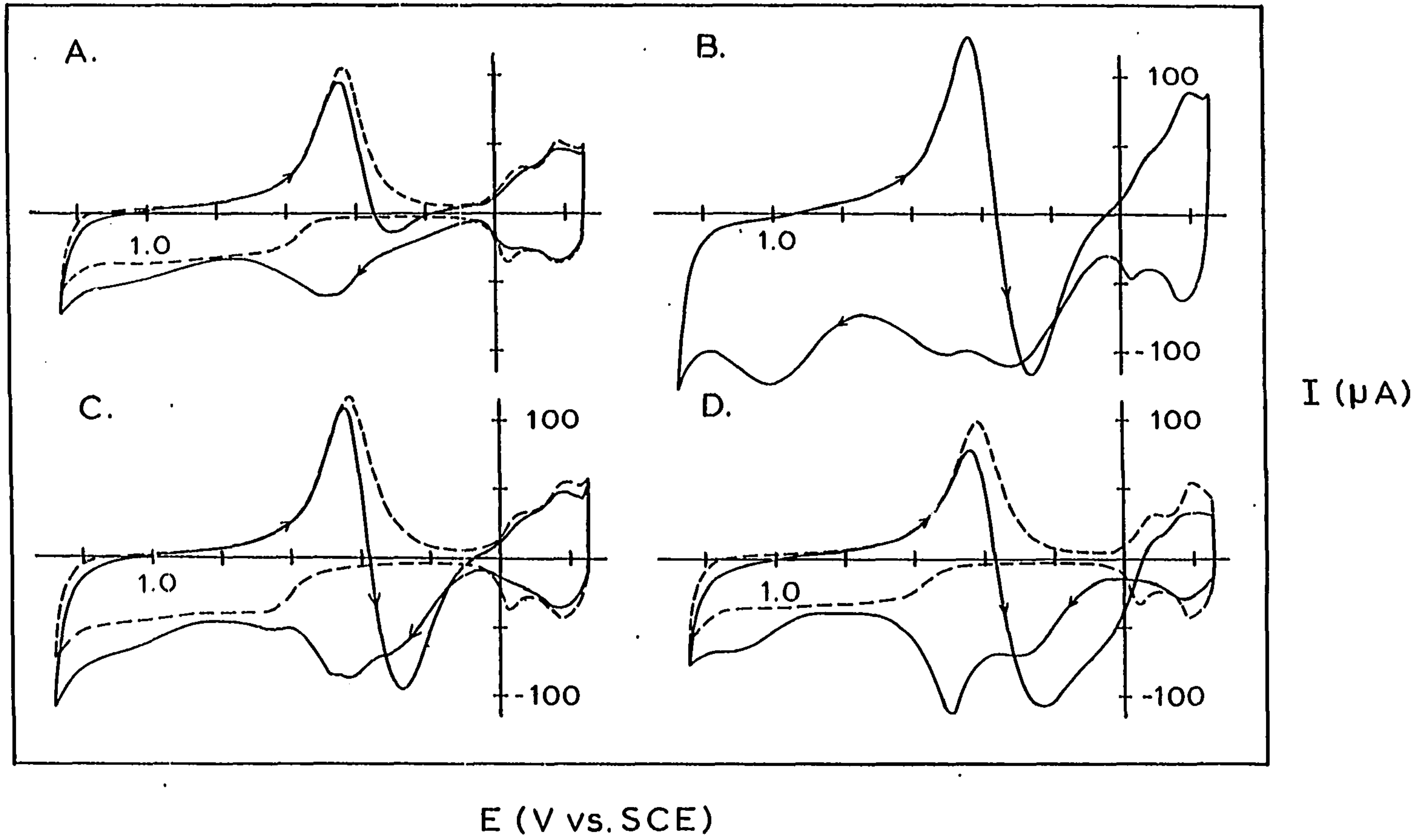
A.
1.0
B.
100
1.0
-100
C.
100
1.0
-100
D.
100
1.0
-100
I (μA)
E (V vs. SCE)

negligible oxidation of the organic compounds at the surface of an electrode covered by PtO during the negative sweep of potential for $1.2 > E > 0.6$ V. The reduction of PtO commences on the negative sweep for $E < 0.6$ V producing a cathodic peak. The production of platinum sites free of surface oxide enables adsorption of organic compounds from solution resulting in their dehydrogenation and subsequent oxidation. The net current shifts to an anodic value on the negative sweep at $E \simeq 0.4$ V, with the half-wave potential at approximately 0.2 V. No oxidation occurs for $E < 0.1$ V.

The cathodic and anodic peaks observed in the vicinity of 0.0 V in the absence of organic compounds correspond to the reversible formation and dissolution, respectively, of adsorbed hydrogen atoms at the platinum surface. The size of these peaks is diminished slightly with the addition of the organic materials to the solution as the result of the preferential adsorption of the compounds. During the positive scan of potential, the oxidation of organic compounds resumes as the adsorbed hydrogen is removed from the electrode ($E > 0.0$ V). The oxidation current reaches maximum value and then decays to a minimum at $E \simeq 0.6$ V. The decrease in anodic current is the result of two factors;

the accumulation of the adsorbed oxidation products on the electrode and the onset of PtO formation which blocks available adsorption sites on the electrode. Anodic current again increases for $E > 0.8$ V as the adsorbed dehydrogenation products are oxidatively removed.

The heights of the anodic peaks observed on the positive sweep of potential for the compounds tested, as is represented by ethanol in Figure IV-2, vary in proportion to the rate of potential scan (ϕ). This indicates that the quantity of charge, i.e. the integral of the I-t curve corresponding to these anodic processes, remains constant with increased ϕ. This property is indicative of surface controlled reactions and, hence, the oxidation of these organic molecules are concluded to be surface-controlled processes. Addition of small quantities of the sodium salts of chloride, bromide and iodide, known for adsorbing strongly at platinum surfaces, completely eliminates the response to the organic compounds. Therefore, the affinity of the platinum surface for adsorption is essential in promoting the oxidation of the organic compounds. The overall anodic processes are designated as being "surface-catalyzed" because there is no evidence that the reactions could occur in the absence of the adsorption step.

Figure IV-2. Current-voltage curves at a platinum RDE by cyclic voltammetry

9.32 mM ethanol in 0.10 M H_2SO_4
$\omega = 41.9$ rad s^{-1}

Scan rate (ϕ, V min^{-1}):

a. 1.0
b. 2.0
c. 3.0
d. 4.0

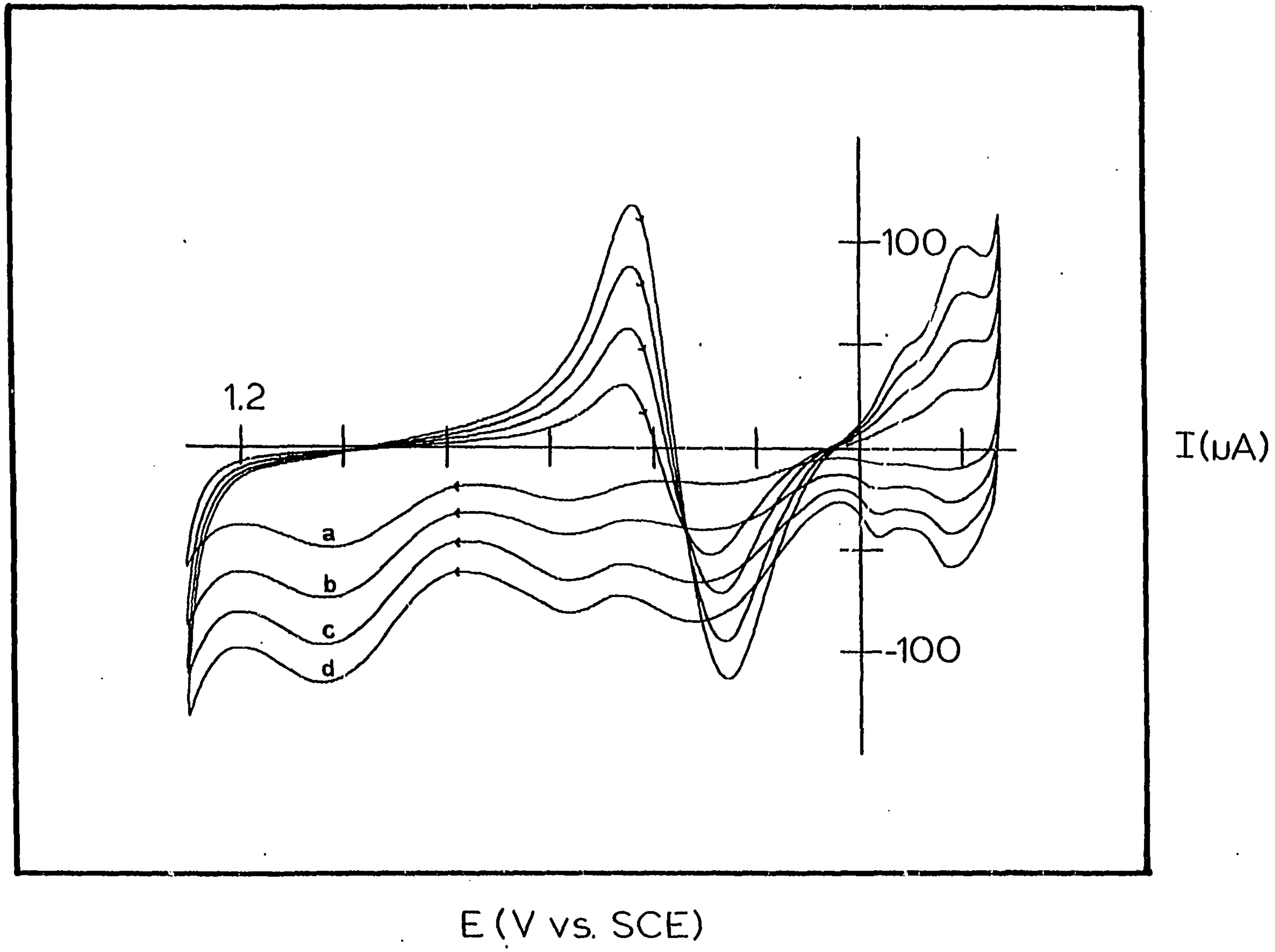
1.2
100
-100
a
b
c
d
I(µA)
E (V vs. SCE)

B. Calibration Curves

A representative set of cyclic voltammograms with increasing methanol concentration is shown in Figure IV-3. The faradaic signal for the compounds studied was observed to increase non-linearly with the bulk concentration (C^b). The peak current (I_p), measured at $0.6\ V > E > 0.0\ V$ on the positive sweep for the four compounds, was observed to be a linear function of C^b only for $C^b < 1$ mM. A linear plot was produced for $-1/I_p$ vs. $1/C^b$ over the entire range of C^b (Figure IV-4). Such behavior is concluded to be consistent with a mechanism whereby the faradaic signal is proportional to the fractional surface coverage by the adsorbed organic compound, $\theta_{\underline{RH}}$. In this discussion, RH is used to represent the organic compound to be detected anodically and the underline designates the adsorbed state of the molecule. The fractional surface coverage, $\theta_{\underline{RH}}$, is related to the molar coverage of the surface by $\theta_{\underline{RH}} = \Gamma_{\underline{RH}}/\Gamma_{\underline{RH},max}$, where $\Gamma_{\underline{RH},max}$ is the limiting coverage (mole cm^{-2}) at an infinite value of C^b_{RH}. The adsorption reaction can be described by

$$RH + \underline{H_2O} \underset{k_{-1}}{\overset{k_1}{\rightleftarrows}} \underline{RH} + H_2O \qquad (IV\text{-}1)$$

Figure IV-3. Current-voltage curves at a platinum RDE by cyclic voltammetry

$\omega = 41.9$ rad s^{-1}

$\phi = 3.0$ V min^{-1}

0.10 M H_2SO_4

Methanol concentration (mM):

1. 0.00
2. 2.19
3. 3.27
4. 4.35
5. 5.44
6. 6.50
7. 7.55

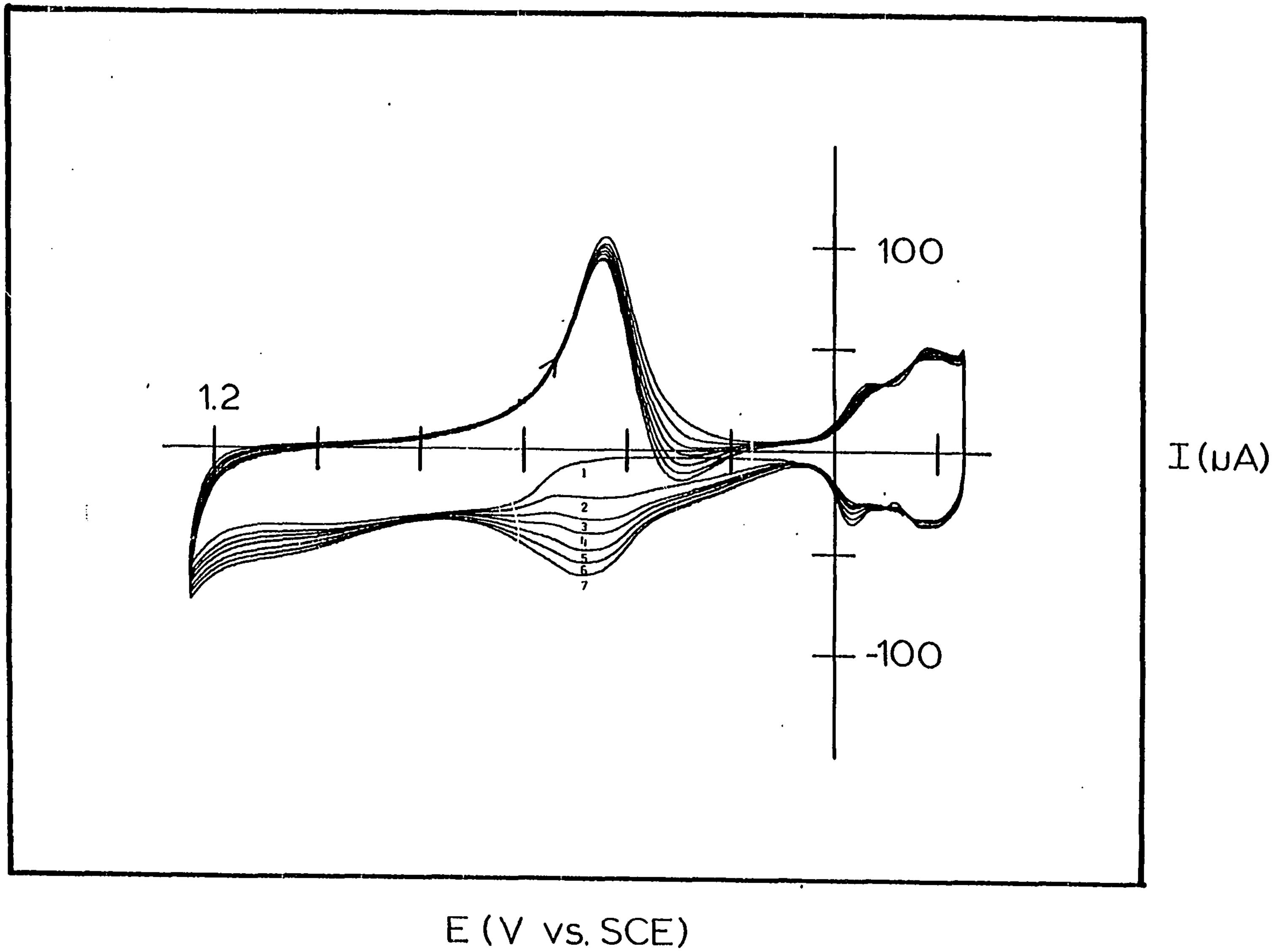
1.2
100
-100
1
2
3
4
5
6
7
I (µA)
E (V vs. SCE)

Figure IV-4. Calibration curves for methanol by cyclic voltammetry at $E = 0.48$ V

Conditions identical to Figure IV-3.

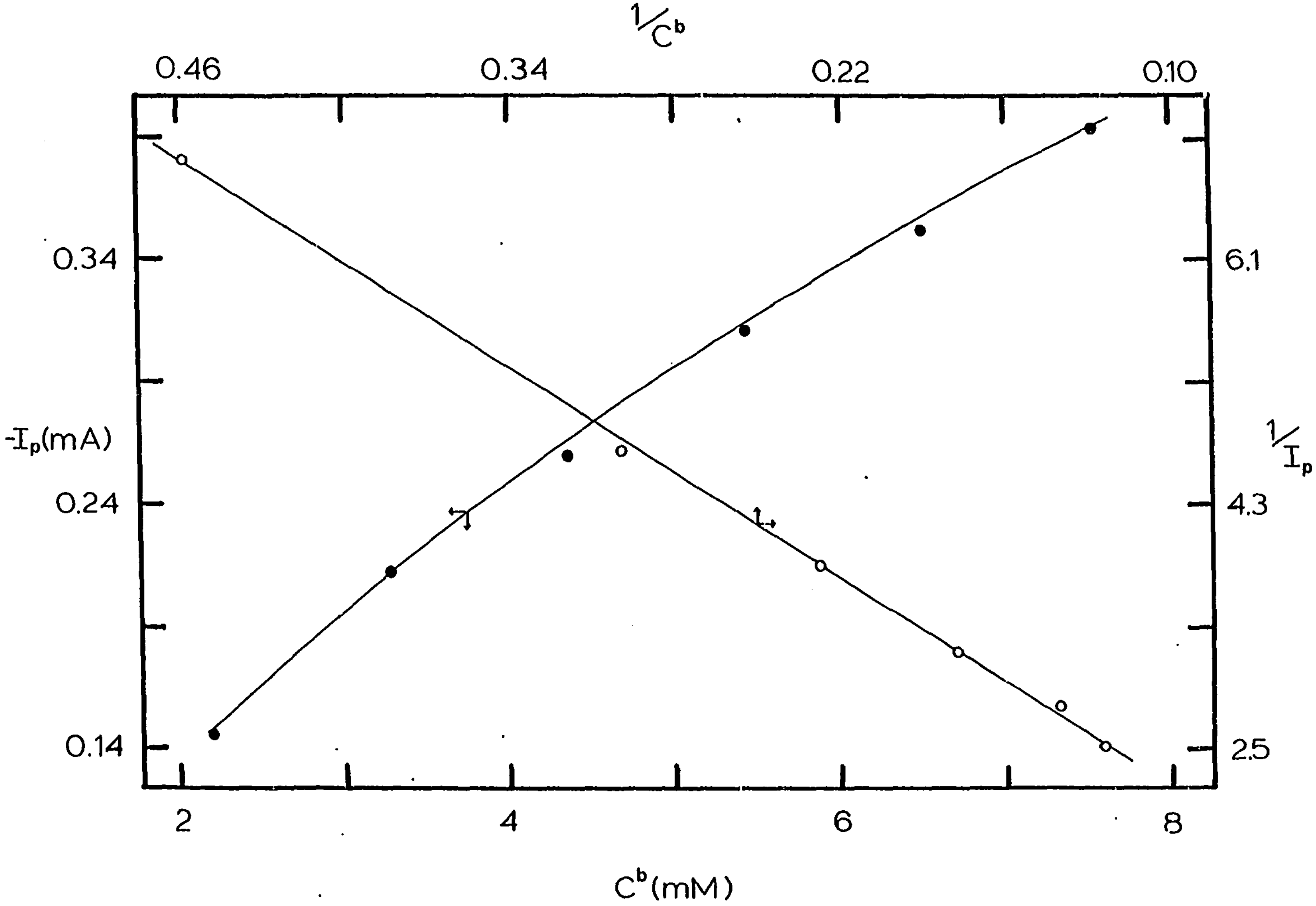
1/C^b
0.46
0.34
0.22
0.10
-Ip(mA)
0.34
0.24
0.14
1/Ip
6.1
4.3
2.5
2
4
6
8
C^b(mM)

where k_1 and k_{-1} are the rate constants for adsorption and desorption respectively. At equilibrium

$$k_1\{RH\}\{\underline{H_2O}\} = k_{-1}\{\underline{RH}\} \qquad \text{(IV-2)}$$

where the brackets indicate chemical activity and $\{H_2O\}$ being constant for dilute solutions is incorporated into k_{-1}. Assuming that $\underline{RH}$ and $\underline{H_2O}$ are the only adsorbed species,

$$\theta_{\underline{H_2O}} + \theta_{\underline{RH}} = 1. \qquad \text{(IV-3)}$$

Since
$$\{\underline{RH}\} \equiv \theta_{\underline{RH}} \qquad \text{(IV-4)}$$

and
$$\{\underline{H_2O}\} \equiv \theta_{\underline{H_2O}} = 1 - \theta_{\underline{RH}} \qquad \text{(IV-5)}$$

then Eq. IV-2 becomes

$$k_1\{RH\}(1 - \theta_{\underline{RH}}) = k_{-1}\theta_{\underline{RH}}. \qquad \text{(IV-6)}$$

Solving Eq. IV-6 for $\theta_{\underline{RH}}$ results in

$$\theta_{\underline{RH}} = \frac{KC^b_{RH}}{1 + KC^b_{RH}} \qquad \text{(IV-7)}$$

where $K = k_1/k_{-1}$, and $C^b_{RH} = \{RH\}$.

The anodic reaction is irreversible, i.e. $k_{-2} = 0$, and

$$\underline{RH} \xrightarrow{k_2} \underline{R} + H^+ + e^- \qquad \text{(IV-8)}$$

I_p is given by

$$I_p = -nFA(d\Gamma_{\underline{RH}}/dt) = -nFAk_2\Gamma_{\underline{RH},max}\theta_{\underline{RH}}. \qquad \text{(IV-9)}$$

The combination of Eqs. IV-7 and IV-9 yields

$$I_p = \frac{-K'C^b_{RH}}{1 + KC^b_{RH}} \qquad \text{(IV-10)}$$

where $K' = nFA\Gamma_{\underline{RH},max}k_2K$. The plot of $-1/I_p$ vs. $1/C^b_{RH}$ is, therefore, expected to be linear. Also, for $KC^b_{RH} << 1$, i.e. low C^b_{RH}, the plot of $-I_p$ vs. C^b_{RH} is predicted to be linear.

Eq. IV-7 has the same form as the equation for the Langmuir adsorption isotherm. Langmuir adsorption assumes no lateral interaction between adsorbed species and that the adsorption sites exhibit a single adsorption energy. These assumptions are reasonable at low analyte concentration when $\theta_{\underline{RH}} << 1$. For small $\theta_{\underline{RH}}$ the adsorbed species can remain far apart from each other minimizing lateral interaction. Even though many adsorption reactions at platinum have been demonstrated to occur with a range of adsorption energies (10), in the limit of small $\theta_{\underline{RH}}$ only adsorption sites of similarly high adsorption energy are utilized, i.e. the surface behaves homogeneously.

C. Effect of the Rotational Velocity of the Electrode

Based on the assumption that $\theta_{\underline{RH}}$ has reached its equilibrium value prior to the anodic reaction, the concentration of RH at the electrode surface in the diffusion layer, C^{s}_{RH}, has become equal to the value C^{b}_{RH}. Therefore, variation of rotational velocity, ω, of the electrode is not predicted to alter $\theta_{\underline{RH}}$ and should not influence I_p. The value of I_p was in fact observed to decrease with increases in ω. A similar negative dependence of faradaic signal on ω has been reported by Breiter and Gilman for methanol at a platinum electrode in 1 M $HClO_4$ (11). The explanation for this phenomenon as suggested by these investigators is that reaction intermediates formed by the initial charge-transfer step can either undergo further anodic reaction or they can be lost from the surface by desorption followed by mass transport. Increased rates of stirring result in an increased likelihood that subsequent oxidation steps do not occur and the net anodic signal is decreased. Plots of $-I_p$ vs. $\omega^{\frac{1}{2}}$ for the compounds studied were linear with a slope of -1. This result is consistent with a process in which a reaction intermediate is lost at a mass-transport limited rate (70).

D. Triple Pulse Voltammetry at the RDE

The potential waveform used for TPA is shown in Figure IV-5. The faradaic signal is sampled at electrode potential E1. Anodic cleaning with subsequent formation of PtO occurs at potential E2 and the oxide is subsequently reduced at electrode potential E3. Triple pulse voltammetry (TPV) at the RDE was used to select the appropriate value of E1 which would produce maximum sensitivity for TPA detection of organic compounds in the flow-through detector. Values of E2 and E3 were 1.25 and 0.00 V, respectively. E2 corresponds approximately to the positive potential limit of the solvent where the electrode is anodically cleaned without the formation of gaseous O_2. E3 is just positive of the electrode potential at which hydrogen adsorption occurs. The time periods for application of E2 and E3 in the waveform were 0.4 and 0.8 s respectively. These time periods were found empirically to be sufficiently long for the corresponding currents to decay to negligible values.

Figure IV-5. Triple pulse potential waveform

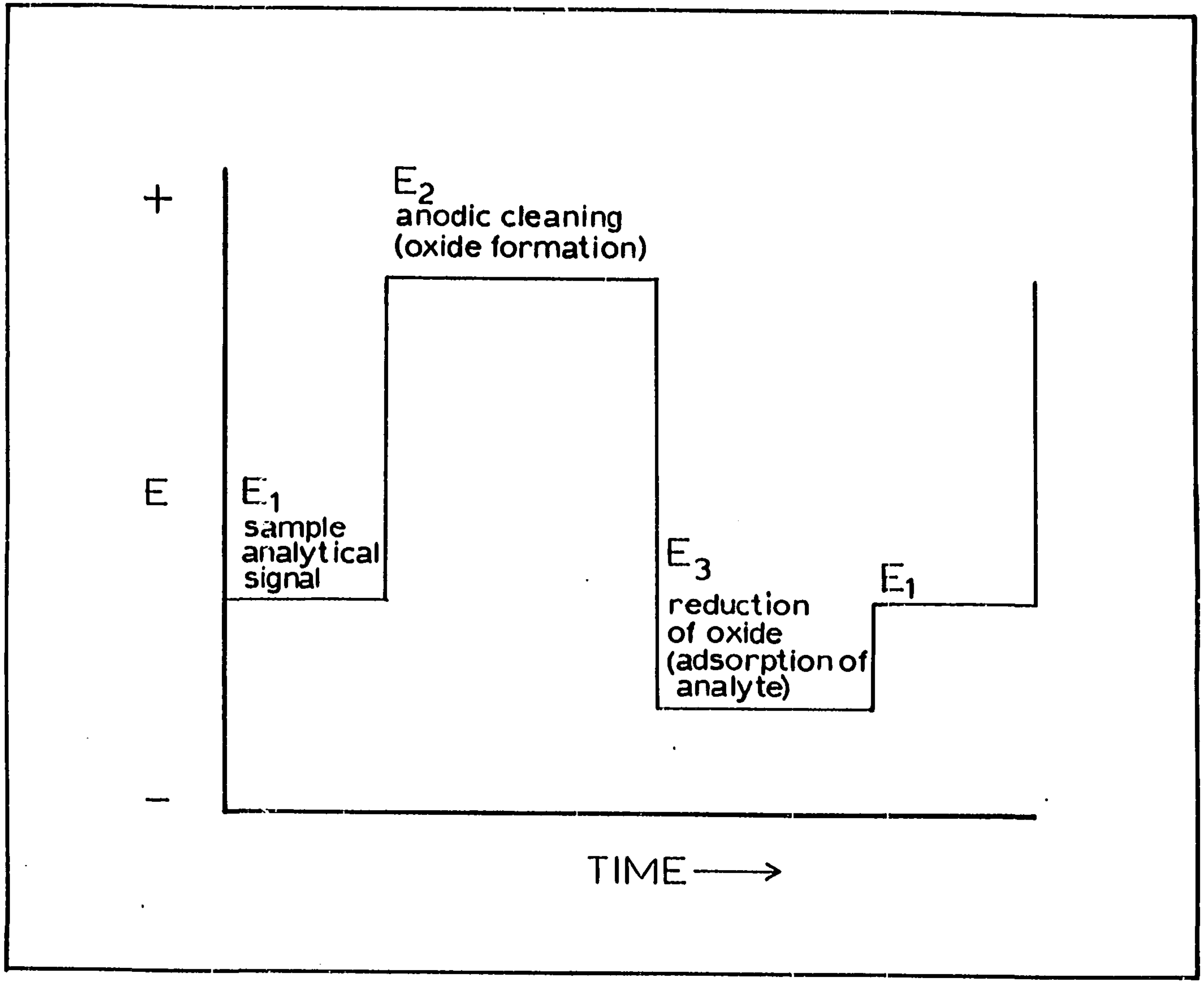
+
E
−
E_2
anodic cleaning
(oxide formation)
E_1
sample
analytical
signal
E_3
reduction
of oxide
(adsorption of
analyte)
E_1
TIME ⟶

In place of the constant voltage applied as E1, a linear voltage scan was substituted, E_s (5 mV s^{-1}), establishing a new value of E1 for each cycle of the waveform. The delay time for measurement of the pulse current following application of E1 = E_s was 45 ms which was sufficient for the charging current to decay to a negligible value; the sample-hold circuit was in the "sample" state for 8.0 ms. The total time at E1 = E_s was 0.2 s. Hence, the total period for completion of the waveform was 1.4 s. Triple pulse voltammograms for ethanol at the platinum RDE are illustrated in Figure IV-6. Also shown is the I-E curve obtained by the conventional (i.e., d.c.) linear scan cyclic voltammetry in the absence of ethanol. From Figure IV-6, a value of E1 = 0.26 V is concluded to be optimum for the triple pulse amperometric detection of ethanol. The other compounds tested exhibited responses similar to ethanol and it was concluded that the optimum waveform for detection of ethanol by TPA was adequate for the other organic compounds studied.

E. Triple Pulse Amperometry at the RDE

TPA detection with a constant value of E1 = 0.26 V is compared to d.c. detection at the RDE in Figure IV-7 for ethanol. For d.c. detection, the potential of the

Figure IV-6. Current-potential curves for ethanol obtained by triple pulse voltammetry at the platinum RDE

ω = 41.9 rad s^{-1}
0.10 M H_2SO_4

(•••) Background I-E curve by linear sweep voltammetry

50 µA div^{-1}
ϕ = 3.0 V min^{-1}

(——) Triple pulse voltammetry

100 µA div^{-1}
E1 = E_s (0.20 s)
E2 = 1.25 V (0.80 s)
E3 = 0.00 V (0.40 s)
ϕ = 0.30 V min^{-1}

Ethanol (mM)

A. 0.00
B. 1.14
C. 2.28
D. 3.41
E. 4.56
F. 5.66
G. 6.78
H. 7.89

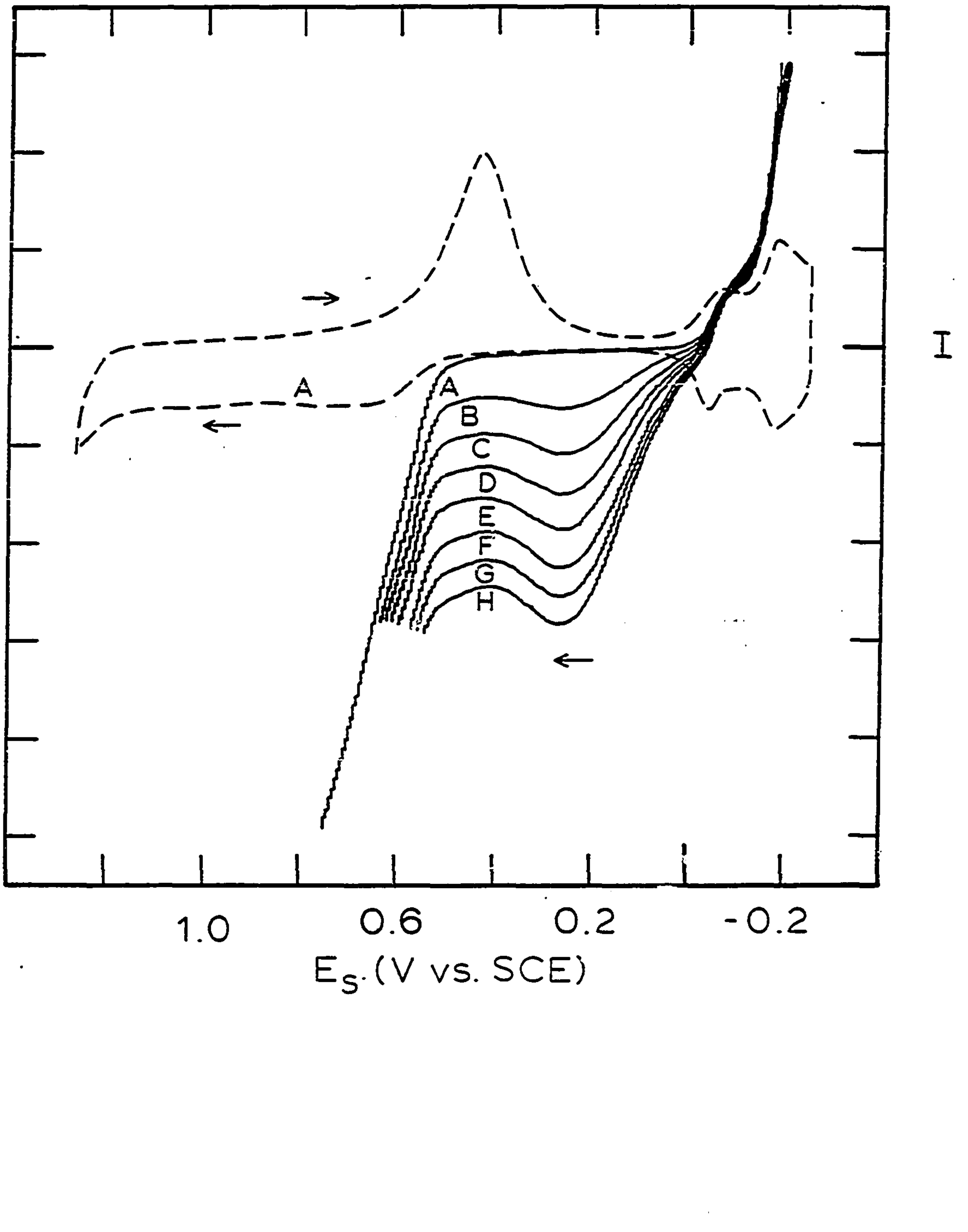
A
A
B
C
D
E
F
G
H
I
1.0
0.6
0.2
-0.2
E_S (V vs. SCE)

Figure IV-7. Comparison of stability of response for ethanol at the platinum RDE by TPA and d.c. detection

ω = 41.9 rad s^{-1}
0.10 M H_2SO_4

7.89 mM ethanol

Curves:

A. d.c. detection

E = 0.26 V

B. TPA detection

E1 = 0.26 V (0.20 s)
E2 = 1.25 V (0.80 s)
E3 = 0.00 V (0.40 s)

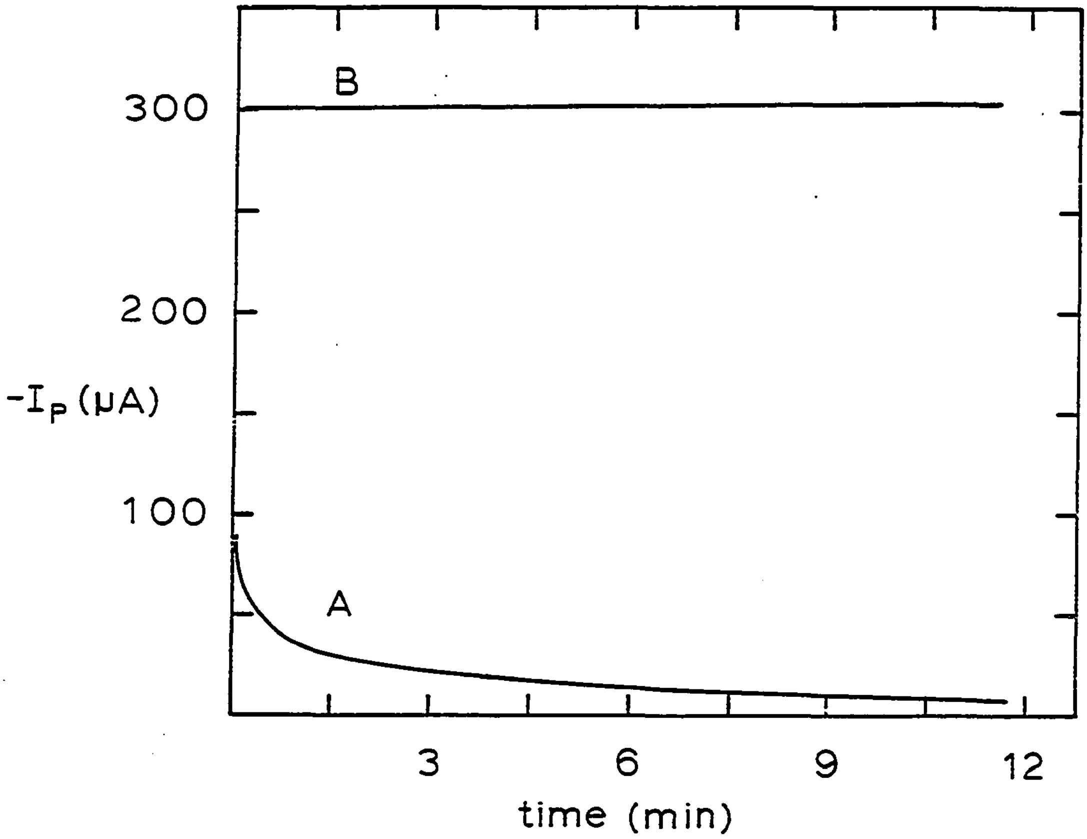
B
A
300
200
100
-I_P (μA)
3
6
9
12
time (min)

platinum electrode was repeatedly switched between 1.25 and 0.00 V to insure a clean electrode surface prior to recording the I-t curve at the constant potential 0.26 V. The signal for the TPA detection was observed to remain constant for 0.5 hr at which time the experiment was discontinued.

A calibration curve was constructed for ethanol at concentrations of 1 to 10 mM with TPA detection. The plot of $-1/I_p$ vs. $1/C^b$ was linear over the entire concentration range, as predicted by Eq. IV-10. The reader is reminded that Eq. IV-10 was derived assuming that the adsorption reaction

$$RH + \underline{H_2O} \underset{k_{-1}}{\overset{k_1}{\rightleftarrows}} \underline{RH} + H_2O \qquad \text{(IV-11)}$$

had reached equilibrium. Bagotzky and Vassiliev (10) determined that the time to reach adsorption equilibrium for 10 mM methanol on platinum is greater than 100 s. It is obvious, therefore, that the 200 ms spent at potential E1 was not sufficiently long to reach the same condition of equilibrium observed by Bagotzky and Vassiliev. However, the adsorption process which these investigators studied is concluded to be different from the adsorption described by

Eq. IV-11. The electrode potential used in their experiments was sufficiently positive to oxidize the adsorbed methanol. After 100 s at this potential, the anodic current for the methanol had dropped to a negligible value. This indicates that the form of the adsorbed molecules which Bagostzky and Vassiliev studied was not RH but its adsorbed oxidation product, and, therefore, the conclusions made by those authors are not applicable to the interpretation of data obtained in this research.

F. Summary

The anodic response of methanol, ethanol, ethylene glycol and formic acid on a platinum RDE has been illustrated. Prior adsorption of the compound is concluded to be a prerequisite for oxidation. The oxidation current is proportional to the fractional surface coverage, as described by the Langmuir adsorption equation, and plots of $-1/I_p$ vs. $1/C^b$ are linear. Application of a triple pulse waveform has been demonstrated to maintain a uniform level of electrode activity during detection of all compounds studied. The repeated execution of the waveform incorporates the cleaning and reactivation of the platinum electrode, by alternate anodic and cathodic polarization, with measurement of the faradaic signal for the analyte at the reduced electrode surface. The waveform is completed within approximately 1.5 s and the faradaic signal exhibits no decay with time as would be the case for amperometric detection at a constant applied potential.

V. OXIDATION OF CARBOHYDRATES ON PLATINUM ELECTRODES

Having demonstrated the feasibility of continuous electrode reactivation by application of a triple pulse waveform for the detection of simple alcohols, the application of this technique for detection of carbohydrates was investigated. The anodic behavior of ten simple carbohydrates at a platinum RDE in 0.1 M NaOH was determined by linear scan cyclic voltammetry. Interrupted scan and flow-injection voltammetric experiments were also performed to characterize the adsorption behavior of the carbohydrates. TPV at the RDE was used to optimize experimental conditions for later use in the detection of dextrose and sorbitol by TPA in a flowing stream.

A. Cyclic Voltammetry

The compounds studied, listed in Table V-1, include a ketose, aldoses and several sugar alcohols. By way of brief review, structures are compared below for fructose, dextrose and sorbitol (1). The choice of 0.10 M NaOH as the supporting electrolyte was made because the anodic sensitivity for the carbohydrates was observed to improve with increasing pH.

Preliminary characterization of the anodic response

Table V-1. Carbohydrates studied

Compound	Formula
Dextrose	$C_6H_{12}O_6$
Galactose	$C_6H_{12}O_6$
Mannose	$C_6H_{12}O_6$
Rhamnose	$C_6H_{12}O_5$
Arabinose	$C_5H_{10}O_5$
Xylose	$C_5H_{10}O_5$
Fructose	$C_6H_{12}O_6$
Perseitol	$C_7H_{16}O_7$
Mannitol	$C_6H_{14}O_6$
Sorbitol	$C_6H_{14}O_6$

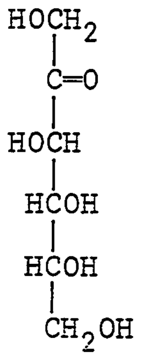

Fructose

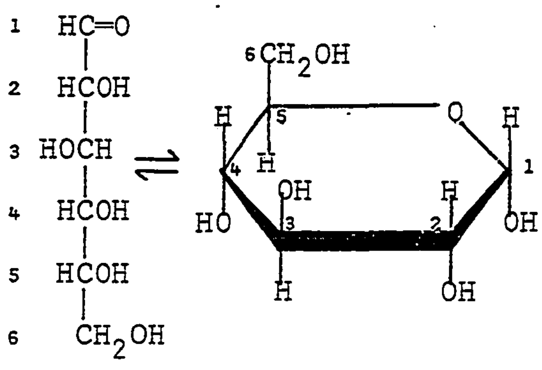

Dextrose

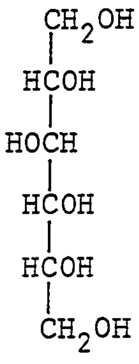

Sorbitol

of the compounds tested was based on I-E curves obtained by cyclic voltammetry at the platinum RDE. Representative curves are shown in Figure V-1 for dextrose and sorbitol. For the purpose of discussion, the potential axis is divided into three segments and named on the basis of characteristic processes occurring at the platinum RDE in the absence of the carbohydrates. In the hydrogen region (-0.6 to -0.9 V), cathodic and anodic peaks are observed for the supporting electrolyte corresponding to the formation (negative scan) and dissolution (positive scan), respectively, of adsorbed H-atoms. Virtually no faradaic reaction of the electrode surface occurs in the double-layer region (-0.2 to -0.5 V) and in the absence of electroactive solute the small observed current corresponds to charging of the electrical double layer at the electrode-solution interface. The oxide region (+0.6 to -0.1 V) corresponds to the range of potentials for which a layer of platinum oxide is formed on the electrode surface. The cathodic peak observed on the negative scan at -0.3 V corresponds to reduction of the oxide.

Dextrose and the other aldoses produced anodic peaks on the positive scan in the hydrogen region as well as in the double layer region. The ketose and sugar alcohols

Figure V-1. Current-voltage curves at a platinum RDE by cyclic voltammetry

$\omega = 41.9$ rad s^{-1}
$\phi = 3.0$ V min^{-1}

(---) Residual curve for 0.10 M NaOH

(——) Carbohydrate present

A: 0.40 mM dextrose

B: 0.40 mM sorbitol

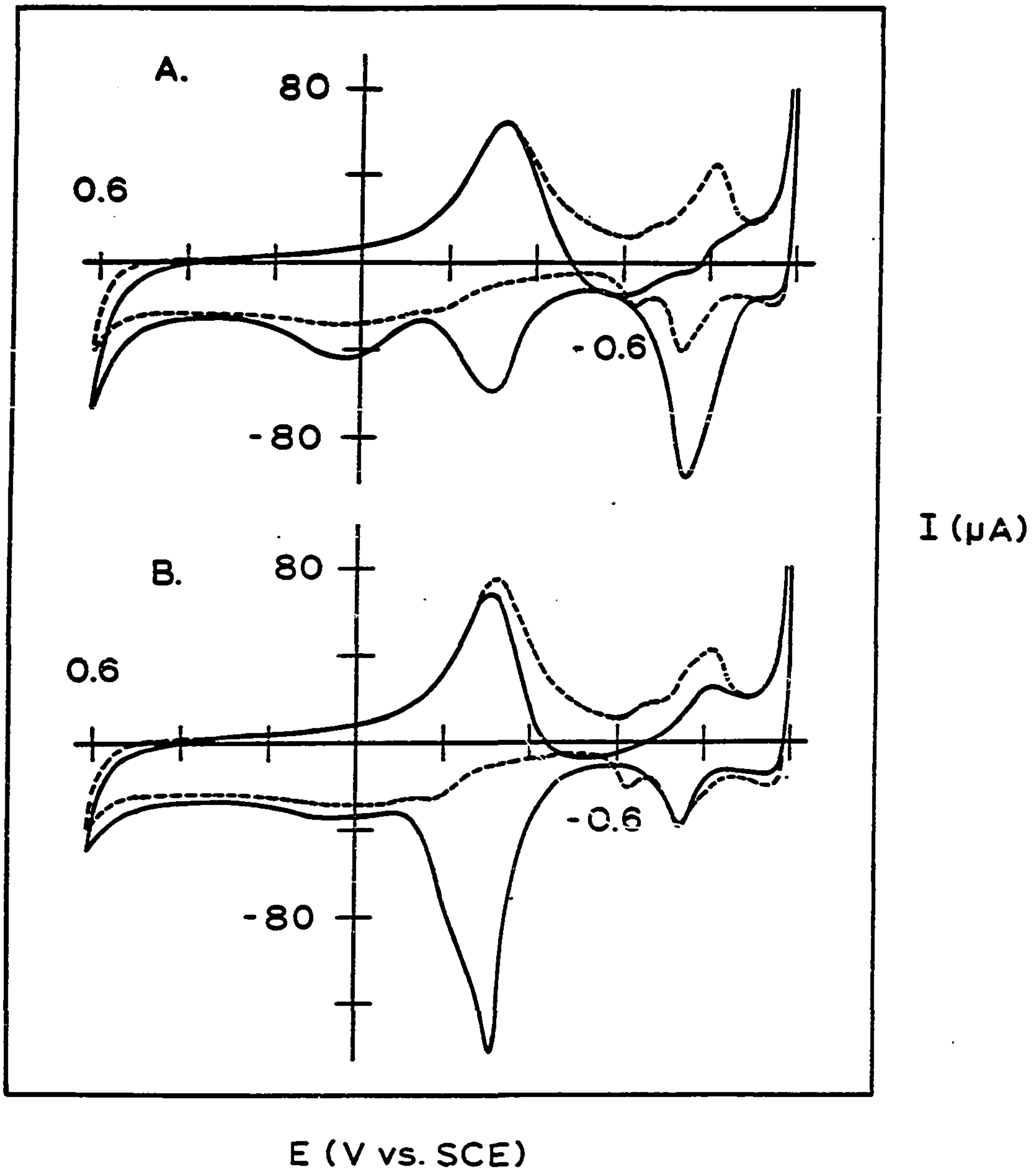
A.
80
0.6
-0.6
-80
B.
80
0.6
-0.6
-80
I (μA)
E (V vs. SCE)

produced anodic peaks in the double-layer region but virtually no increase occurred for the peak for anodic dissolution of adsorbed H-atoms in the hydrogen region. The height of all anodic peaks obtained on the positive scan for the carbohydrates tested varied in a linear fashion with changes in the rate of potential scan (ϕ) and these reactions are concluded to be surface controlled. Furthermore, a linear correspondence was obtained for the reciprocal of peak current and the reciprocal of the concentration of the carbohydrates. This observation is consistent with a mechanism whereby the faradaic signal is proportional to the fractional surface coverage by the adsorbed organic compounds with adsorption according to the Langmuir isotherm (Sec. IV-B).

Ernst, et al. (15) working in phosphate buffer at pH 7.5, observed an identical potential dependence for the adsorption of H-atoms and the adsorption of dextrose at platinum in the hydrogen region. They proposed a reaction mechanism whereby adsorbed H-atoms promote adsorption of dextrose by hydrogen bonding to the OH-group on the C_1-atom for the hemiacetal form of the dextrose molecule. Although hydrogen bonding should also promote the adsorption of the sugar alcohols, the absence of an anodic peak for sorbitol at pH 7.5 was attributed, by Ernst et al., to the absence of the easily oxidized hemiacetal form for that compound. A similar benefit from H-atoms was observed for the compounds tested in this study as illustrated for dextrose and sorbitol in Figure V-2. When the negative limit of the cyclic potential scan was shifted from -1.0 to -0.6 V, a pronounced decrease was observed for the anodic peaks in the double-layer region.

B. Cyclic Voltammetry with Interrupted Scan

The absence of any significant change in the anodic peak for adsorbed H-atoms in the I-E curves obtained by cyclic voltammetry (Figure V-1) upon addition of sorbitol might be concluded as evidence that oxidation of sorbitol by a mechanism involving surface-catalyzed dehydrogenation does not occur for sorbitol. That such a conclusion is tentative at best is apparent from the recognition that sorbitol is oxidized in the double-layer region during the negative scan of potential (see Figure V-1). Since the product of that reaction is believed to be strongly adsorbed, there is probably an insufficient quantity of unoxidized sorbitol present on the electrode surface at the start of the subsequent positive scan to produce a signif-

Figure V-2. Effect on I-E curves of decreased limit of negative scan

$\omega = 41.9$ rad s^{-1}

$\phi = 3.-$ V min^{-1}

(---) Residual curve for 0.10 M NaOH

(——) Carbohydrate present

A: 0.22 mM dextrose

B: 0.22 mM sorbitol

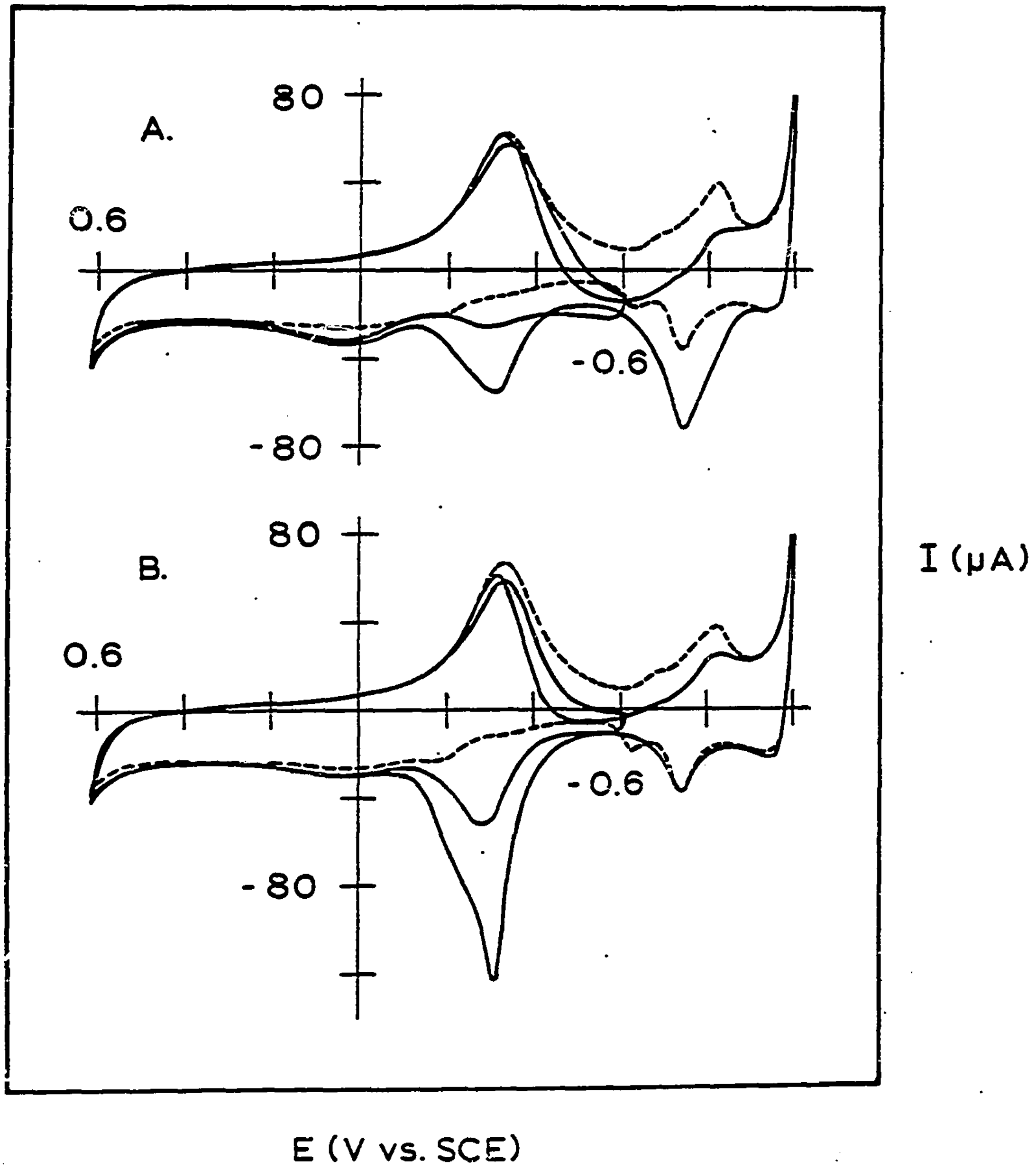
A.
80
0.6
-0.6
-80
B.
80
0.6
-0.6
-80
I (μA)
E (V vs. SCE)

icant anodic peak in the hydrogen region. To test this possibility, the potential of the platinum-RDE was stepped rather than scanned from 0.60 V to -0.94 V following completion of the positive scan. The value of electrode potential was maintained at -0.94 V for 4 s and the I-E curve recorded for the positive scan of potential. The curves are shown in Figure V-3 for sorbitol and dextrose along with I-E curves for the background processes obtained under the same conditions but without the carbohydrates. A substantial peak was obtained for sorbitol, as well as dextrose, in the hydrogen region. It is concluded that sorbitol, as well as dextrose, undergo substantial dehydrogenation on the platinum electrode surface. Three possible reasons why the peak for sorbitol in the hydrogen region is smaller than the peak for dextrose are: that the surface coverage by sorbitol at equilibrium is less than for dextrose at the same concentration, the rate of desorption of the primary oxidation product is faster for dextrose than for sorbitol, and/or the rate of catalytic dehydrogenation is less for sorbitol.

C. Flow-Injection Voltammetry

It is expected that significant new information about the voltammetric response of surface-controlled reactions

Figure V-3. Current-voltage curves at platinum RDE by cyclic voltammetry with interrupted scan

Positive scan only is shown

$\omega = 41.9$ rad s^{-1}

$\phi = 3.0$ V min^{-1}

A: Cyclic voltammetry without interruption

B: Cyclic voltammetry with interruption of scan

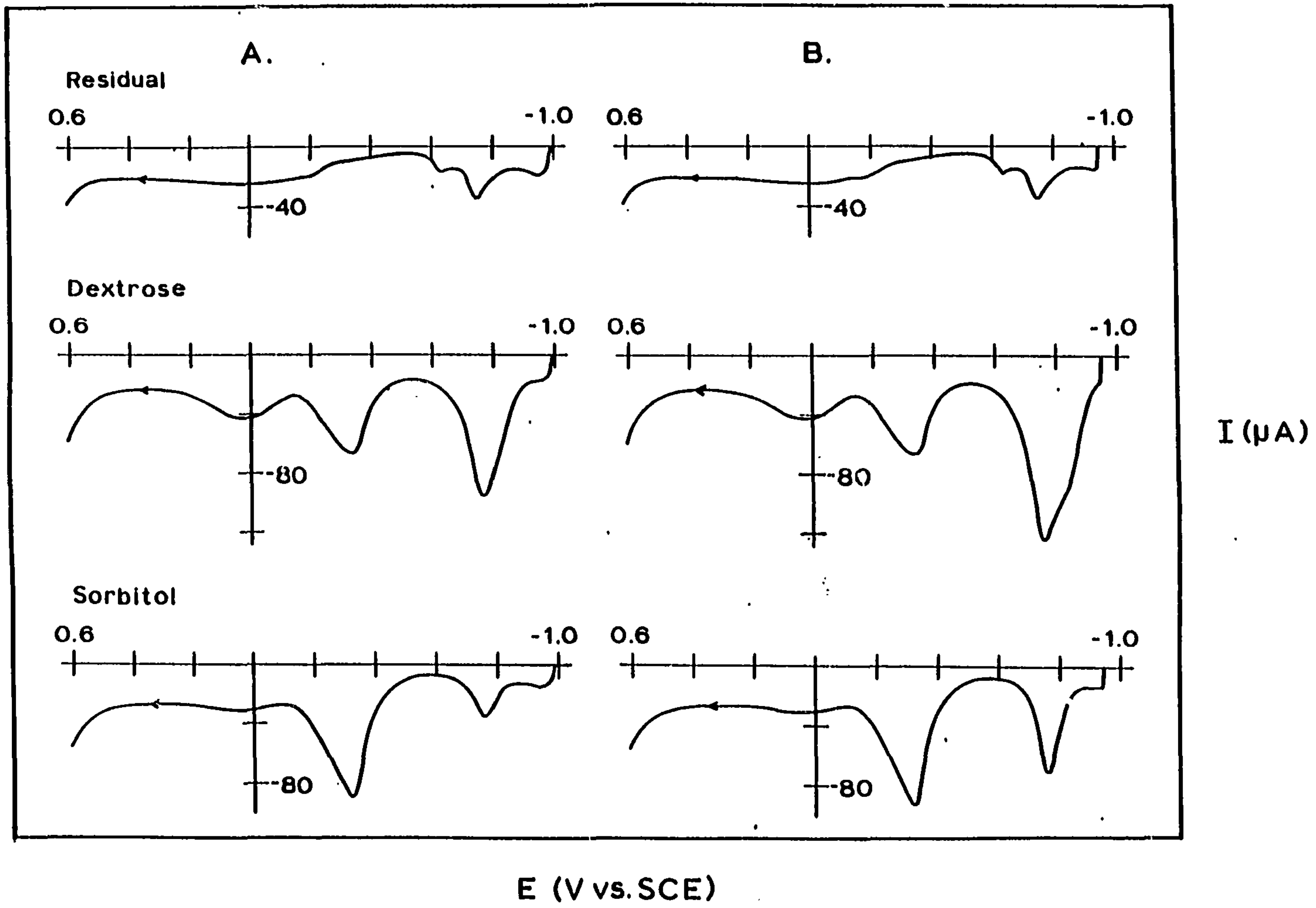
A.
B.
Residual
0.6
-1.0
-40
0.6
-1.0
-40
Dextrose
0.6
-1.0
-80
0.6
-1.0
-80
Sorbitol
0.6
-1.0
-80
0.6
-1.0
-80
I (μA)
E (V vs. SCE)

might be obtained if that response could be measured in the absence of the compound from the bulk solution. This would be particularly useful for differentiating surface-controlled processes resulting from the reaction of adsorbed solute, from those for dissolved solute undergoing reaction controlled by surface transformations. The use of the RDE under conditions of media exchange is cumbersome and accomplishment of this goal by flow-injection voltammetry was investigated. In these experiments, a specified volume of sample was injected into the stream of supporting electrolyte for a constant electrode potential and the resulting I-t curve was recorded. When all the dissolved sample had been flushed from the detector by the continuous flow of supporting electrolyte, the I-E curve was recorded for a positive, linear sweep of potential. Data obtained in this manner are shown for sorbitol and dextrose in Figure V-4. Note that the direction of the potential axes have been reversed in the figure to be consistent with the time axes of the I-t curves. Clearly, oxidation of both sorbitol and dextrose occurs for injections at E = -0.80 V. The I-E curves obtained 45 s after injection, when all the carbohydrate had been washed from the detector cell, clearly show anodic peaks in the hydrogen and double-layer regions

Figure V-4. Current-time and I-E curves for the platinum-disc flow-through electrode following injections of sorbitol and dextrose

V_s = 100 µL
v_f = 0.375 ml min^{-1}
C^b = 2.5 mM

I-t curves

A: -0.94 V
B: -0.80 V

I-E curves

ϕ = 3.0 V min^{-1}
(---) Residual in absence of carbohydrate
E during injections

A: -0.94 V
B: -0.80 V

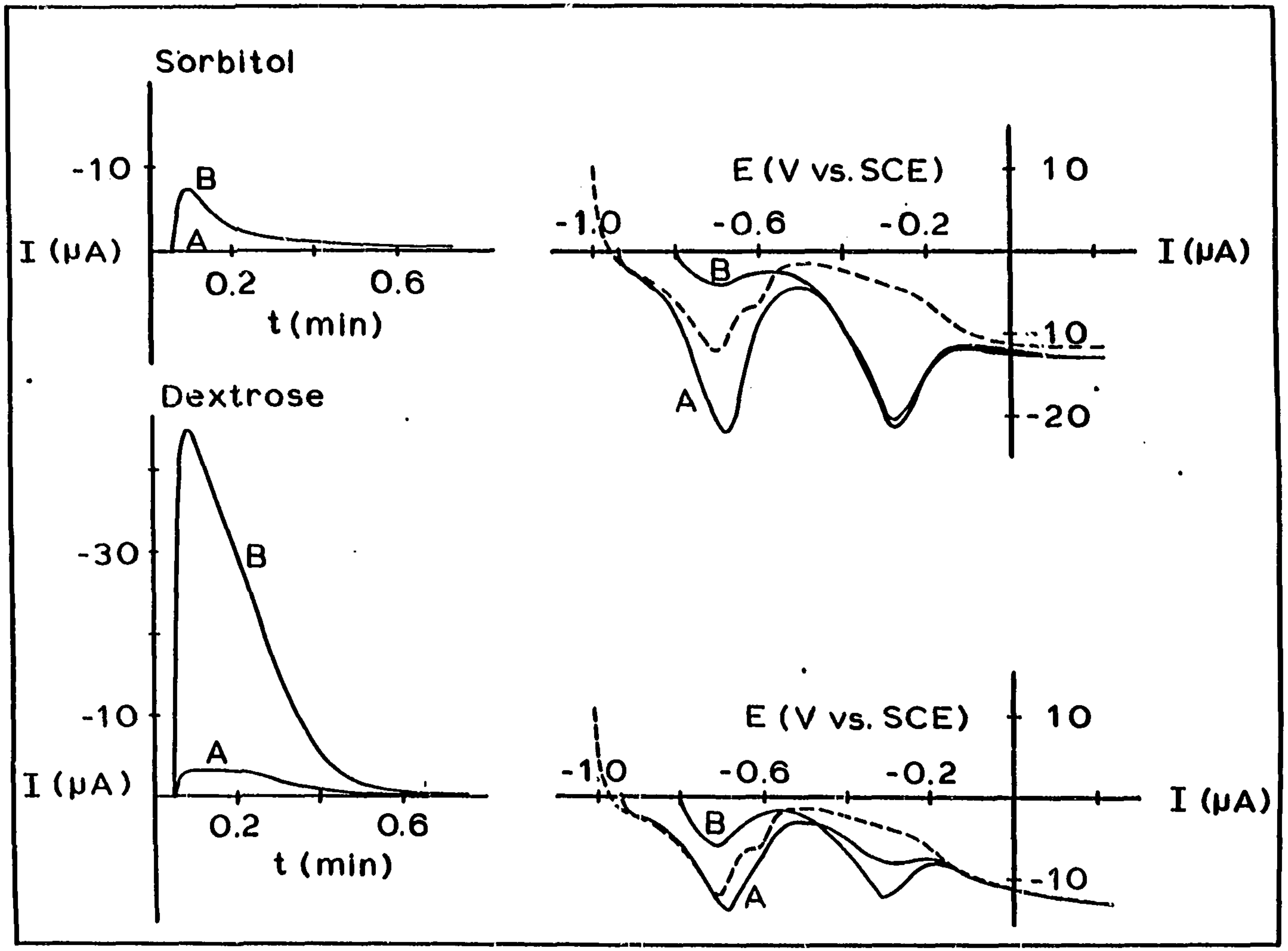
Sorbitol
-10
B
A
I (μA)
0.2
0.6
t (min)
E (V vs. SCE)
10
-1.0
-0.6
-0.2
I (μA)
B
-10
A
-20
Dextrose
-30
B
-10
A
I (μA)
0.2
0.6
t (min)
E (V vs. SCE)
10
-1.0
-0.6
-0.2
I (μA)
B
A
-10

for both sorbitol and dextrose. These peaks can originate only from the adsorbed carbohydrates. When a period greater than 45 s was allowed to transpire before recording the I-E curves, the anodic peaks in the double-layer region were smaller than for 45 s, undoubtedly because of the slow desorption of the reaction products of the oxidation in the hydrogen region.

D. Effect of Rotational Velocity

For an increase in rotational velocity (ω) of the platinum-RDE, the anodic peak for dextrose in the hydrogen region of the I-E curves obtained by cyclic voltammetry increased whereas the peak in the double-layer region decreased. The anodic peak for sorbitol in the double-layer region also decreased with increases of ω. The values of peak currents are plotted in Figure V-5 as a function of $\omega^{\frac{1}{2}}$ for typical conditions of concentration. Linearity of plots of faradaic signal vs. $\omega^{\frac{1}{2}}$ are traditionally regarded as diagnostic evidence of mass-transport control in the reaction mechanism at an RDE (71). Although the best linear fits of data are shown in Figure V-5, it is apparent that the data would conform better to a curvilinear model. A negative dependence of the anodic peak for dextrose in the

Figure V-5. Effect of rotational velocity on anodic peaks from cyclic voltammetry at the platinum RDE

ϕ = 3.0 V min^{-1}

(●) Peak in hydrogen region for 0.40 mM dextrose

(○) Peak in double-layer region for 0.40 mM dextrose

(■) Peak in double-layer region for 4.94 mM sorbitol

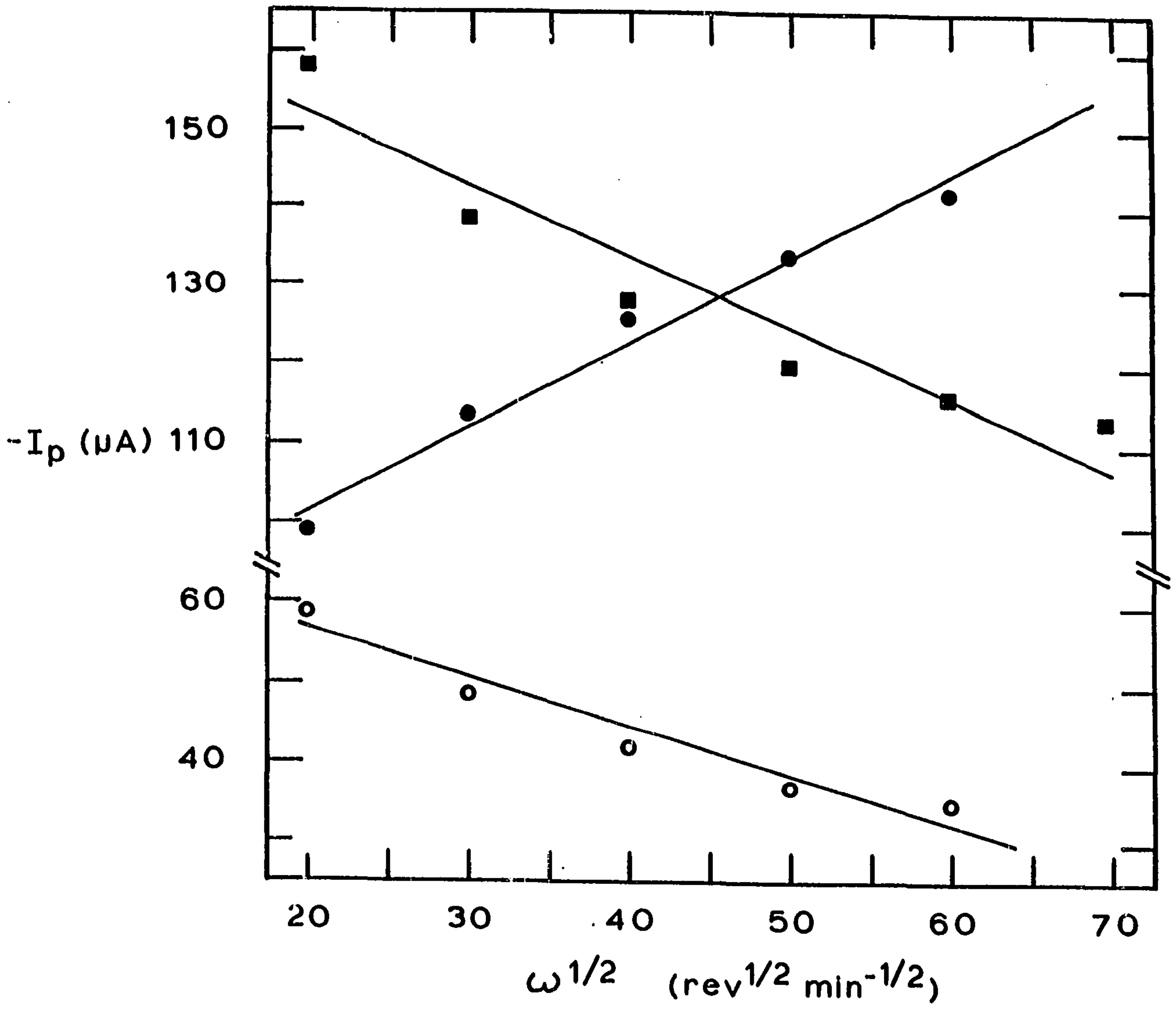
150
130
-Ip (μA) 110
60
40
20
30
40
50
60
70
ω 1/2 (rev1/2 min-1/2)

double-layer region for 1 M H_2SO_4 has been reported by Skou (17). This was explained by a mechanism involving desorption and diffusional loss of the enediol-form of dextrose reportedly produced on the electrode surface prior to oxidation. Alternately, similar results would be expected for a mechanism in which intermediate products of a multi-electron oxidation involving sequential charge-transfer steps are lost from the electrode surface by desorption and convective-diffusional mass transport.

The positive dependence of the anodic peak for dextrose in the hydrogen region is expected if the product of that oxidation is lost by desorption and mass transport to regenerate active surface sites. It is concluded then that for carbohydrates the anodic process in the double-layer region corresponds to sequential oxidation steps for the adsorbed product of the primary oxidation occurring in the hydrogen region. A simplified sequence is proposed below which accounts qualitatively for the anodic response of the carbohydrates.

$S + R \rightleftarrows S\text{-}\underline{R}$	(adsorption)	V-1
$S\text{-}\underline{R} \rightarrow S\text{-}\underline{R}' + ne$	(primary anodic reaction in hydrogen region)	V-2
$S\text{-}\underline{R}' \rightarrow S + R'$	(slow desorption to regenerate active surface site)	V-3
$S\text{-}\underline{R}' \rightarrow S\text{-}\underline{R}'' + n'e$ $\hookrightarrow S + R''$	(secondary anodic reactions and desorption in the double-layer region)	V-4

In the mechanism above: S represents an active surface site, R is the reactant dissolved in the bulk solution of supporting electrolyte, R'-R'' represent successively higher oxidation states of R, and the underline denotes that the indicated species is in the adsorbed state. The anodic signal in the hydrogen region is enhanced for an increased rate of desorption by Eq. V-3. Since the anodic current in the double-layer region results from oxidation of adsorbed species by Eq. V-4, the signal is decreased if desorption of R' and R'' is increased.

E. Triple Pulse Voltammetry at the RDE

The selection of the appropriate potential values for the triple pulse waveform was made on the basis of triple pulse voltammetry at the platinum-RDE wherein a linear potential sweep (E_s, 0.3 V min^{-1}) was substituted for a constant value of E1. The potential E1 = E_s was applied for a total time of 125 ms with the measurement of current (1 ms) executed after 100 ms. The potential value and duration of E2 was 0.70 V for 500 ms. The optimum value for the reduction potential (E3) was determined by recording triple pulse voltammograms in a solution containing 1.0 mM sorbitol and observing the maximum current obtained in the double-layer potential region for different values of E3 (250 ms). A plot of $-I_p$ vs. E3 is shown in Figure V-6. It is evident from this plot that maximum sensitivity is obtained for E3 = -1.0 V, the negative limit for the solution. This is concluded to be due to the increased extent of adsorption of carbohydrate on an electrode which contains adsorbed hydrogen.

Having determined the optimum potential for E3 (i.e., -1.0 V), the optimum value for E1 was determined, again by triple pulse voltammetry. Representative curves obtained by this method are shown in Figures V-7 and V-8 for dextrose and sorbitol, respectively. Curves are also shown which were obtained for the supporting electrolyte alone. A substantial increase of the anodic peaks in the hydrogen region was obtained with addition of sorbitol and dextrose. The enhanced peaks have the identical shape and position as the peaks observed in the absence of the organic compounds and the conclusion is reaffirmed that the enhanced signal is from adsorbed H-atoms produced by surface-catalyzed dehydrogenation of the carbohydrates.

Anodic peaks were also obtained for both sorbitol and dextrose in the double-layer region with peak potentials of -0.30 V for sorbitol and -0.38 V for dextrose. The background current for these faradaic peaks was minimal. The

Figure V-6. Plot of $-I_p$ vs. E3 for sorbitol at a platinum RDE by triple pulse voltammetry

ω = 41.9 rad s^{-1}
ϕ = 0.30 V min^{-1}
1.0 mM sorbitol in 0.10 M NaOH

$-I_p$ taken at E_s = -0.30 V (125 ms)
E2 = 0.70 V (500 ms)
E3 = (250 ms)

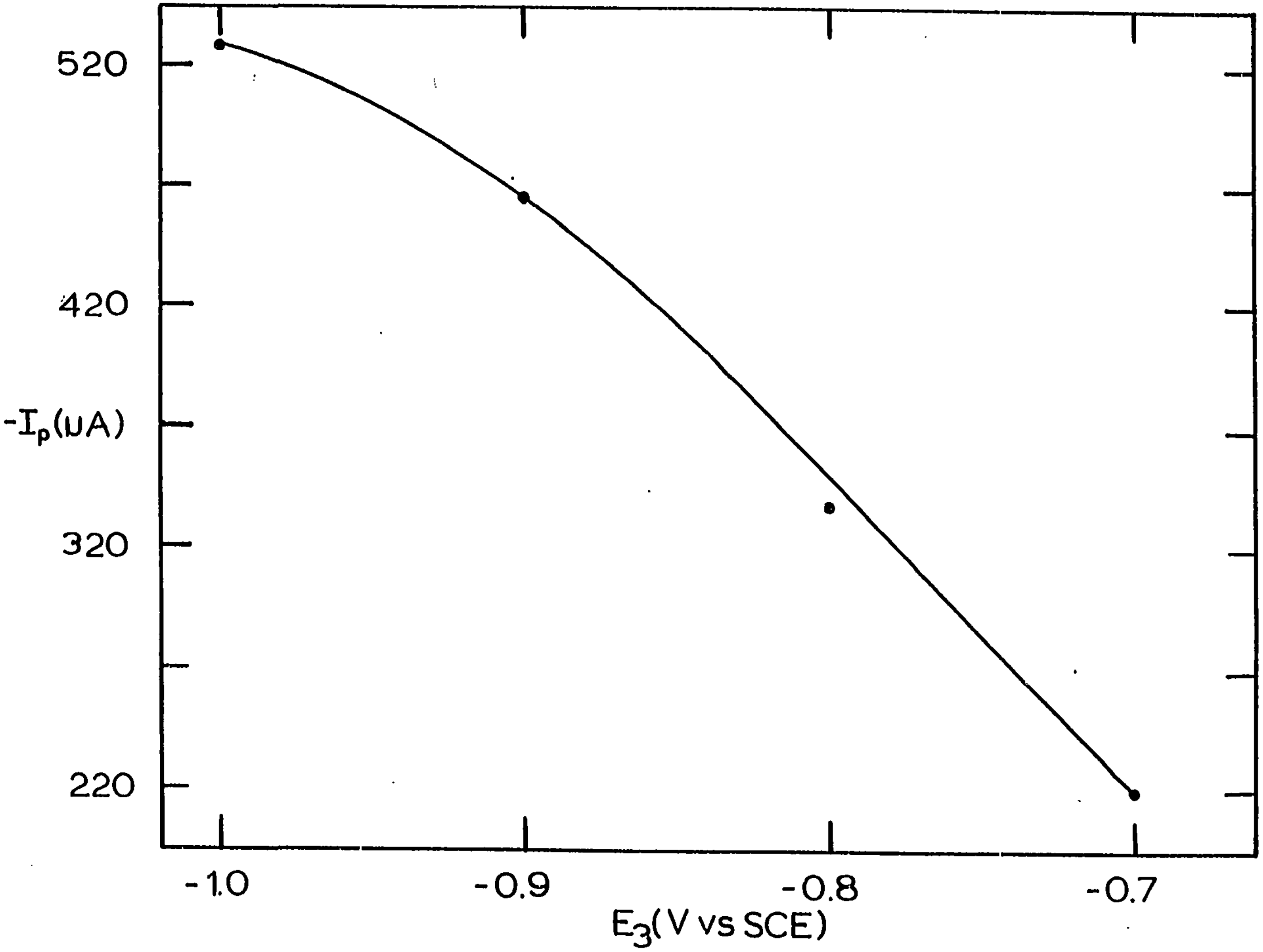
520
420
-I_p(μA)
320
220
-1.0
-0.9
-0.8
-0.7
E3(V vs SCE)

Figure V-7. Current-voltage curves for dextrose at a platinum RDE by cyclic voltammetry and triple pulse voltammetry

ω = 41.9 rad s^{-1}

(——) Cyclic voltammetry

ϕ = 3.0 V min^{-1}

A: Residual curve for 0.10 M NaOH
B: 0.50 mM dextrose

(•••) Triple pulse voltammetry

ϕ = 0.30 V min^{-1}
E1 = E_s (125 ms)
E2 = 0.70 V (500 ms)
E3 = -1.0 V (250 ms)

A: Residual curve for 0.10 M NaOH
B: 2.5 mM dextrose

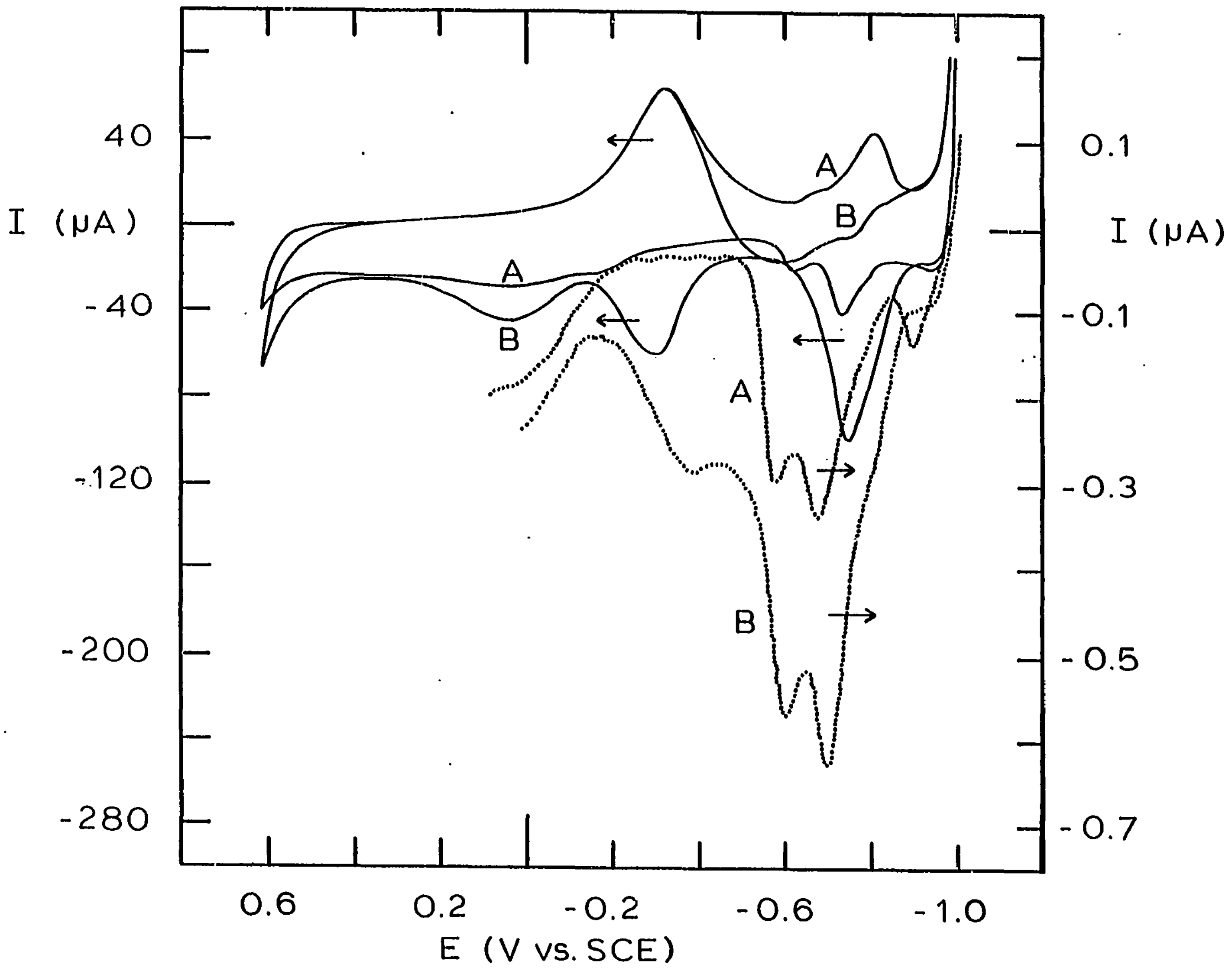
40
-40
-120
-200
-280
I (μA)
0.1
-0.1
-0.3
-0.5
-0.7
I (μA)
A
B
A
B
A
B
0.6
0.2
-0.2
-0.6
-1.0
E (V vs. SCE)

Figure V-8. Current-voltage curves for sorbitol at a platinum RDE by cyclic voltammetry and triple pulse voltammetry

Conditions identical to Figure V-7 except that sorbitol was substituted for dextrose.

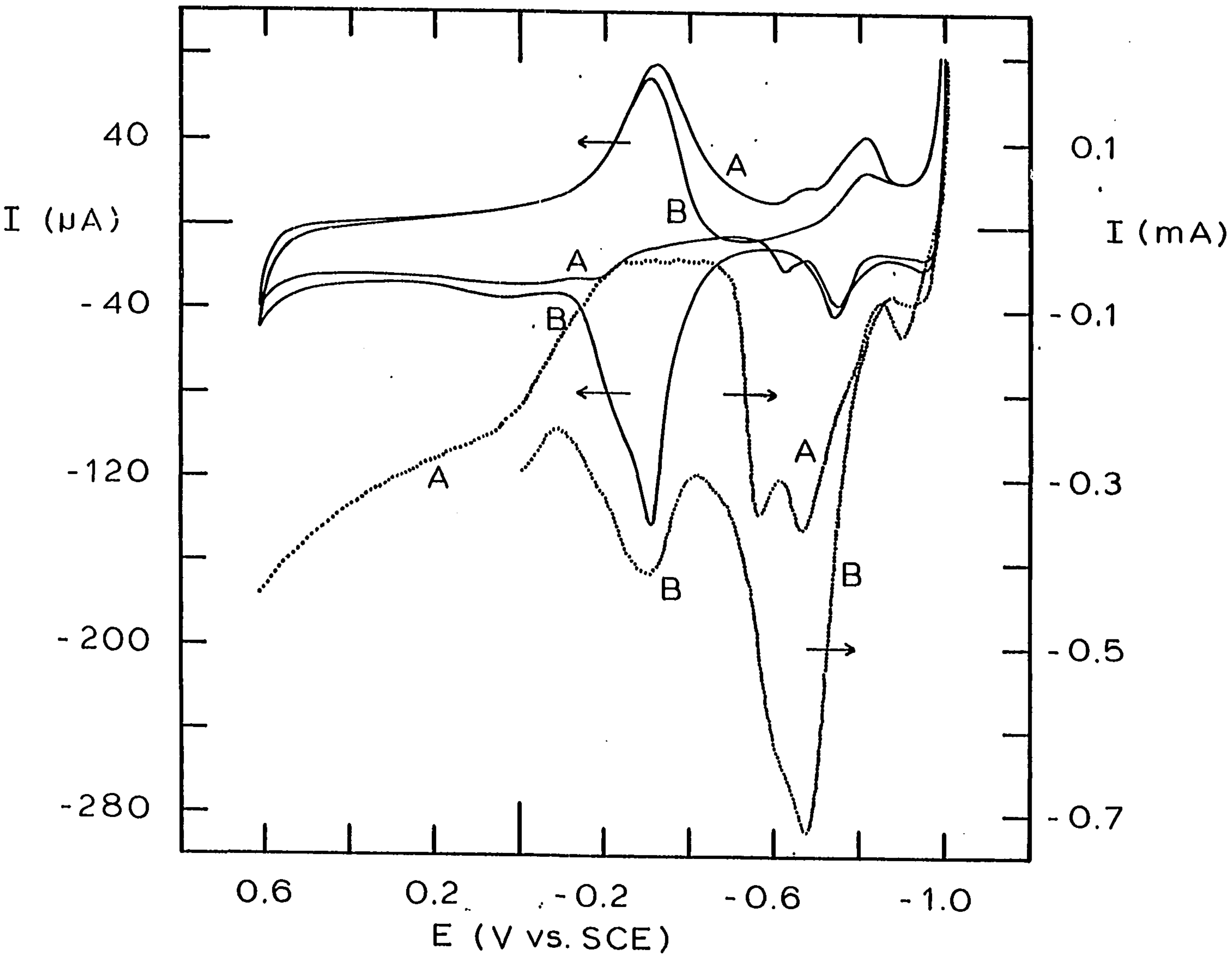

I (µA)
40
-40
-120
-200
-280
I (mA)
0.1
-0.1
-0.3
-0.5
-0.7
0.6
0.2
-0.2
-0.6
-1.0
E (V vs. SCE)
A
B
A
B
A
B
A
B

electrochemical behavior of all sugar alcohols tested was similar to that of sorbitol and the behavior of the aldoses and ketose tested was similar to that of dextrose. An optimum value of E1 for the detection of aldoses in 0.1 M NaOH was concluded to be -0.40 V and the value for the alcohols and ketoses was concluded to be -0.30 V. The value of -0.40 V was chosen as the best single potential applicable for both classes of compounds. At that potential, little change in the analytical signal was observed for small changes of potential and, furthermore, the background was minimal.

F. Summary

The anodic response of ten simple carbohydrates was investigated. Prior adsorption of the analyte on the platinum electrode is a necessary condition for oxidation. The adsorption of carbohydrate is enhanced by the presence of hydrogen adsorbed on the electrode in the potential range -0.6 to -1.0 V for 0.10 M NaOH. The oxidation process is believed to occur in sequential steps with the primary oxidation step occurring at potentials in the hydrogen region. Conditions for TPA were optimized for the detection of dextrose and sorbitol in 0.10 M NaOH.

VI. FLOW-INJECTION DETECTION

The triple pulse amperometric technique at the platinum-disc flow-through detector was evaluated for application to flow-injection detection. Sample plugs were introduced into a flowing stream of 0.10 M NaOH and the peak current (I_p) was measured. The precision of the technique as well as the dependence of I_p on the analyte concentration of the sample (C^b) was investigated. The value of I_p for injection of a small volume of analyte of concentration C^b in a flow-injection system is less than that which would be observed for continual flow of a solution containing the analyte at a concentration of C^b. The peak concentration in the flow stream (C_p) is less than the analyte concentration in the injected sample because of dispersion within the stream. However, since dispersion is constant in a well-managed flow system, C_p/C^b is constant for a given compound (71), and the dependence of I_p on C_p is expected to be identical to the I_p vs. C^b dependence reported previously for the RDE (Sec. IV,V).

A. Flow Injection-Detection of Alcohols

TPA detection of alcohols was evaluated with the flow system described in Sec. III-E. The flow rate of 0.10 M

H_2SO_4 was adjusted to 0.5 ml min^{-1}. The alcohol solutions were prepared in oxygen-free 0.10 M H_2SO_4. The conditions for the triple pulse waveform were the same as described in Sec. IV-E. The successful maintenance of electrode activity by application of the triple pulse waveform is illustrated in Figure VI-1 for flow-injection detection of ethanol. Peaks for twelve successive injections of 220 µL each containing 52 µg ethanol are shown. The relative standard deviation in I_p is 0.80%. Similar studies for methanol and formic acid yielded comparable results. Detection at a constant (d.c.) applied potential, also shown in Figure VI-1, is useless with no response observed after the second injection.

Calibration studies were made for ethanol by the flow-injection method. Concentrations were in the range 0.17 - 2.4 mM (0.78 - 11 µg per 100 µL sample) and the results are plotted in Figure VI-2. The plot of $-1/I_p$ vs. $1/C^b$ is linear with slope = 0.0866 ± 0.0018, intercept = 0.023 ± 0.004 and r^2 = 0.9989. The uncertainties in slope and intercept represent the 90% confidence intervals.

B. Flow-Injection Detection of Carbohydrates

TPA detection of carbohydrates was investigated in a flow stream of 0.10 M NaOH with a flow rate (V_f) of 0.375

Figure VI-1. Comparison of detection peaks for ethanol in flow-injection detection with d.c. and triple pulse amperometric detection

V_s = 250 µL

V_f = 0.50 ml min^{-1}

5.2 mM ethanol

D.c. detection

E = 0.26 V

Triple pulse amperometric detection

E1 = 0.26 V (0.50 s)
E2 = 1.25 V (1.18 s)
E3 = 0.00 V (0.85 s)

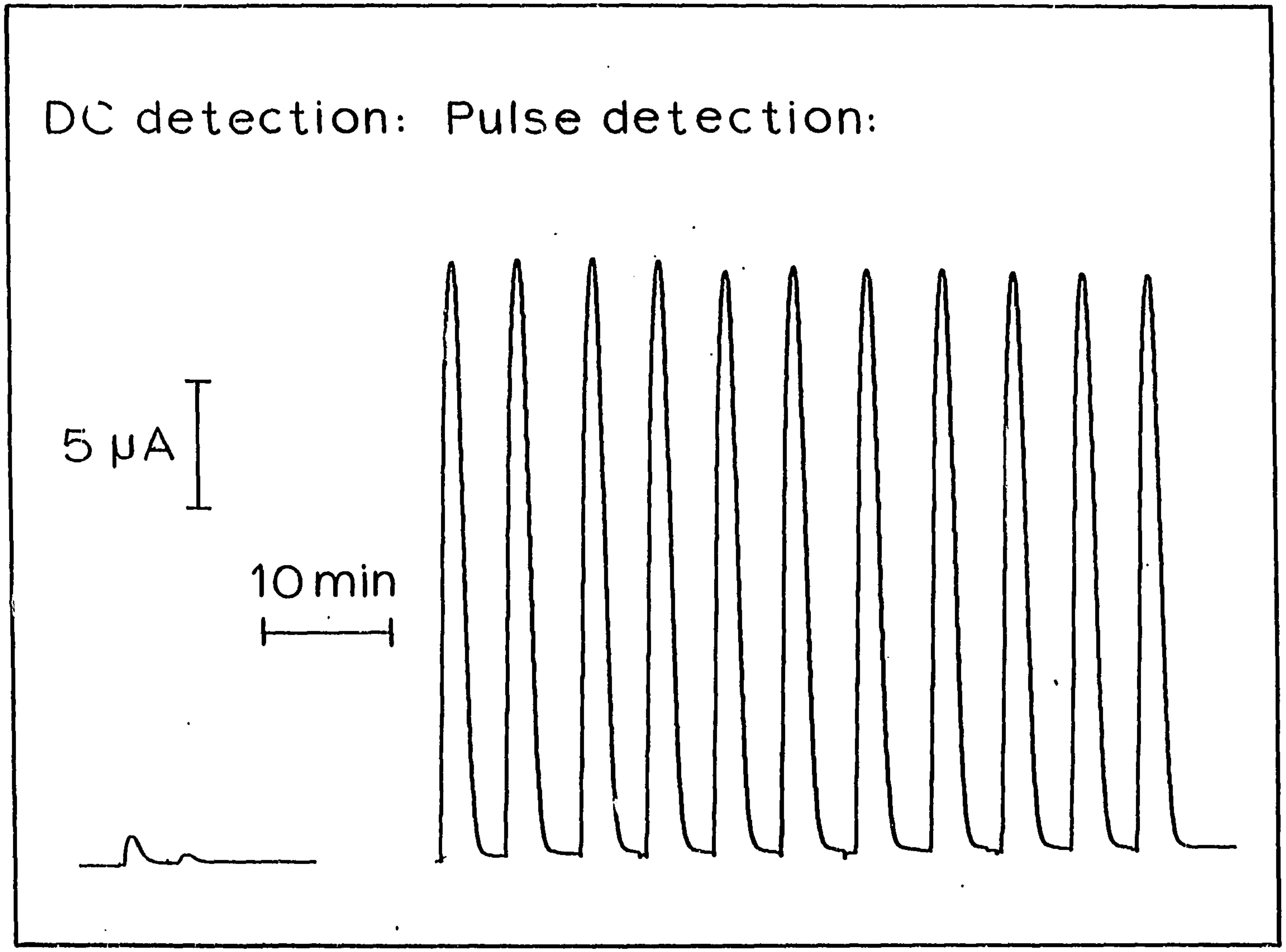
DC detection:
Pulse detection:
5 μA
10 min

Figure VI-2, Calibration curves for ethanol by flow-injection with triple pulse amperometric detection

V_s = 100 μL
V_f = 0,375 ml min^{-1}

E1 = 0.26 V (0,2 s)
E2 = 1.25 V (0.7 s)
E3 = 0,00 V (0.4 s)

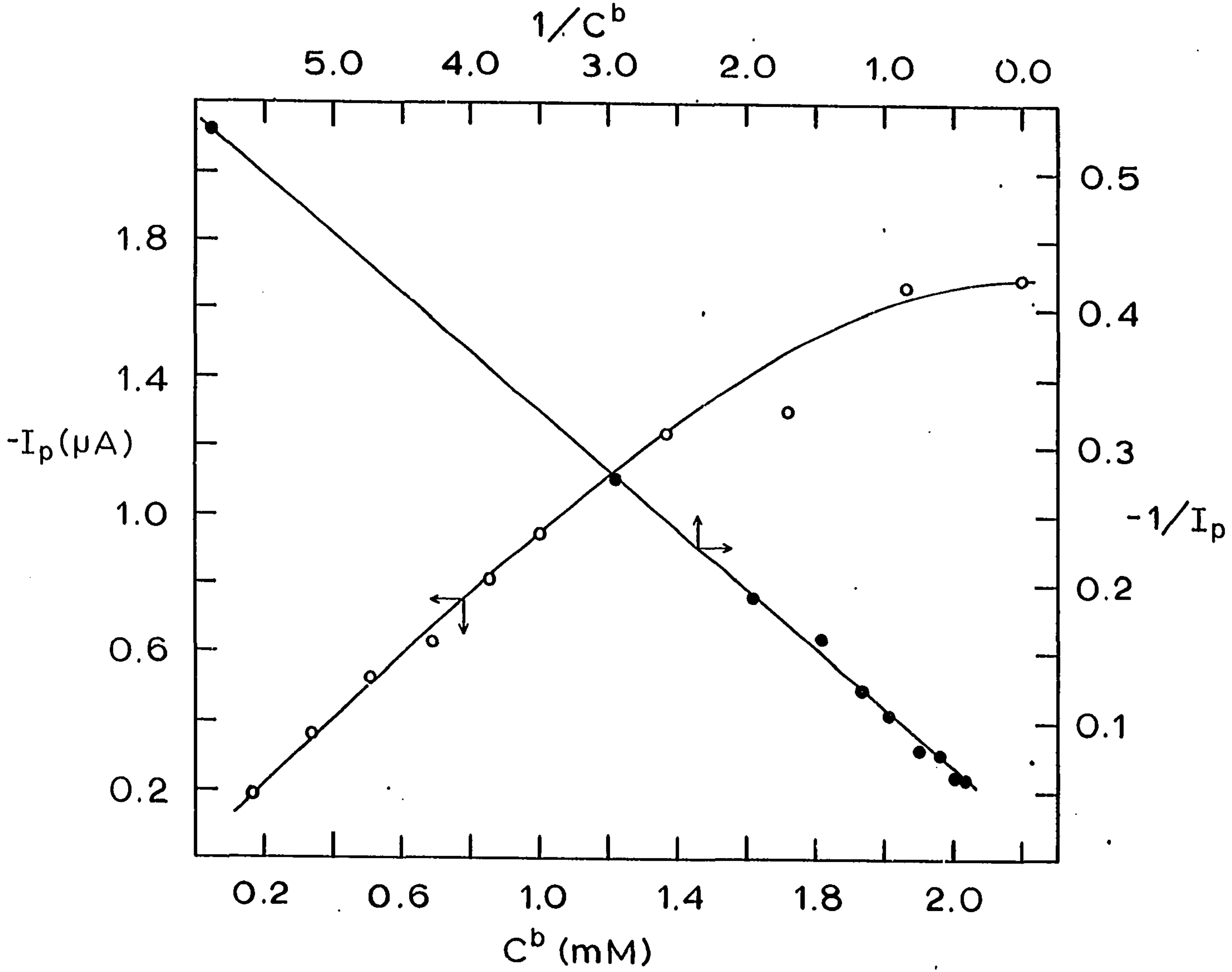
1/C^b
5.0
4.0
3.0
2.0
1.0
0.0
1.8
1.4
1.0
0.6
0.2
-I_p(μA)
0.5
0.4
0.3
0.2
0.1
-1/I_p
0.2
0.6
1.0
1.4
1.8
2.0
C^b (mM)

ml min^{-1}. All solutions of carbohydrates were prepared in oxygen-free 0.10 M NaOH just prior to use to minimize decomposition under the alkaline conditions. The response for dextrose was observed to be a function of the time periods for application of each of the three potentials in the triple pulse waveform. The faradaic response of dextrose for E1 = -0.40 V was observed to increase in a nearly linear fashion, when the time at E3 = -1.0 V was increased from 100 to 223 ms. This probably happens because increased time at the cathodic potential results in the accumulation of a greater quantity of adsorbed compound. Beyond 223 ms, however, the faradaic signal decreased, probably because electrode fouling was appreciable resulting from the more extensive dehydrogenation at E1. The value of E2 was increased to 0.80 V and the time of oxidative cleaning was decreased to 185 ms, from the values used in Sec. V. These values of potential and time were sufficient for complete cleaning of the electrode surface as indicated by the reproducibility of the faradaic signals at E1. The value of E1 was set at -0.40 V, as discussed in Sec. V, for a total time of 155 ms. Current measurement was achieved in a period of 1 ms initiated 118 ms after application of E1. The total cycle time for this waveform was 563 ms.

Calibration studies were conducted for dextrose and sorbitol by the flow-injection method. Concentrations were in the range 0.10 - 1.00 mM (1.8 - 18 µg per 100 µL for dextrose). Three injections were made for each concentration. The peaks obtained for dextrose are shown in Figure VI-3, and values of peak current are plotted in Figure VI-4. As expected for detection of an adsorbed analyte (Sec. IV-B), plots of $-1/I_p$ vs. $1/C^b$ were linear for both dextrose and sorbitol. Least-squares statistics describing the plots are given in Table VI-1. In comparison, peaks recorded (not shown) for a constant applied potential were negligibly small after two injections and were useless for detection

Table VI-1. Least-squares statistics for plots of $-1/I_p$ vs. $1/C^b$[a]

Parameter	Dextrose	Sorbitol
slope (mM μA^{-1})	$(5.9 \pm 0.2) \times 10^{-3}$	$(4.4 \pm 0.1) \times 10^{-3}$
intercept (μA^{-1})	$(11.0 \pm 0.9) \times 10^{-3}$	$(14.5 \pm 0.2) \times 10^{-3}$
r^2	0.9963	0.9995

[a] Data obtained by flow injection for three runs on each of ten concentrations between 0.1 and 1.0 mM. Conditions identical to Figure VI-3. Uncertainties represent the 90% confidence limits.

Figure VI-3. Peaks obtained with the flow-injection system for dextrose in 0,10 M NaOH

V_s = 100 µL
V_f = 0,375 ml min^{-1}
Concentration given below peaks as mM

E1 = -0,40 V (155 ms)
E2 = +0,80 V (185 ms)
E3 = -1,00 V (223 ms)

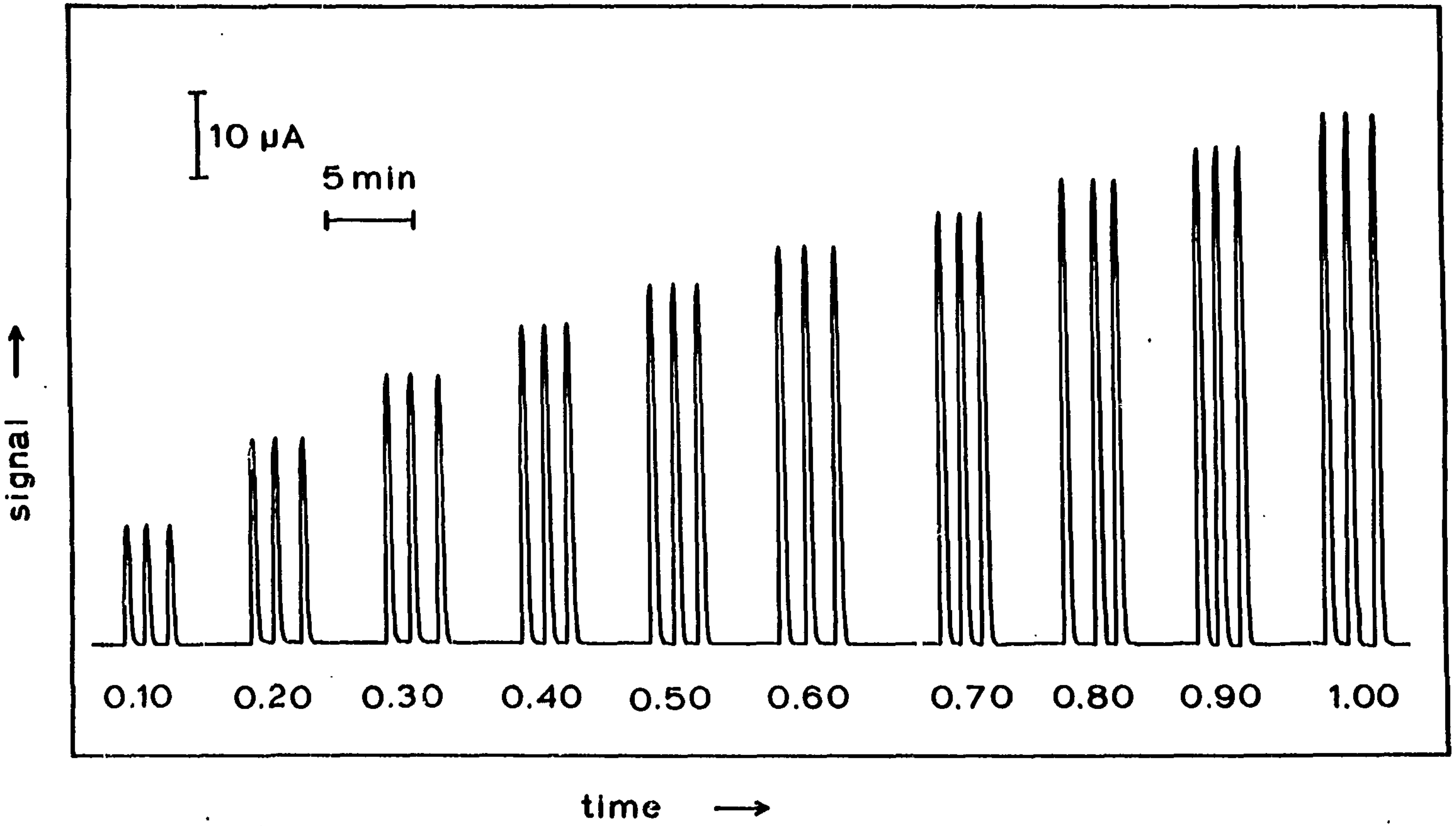
10 µA
5 min
signal
0.10
0.20
0.30
0.40
0.50
0.60
0.70
0.80
0.90
1.00
time

Figure VI-4. Calibration curves for dextrose by flow-injection with triple pulse amperometric detection

Conditions identical to Figure VI-3.

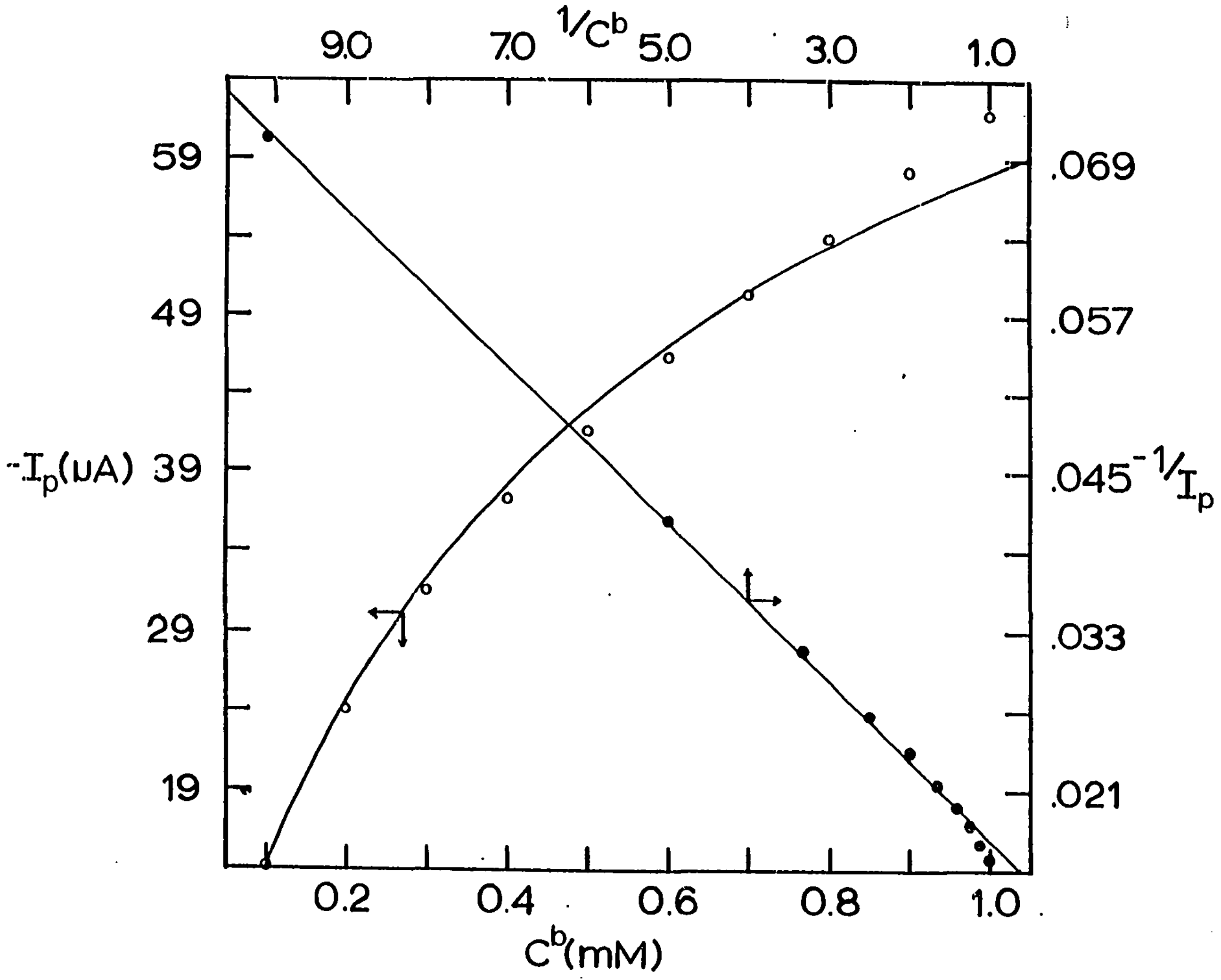
1/C^b
9.0
7.0
5.0
3.0
1.0
-I_p(μA)
59
49
39
29
19
.069
.057
.045
.033
.021
-1/I_p
0.2
0.4
0.6
0.8
1.0
C^b(mM)

of carbohydrates as had been the case for detection of simple alcohols at constant E.

The sensitivities of the responses for the ten carbohydrates examined in Sec. V were compared. Injection of 100 µL aliquots of 0.50 mM solutions for each compound were made and the resulting peak currents measured. The results are summarized in Table VI-2.

Table VI-2. Comparison of peak currents for compounds tested by flow-injection detection

Compound	$-I_p(\mu A)$[a]
dextrose	39.1
galactose	33.6
mannose	29.4
rhamnose	18.3
arabinose	34.4
xylose	33.8
fructose	16.9
perseitol	38.0
mannitol	39.2
sorbitol	41.7

[a] Sample: 100 µL of 0.5 mM carbohydrate in 0.1 M NaOH injected into a stream of 0.1 M NaOH. Conditions given in Figure VI-3.

C. Summary

The applicability of TPA detection of alcohols and carbohydrates injected in a flow stream was demonstrated. The precision for replicate injections was excellent with relative standard deviations of I_p less than 1%. Plots of $-1/I_p$ vs. $1/C^b$ were linear for the range of concentrations tested.

VII. HIGH PERFORMANCE LIQUID CHROMATOGRAPHY

Without the benefit of prior separation the triple pulse amperometric technique has virtually no applicability for the selective determination of a specific carbohydrate. in a mixture. The eventual utilization of TPA was viewed strictly in terms of detection in liquid chromatography. The major difficulty to be overcome was the compatibility of the eluent composition, selected to optimize the separation and ensure stability of the chromatographic column, with the 0.10 M NaOH electrolyte required for TPA detection.

Eluents which contain acetonitrile, commonly used with chemically modified silica columns, are totally incompatible with TPA detection. Acetonitrile molecules are strongly adsorbed on platinum electrodes thereby severely limiting the surface activity (72) and, hence, the ability to anodically detect organic compounds.

Pure water is used as the mobile phase for cation-exchange columns in separation of carbohydrates with the column temperature in the range of 80° to 90° C. Whereas the resins are stable for eluents up to pH 13, eluents having high alkalinity are not useful for the separation of carbohydrates. Dextrose in dilute base at 25° C is not stable forming an equilibrium mixture of dextrose, fructose and mannose. At high temperatures, further rearrangement and fragmentation can occur (1). In addition, it was found that with an eluent of high pH the carbohydrates were irreversibly retained by the column.

Water was chosen as the eluent for separation of carbohydrates in the cation-exchange column and a solution of NaOH was mixed into the effluent stream prior to entrance into the detector. To minimize band broadening, the stream of NaOH (6.1 M) was pumped at a low flow rate (0.01 ml min^{-1}) with respect to the flow rate of the effluent stream from the chromatographic column (0.5 ml min^{-1}). This resulted in an electrolyte concentration of approximately 0.1 M NaOH at the detector.

Steady pumping of the NaOH stream at the low rate of flow proved to be difficult. The peristaltic pump used for this purpose caused the electrolyte concentration in the detector to fluctuate at the frequency of the pump drive producing an oscillatory baseline. The data presented later in Figures VII-8 and VII-10 contain examples of these fluctuations. With development of the computerized data acquisition system (Sec. III-D-3), the fluctuations in the baseline were minimized by performing a moving average of the detector current. An average which contained 30 points collected at 1 s intervals was found to smooth the baseline while having minimal effects on the magnitude of peak currents and retention times. This method of data smoothing was used for all of the chromatograms presented in this section with the exceptions of Figures VII-8 and VII-10.

The conditions of the TPA waveform used for the HPLC studies are given in Figure VII-1. The chromatographic column was maintained at 85° C and the detector temperature was controlled at 60° C, except for the experiments in which the effect of temperature was studied. It was discovered that there was no detector response for oxygen in air-saturated blank samples injected into the chromatographic system. Hence, samples were injected without the removal of dissolved oxygen.

A. Synthetic Samples

1. Precision

The precision of the TPA technique for HPLC was investigated, using the Hamilton column. Ten injections of a solution containing 0.40 mg ml^{-1} dextrose were made at 3 min intervals. The resulting peaks are shown in Figure VII-2. The average peak height was 10.03 μA with a relative stan-

Figure VII-1. Triple pulse potential waveform used for all HPLC studies

E1 = -0.40 V (182 ms)
E2 = +0.80 V (185 ms)
E3 = -1.00 V (223 ms)

173 ms delay after application of E1, before measurement (1 ms) of the faradaic current.

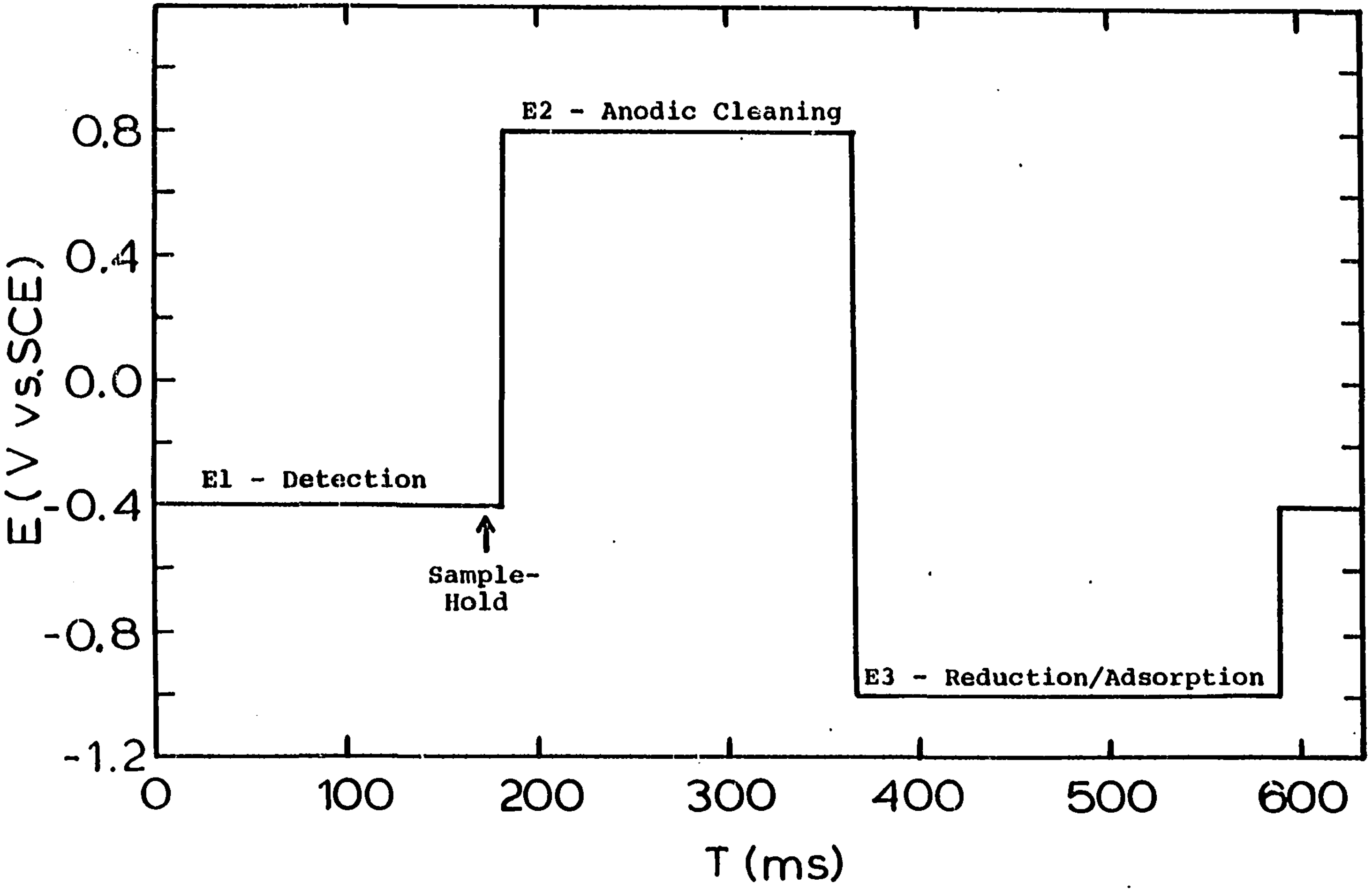
E2 - Anodic Cleaning
E1 - Detection
Sample-Hold
E3 - Reduction/Adsorption
E (V vs.SCE)
0.8
0.4
0.0
-0.4
-0.8
-1.2
0
100
200
300
400
500
600
T (ms)

Figure VII-2. Peaks obtained with the HPLC system for ten injections of 0.40 mg ml^{-1} dextrose

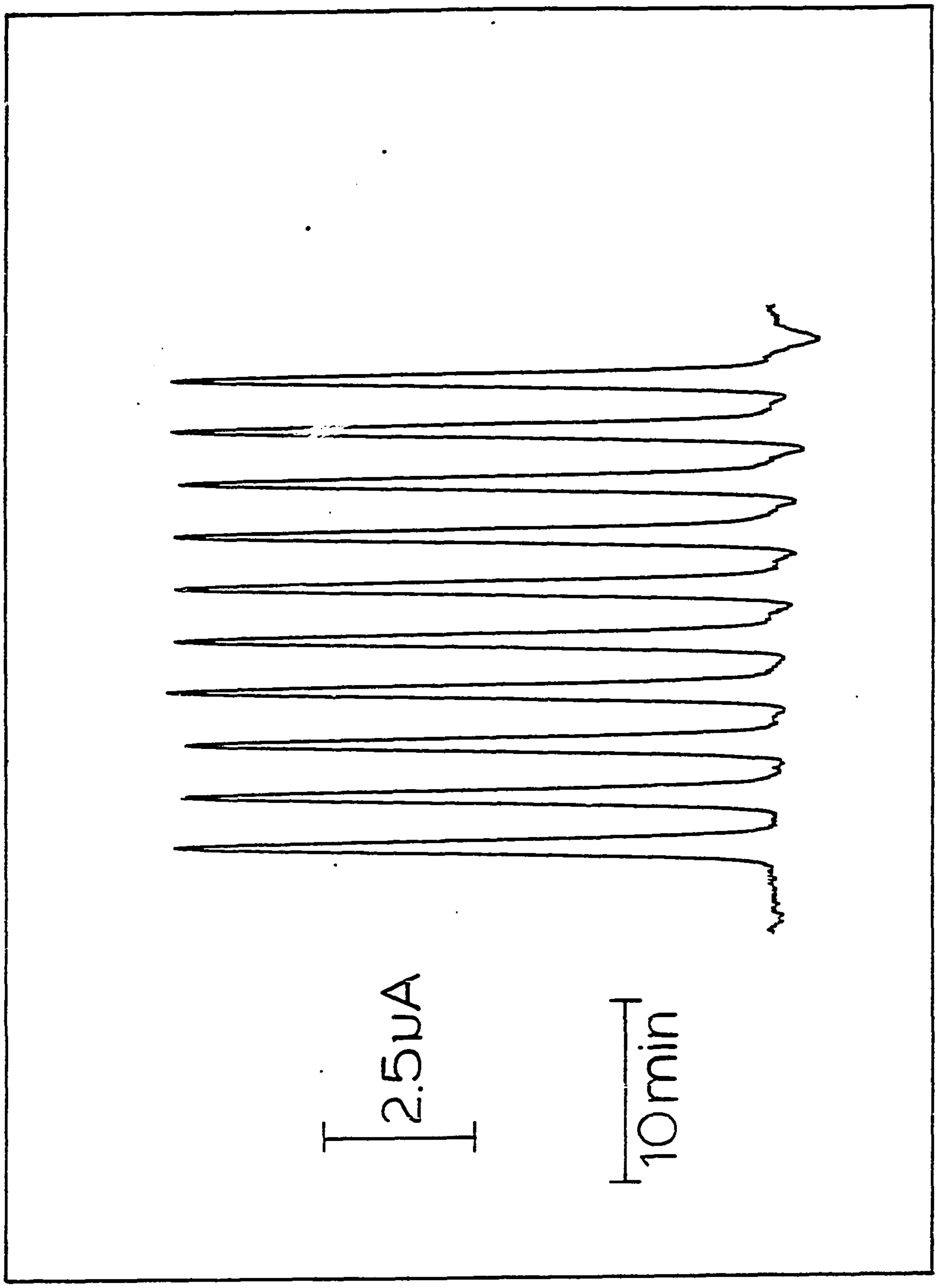
2.5uA
10min

dard deviation of 0,87%.

2. Resolution

The resolution of the Hamilton and Dionex columns was compared. A synthetic sample containing 0.40 mg ml^{-1} each of eight carbohydrates was injected onto each column. The retention times (t_r), number of theoretical plates (n) and height equivalent theoretical plates (h) are listed for each compound in Table VII-1. The chromatograms are shown in Figure VII-3. Even though the Dionex column is 5 cm shorter than the Hamilton column, it exhibited much better resolution. The smaller size of the resin particles in the Dionex column undoubtedly is a factor contributing to the higher resolution. The significance of this comparison of the two columns must be viewed in light of the fact that the Dionex column was new and the Hamilton column had been used for approximately one year prior to this study. Data were not available which represented the resolving power of the Hamilton column when first obtained.

3. Calibration

Calibration curves were produced by injection of samples containing various concentrations of a mixture of carbohydrate standards. The time required to collect data for the calibration depends on the retention times of the com-

Table VII-1. Comparison of performance of Hamilton[a] and Dionex[b] HPLC columns

Carbohydrate[c]	Hamilton			Dionex		
	t_r(min:s)	n[d]	h[e]	t_r	n	h
Maltotriose	10:52	1600	1,88	10:06	1000	2,50
Sucrose	11:42	1100	2,73	10;56	600	4,17
Dextrose	13;42	1000	3.00	13:08	1400	1,79
Xylose	14;47	1100	2,73	14:24	1900	1,32
Fructose	16:12	1400	2,14	16:11	2100	1.19
Glycerol	18:58	1400	2,14	19;50	3200	0,78
Arabitol	20:23	1200	2.50	21;35	3100	0,81
Sorbitol	23:37	1600	1.88	25;33	3900	0,64

---

[a] Hamilton column: 10-15 μm particle size, 7½% cross-linking, 30 cm long.

[b] Dionex column: 7½ μm particle size, 7% cross-linking, 25 cm long.

[c] 0.40 mg ml^{-1}.

[d] $n = 16(t_r/W)^2$; where W = peak width.

[e] $h = L/n$; where L = column length (mm).

Figure VII-3. Comparison of separation of eight carbohydrates by Hamilton and Dionex HPLC columns

I. Hamilton column
II. Dionex column

m	maltotriose
s	sucrose
d	dextrose
x	xylose
f	fructose
g	glycerol
a	arabitol
s'	sorbitol

All carbohydrates have concentrations of 0.40 mg ml^{-1}

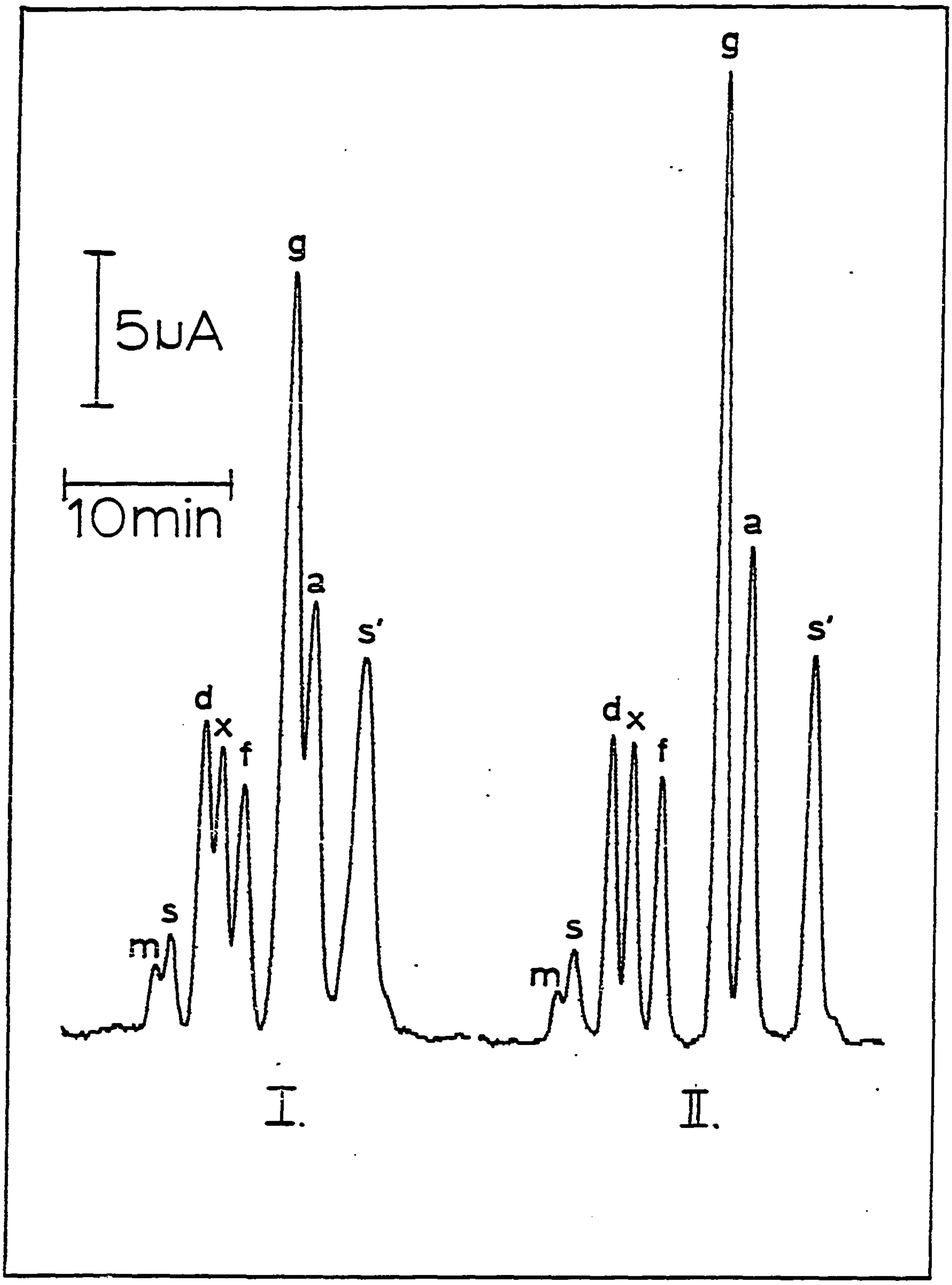
5uA
10min
g
a
s'
d
x
f
s
m
I.
g
a
s'
d
x
f
s
m
II.

ponents for which the system is being calibrated. As an extreme, calibration for all eight carbohydrates listed in Table VII-1, using five concentrations in the series, would require approximately 2.5 hr. If the system is to be calibrated for only one carbohydrate, the standards can be injected at approximately 3-min intervals, requiring a calibration time of 15 min plus the retention time of the carbohydrate. Figure VII-4 shows the peaks for a calibration of glycerol which required only 35 min. As expected, plots of $-1/I_p$ vs. $1/C^b$ were linear. Calibration was performed daily to compensate for small variations in the system. The predominant sources of variation were the increased surface area of the electrode due to platinization resulting from repeated application of the potential waveform (22), wear of the tubing in the head of the peristallic pump which caused variation of the NaOH flow rate, and altered physical conditions of the chromatographic column causing changes in dispersion of the analyte in the effluent stream.

Some analysts make use of one-point internal standardization in chromatographic analysis for the determination of analyte concentrations in a sample. This practice is reliable only when the response factor (F), defined as

Figure VII-4. Peaks from calibration of the HPLC system for glycerol

Peaks

1. 0.20 mg ml^{-1}
2. 0.50 mg ml^{-1}
3. 0.80 mg ml^{-1}
4. 1.00 mg ml^{-1}
5. 1.50 mg ml^{-1}

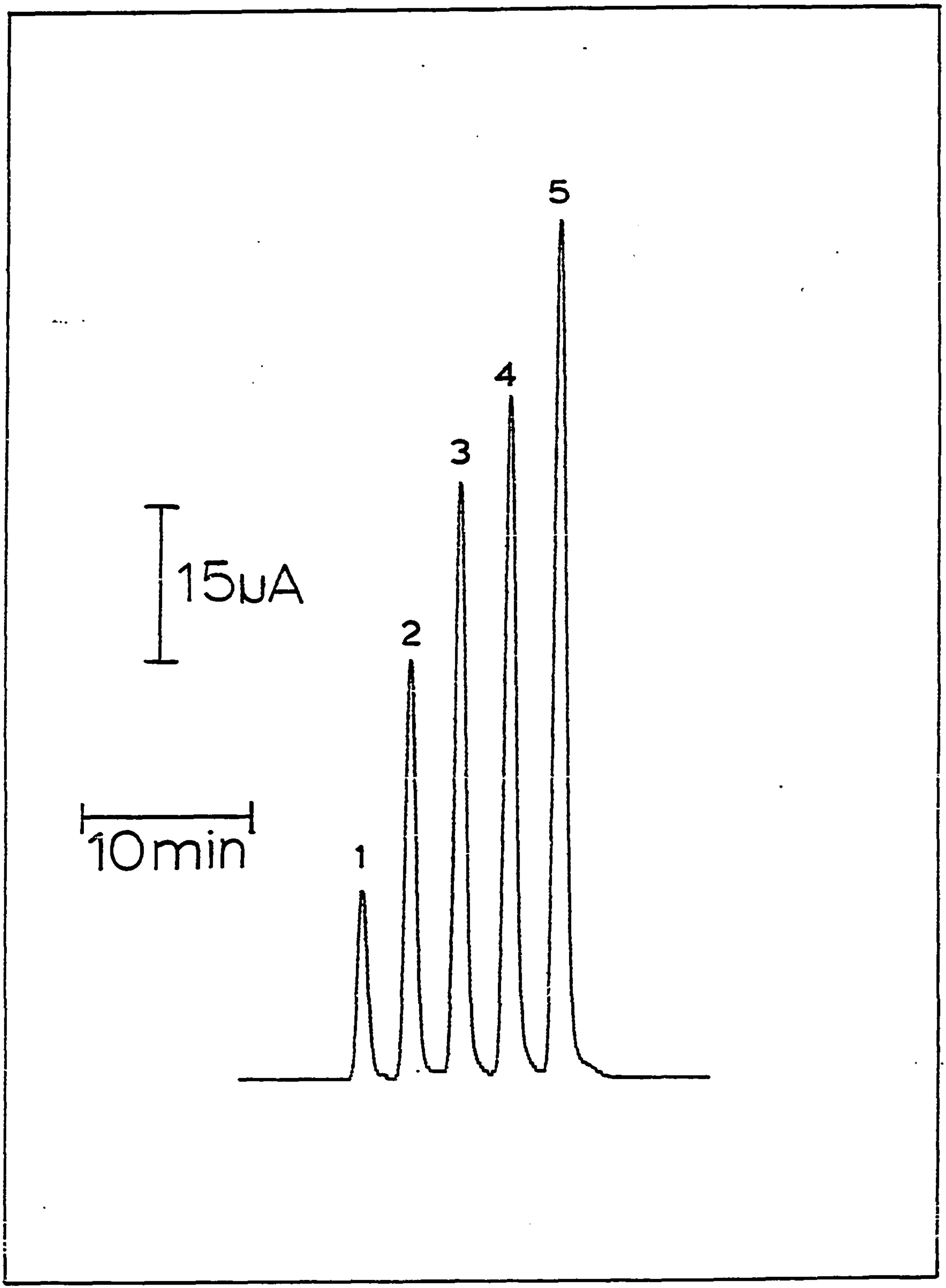
1
2
3
4
5
15µA
10min

the ratio of the detector sensitivity for each analyte and the internal standard, is a constant and independent of concentration. The constancy of F can occur only if the calibration curves for the standard and each analyte are linear with zero intercepts. The detector response for TPA does not have this property; therefore, the method of internal standardization is not valid for this detection method.

The limit of detection for the technique was determined to be approximately 4.6 μg ml^{-1} for dextrose (signal-to-noise ratio = 2). Expected detection limits for the other carbohydrates examined can be made by the comparison of their sensitivites with that for dextrose. The sensitivity of the other monosaccharides examined was similar to that for dextrose with the sugar alcohols exhibiting slightly higher sensitivity. Oligosaccharides showed lower sensitivities than dextrose, which continually decreased with increasing chain length of the saccharide.

4. Variance of quantitative results

Linear calibration curves are obtained by this technique when -1/I is plotted vs. 1/C . The calibration data can be treated by linear regression statistics to define the regression line, i.e. slope and intercept of the calibration curve, and their respective estimated variances.

For the application of the linear calibration curve (-1/I vs. 1/C) to the determination of the concentration (C_s) of an unknown sample based on the measured value of current (I_s), the regression statistics can be used to estimate the variance of C_s. The variance in C_s, V_c, is calculated by Eq. VII-1 by using the standard deviation of 1/C upon -1/I of the calibration curve and the Student t-value at the 90% confidence interval ($t_{0.1}$). In Eq. VII-1, C = concentration, n = number of points in the calibration curve, I = current, and D is given by Eq. VII-2 with the aid of Eq. VII-3.

$$V_c = \pm 0.5 \left[\frac{1}{1/C_s - D} - \frac{1}{1/C_s + D} \right] \qquad \text{VII-1}$$

$$D = (t_{0.1} \times s)(1 + 1/n + I_s^{-2}/\Sigma(-I)^{-2})^{\frac{1}{2}} \qquad \text{VII-2}$$

$$s = \left[\frac{\Sigma(C^{-2}) - (\Sigma(C \times -I)^{-1})^2/\Sigma(-I)^{-2}}{n - 2} \right]^{\frac{1}{2}} \qquad \text{VII-3}$$

Calibration data for standard samples of dextrose at concentrations in the range 0.2 to 1.5 mg ml^{-1} were obtained and the regression line for a plot of -1/I vs. 1/C was determined. The regression statistics are given in Table VII-2.

Table VII-2. Linear regression statistics for dextrose calibration curve

Parameter	Symbol	Value
Slope	B	$(4.05 \pm 0.03) \times 10^{-2}$ mg ml^{-1}μA^{-1}
Intercept	A	$(9.4 \pm 0.8) \times 10^{-3}$ μA^{-1}
Standard error	s	0.014 ml mg^{-1}
Correlation coefficient	r^2	1.0000

The absolute variances for concentrations determined from this calibration are illustrated in Figure VII-5. The center line of Figure VII-5 was generated using the slope and intercept listed in Table VII-2 according to Eq. VII-4.

$$-I = \frac{C}{B + AC} \qquad \text{VII-4}$$

The upper and lower lines represent the confidence limits as generated by Eq. VII-1. Due to the inverse nature of the linearized calibration plot the absolute variances are more severe at higher concentrations. The primary concern of the analyst is that the relative variance (V_c/C_s) be kept at a minimum. A plot of relative variance vs. concentration for the dextrose calibration curve (Figure VII-6) illustrates that the relative variance becomes quite severe for concentrations determined from the upper two

Figure VII-5. Plot of dextrose calibration curve, defined in Table VII-2, showing absolute variances for concentration determined from the curve

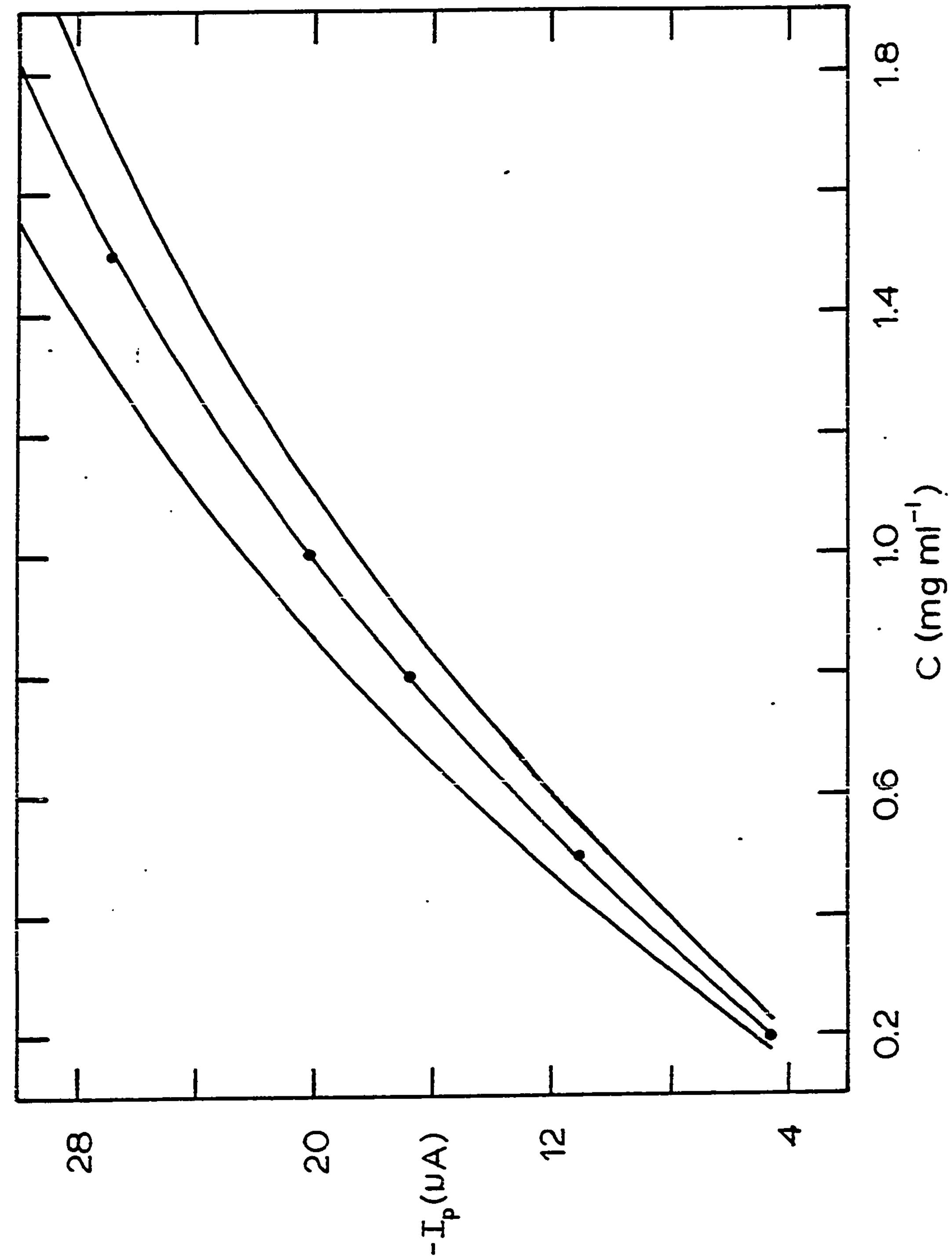
$-I_p$ (μA)
28
20
12
4
C (mg ml^{-1})
0.2
0.6
1.0
1.4
1.8

Figure VII-6. Plot of relative variance vs, concentration for dextrose calibration curve defined in Table VII-2

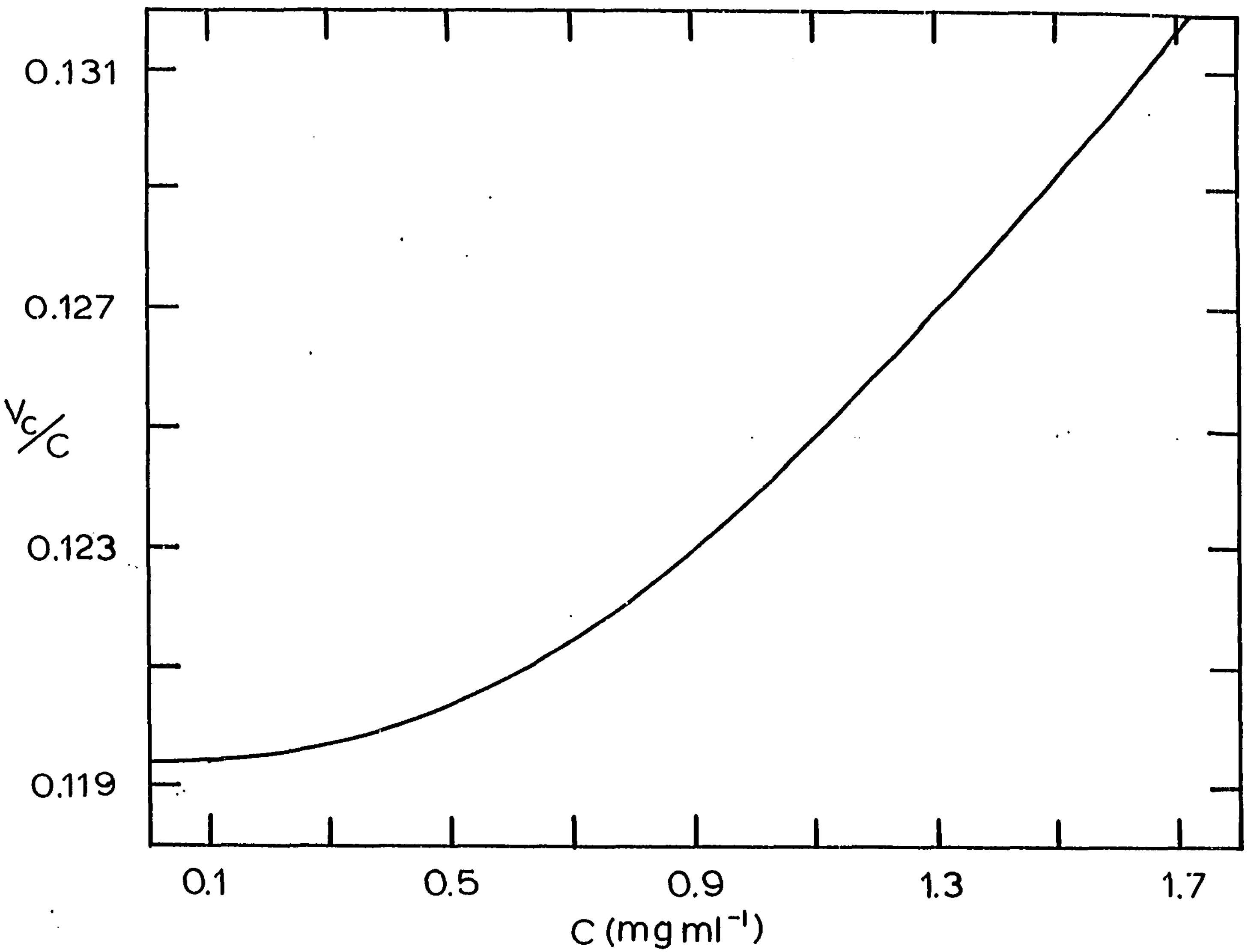
0.131
0.127
0.123
0.119
V_c/C
0.1
0.5
0.9
1.3
1.7
C (mg ml^{-1})

thirds of the curve. Therefore, in order to keep the relative variance at a reasonable level, samples of high concentration should be diluted such that the response of the sample is in the low region of variance of the calibration curve.

B. Detector Temperature

The dependence of detector current on variations of the temperature for the TPA detection of carbohydrates was investigated using the HPLC system. Such a study was not feasible in a batch cell due to the rapid decomposition of carbohydrates in alkali solutions at elevated temperatures. With the HPLC system, the time period between the addition of base to the analyte and its detection was only a few seconds and decomposition was assumed negligible. In addition, because of the capability of separating a mixture in the HPLC system, the effect of temperature could be determined for several carbohydrates in one experiment.

The anodic current obtained by TPA has been shown to be described by

$$|I_p| = \frac{nFAk_2\Gamma_{max}KC^b}{1 + KC^b} \qquad \text{VII-5}$$

where all the symbol are as previously defined (Sec. IV). For small concentration where $KC^b << 1$, Eq. VII-5 can be approximated as

$$|I_p| = nFAk_2\Gamma_{max}KC^b \quad . \qquad \text{VII-6}$$

Taking the natural logarithm of each side of Eq. VII-6 produces Eq. VII-7. In order to predict the effect of

$$\ln|I_p| = \ln(nFAC^b) + \ln k_2 + \ln\Gamma_{max} + \ln K \qquad \text{VII-7}$$

temperature, Eq. VII-7 is differentiated with respect to 1/T, to give Eq. VII-8. The first term of Eq. VII-8 can

$$\frac{d\ln|I_p|}{d(1/T)} = \frac{d\ln k_2}{d(1/T)} + \frac{d\ln\Gamma_{max}}{d(1/T)} + \frac{d\ln K}{d(1/T)} \qquad \text{VII-8}$$

be evaluated as follows. Assuming that the oxidation is irreversible, i.e. no back reaction, then according to Arrhenius theory the rate constant for electron transfer, k_2, is given by

$$k_2 = A_{anod}\exp\{-\Delta G^*_{anod}/RT\}\exp\{\alpha_a F(E - E^o)/RT\} \qquad \text{VII-9}$$

where ΔG^*_{anod} is the energy barrier for the anodic reaction, α_a is the anodic transfer coefficient, E^o is the standard reduction potential and A_{anod} is a constant. Differentiating the $\ln k_2$ with respect to $1/T$ gives Eq. VII-10.

$$\frac{d\ln k_2}{d(1/T)} = \frac{d\ln A_{anod}}{d(1/T)} - \frac{\Delta H^*_{anod}}{R} + \frac{\alpha_a F(E - E^o)}{R} \qquad \text{VII-10}$$

The second term in Eq. VII-8 is more difficult to explicitly evaluate. However, since Γ_{max} was defined as the molar surface coverage at infinite concentration, its change with finite temperature is probably insignificant and it is therefore approximated by zero.

$$\frac{d\ln \Gamma_{max}}{d(1/T)} \simeq 0 \qquad \text{VII-11}$$

In the third term of Eq. VII-8

$$K = \frac{k_1}{k_{-1}}, \qquad \text{VII-12}$$

where k_1 and k_{-1} are the rate constants for the adsorption and desorption reactions respectively (Eq. IV-1). According to Arrhenius theory

$$k_1 = A_{ads}\exp\{-\Delta G^{*}_{ads}/RT\} \qquad \text{VII-13}$$

and

$$k_{-1} = A_{des}\exp\{-\Delta G^{*}_{des}/RT\}. \qquad \text{VII-14}$$

Substituting Eqs. VII-13 and VII-14 into VII-12 gives Eq. VII-15,

$$K = (A_{ads}/A_{des})\exp\{-\Delta G^{o}_{ads}/RT\}\ , \qquad \text{VII-15}$$

where ΔG^{o}_{ads} is the free energy of adsorption and A_{ads} and A_{des} are constants. Differentiating lnK with respect to 1/T gives Eq. VII-16,

$$\frac{d\ln K}{d(1/T)} = \frac{d\ln(A_{ads}/A_{des})}{d(1/T)} - \frac{\Delta H^{o}_{ads}}{R}. \qquad \text{VII-16}$$

Eq. VII-8 is represented by the sum of Eqs. VII-10, VII-11, and VII-16 as shown in Eq. VII-17. If it is assumed here

$$\frac{d\ln|I_p|}{d(1/T)} = \frac{d\ln A_a}{d(1/T)} + \frac{d\ln(A_{ads}/A_{des})}{d(1/T)} - \frac{\Delta H^{*}_{anod}}{R} - \frac{\Delta H^{o}_{ads}}{R} + \frac{\alpha_a F(E - E^{o})}{R}$$

VII-17

that the first two terms of Eq. VII-17 are negligible, i.e. that A_a, A_{ads} and A_{des} are approximately constant with respect to temperature, then Eq. VII-17 reduces to Eq. VII-18.

$$\frac{d\ln|I_p|}{d(1/T)} = \frac{-\Delta H^{*}_{anod}}{R} - \frac{\Delta H^{o}_{ads}}{R} + \frac{\alpha_a F(E - E^{o})}{R} \qquad \text{VII-18}$$

Eq. VII-18 illustrates that the magnitude of the slope for a plot of $\ln|I_p|$ vs. $1/T$ is considered to be a function of three terms. The first term must be negative since from its nature ΔH^{*}_{anod} is taken to have a positive value. The second and third terms, however, probably have positive values; ΔH^{o}_{ads} will be negative since the adsorption reaction is spontaneous making the second term positive, and $(E - E^{o})$ is positive since E is positive of the standard reduction potential. Therefore, depending on the relative values of the three terms in Eq. VII-18, a plot of $\ln|I_p|$ vs. $1/T$ is expected to be linear but the slope may be negative or positive.

Table VII-3 contains the values of peak current obtained for six carbohydrates with detector temperature (T) varied in the range 35^{o} to 85^{o} C. Plots of $\ln|I_p|$ vs. $1/T$

Table VII-3. Peak current obtained by HPLC with TPA detection at varied detector temperature for six carbohydrates[a]

Temperature (^{o}C)	I_p(μA) Lactose	Dextrose	Xylose	Arabinose	Arabitol	Sorbitol
85	2.70	4.67	4.92	5.68	7.89	5.62
75	2.62	4.10	4.32	5.22	7.09	5.58
65	2.15	3.97	4.24	4.82	6.95	5.14
55	1.94	3.70	3.76	4.45	6.39	4.56
45	1.70	3.19	3.42	3.99	5.72	4.48
35	1.29	2.80	2.97	3.41	5.24	3.74

[a] 0.14 mg ml^{-1} Lactose, 0.12 mg ml^{-1} all other carbohydrates.

for the six compounds were all linear with negative slopes. The plot for arabinose is shown in Figure VII-7 as an example.

It was not possible to evaluate from independent experiments the numerical values of ΔH^{*}_{anod}, ΔH^{o}_{ads} and E^{o}. However, a qualitative conclusion is possible: whereas adsorption of the carbohydrate analytes is a prerequisite for detection by TPA, the sensitivity of the technique appears to be controlled more by the kinetics of the irreversible, anodic, charge-transfer reaction than by the finite extent of the adsorption, i.e. K_{ads}.

C. Analysis of Real Samples

A variety of real samples was analyzed using HPLC separation with TPA detection to test the breadth of applicability of the technique. Samples containing a wide range of concentrations of a variety of carbohydrates were analyzed. Qualitative peak identification was made by comparison of retention times to standards. To extend the life of the chromatographic columns, all samples were passed through Amberlite MB-3 (Mallinckrot, Paris, KY) mixed-bed ion-exchange resin, and filtered through a 0.45 μm membrane.

Figure VII-8 shows typical chromatograms obtained for

Figure VII-7. Plot of $\ln(-I_p)$ vs. 1/temperature for injections of 0.12 mg ml^{-1} arabinose

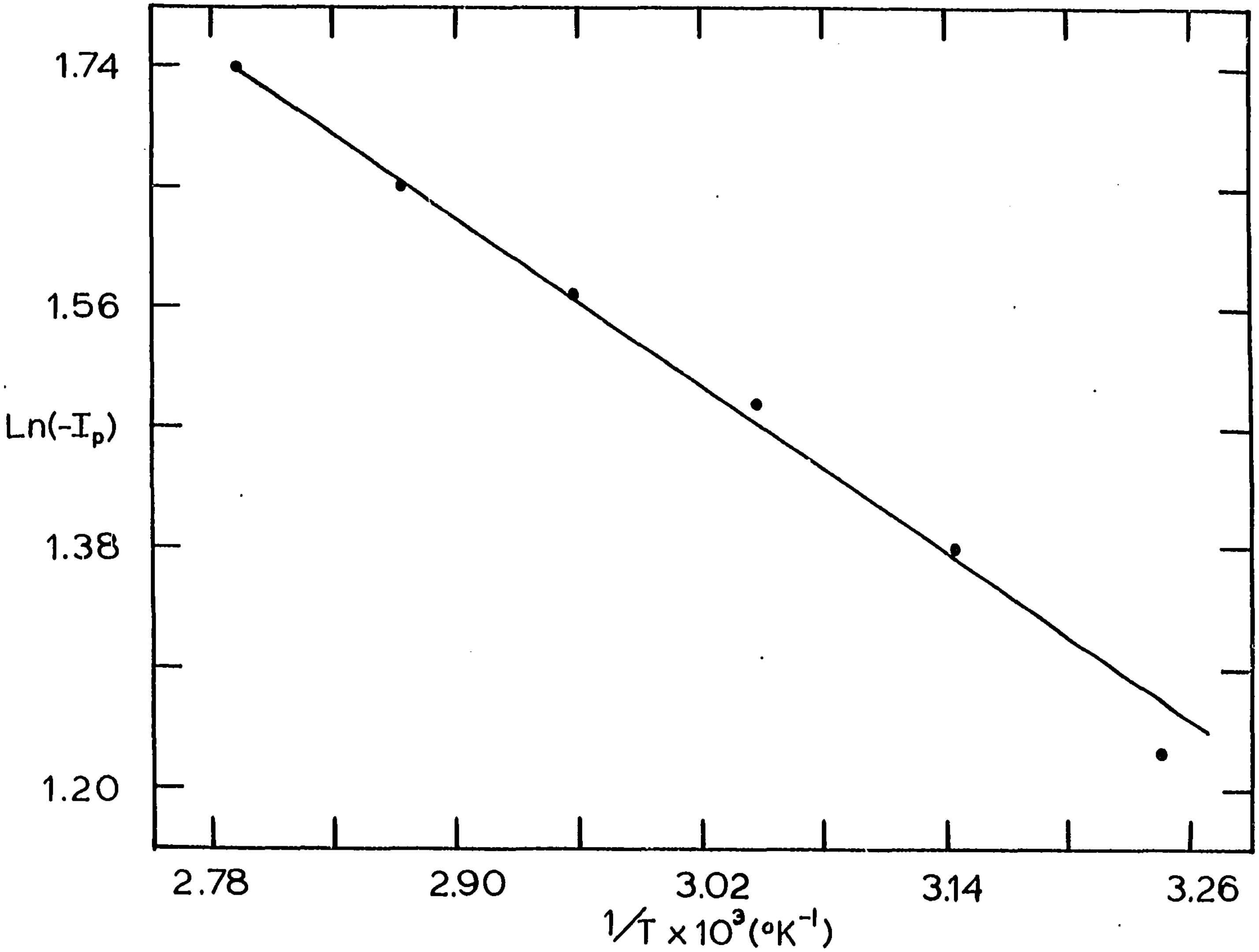
1.74
1.56
Ln($-I_p$)
1.38
1.20
2.78
2.90
3.02
3.14
3.26
$1/T \times 10^3$ (°K^{-1})

Figure VII-8, Chromatographic analysis with Hamilton column

I, Ginger-ale (20:1 dilution before injection)
II, Coconut-milk

Peaks:

s. sucrose
d. dextrose
x. xylose
f. fructose
s', sorbitol

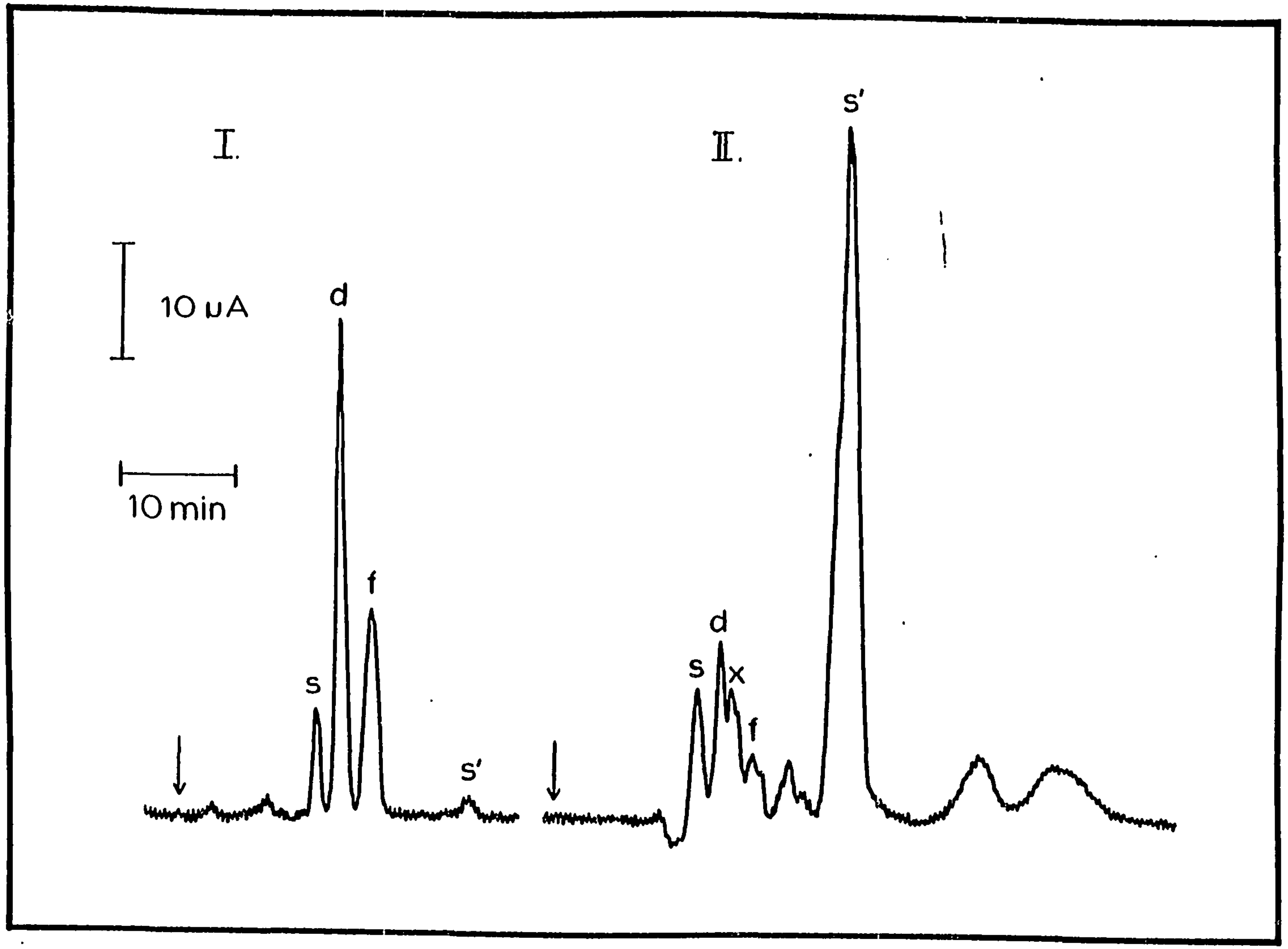
I.
II.
10 µA
10 min
s
d
f
s'
s
d
x
f
s'

samples of ginger-ale and coconut-milk. The ginger-ale sample was diluted 1:20 prior to analysis, whereas the coconut-milk was injected without dilution. Ginger-ale is an example of a manufactured food product sweetened with corn syrup. The coconut milk was unprocessed with the sample extracted from the nut in the laboratory just prior to analysis. The analysis of a physiological sample is illustrated in Figure VII-9, showing the chromatogram resulting from a morning human urine sample. No attempt was made to quantitate the carbohydrates in these samples.

The application of TPA detection for quantitative analysis was demonstrated for several samples of beer and wine. The wine samples were diluted 2:25 and the beer samples were degassed prior to analysis. Chromatograms are shown in Figure VII-10 for two brands of beer at two sensitivities. Figure VII-10-I is for Miller Lite at a low sensitivity. Prominent peaks for dextrose, glycerol and ethanol are observed. Figure VII-10-II contains a chromatogram of Coors beer at the sensitivity used to quantitate the various carbohydrates. The identity of the first eluting peak was not determined but is thought to be maltotetrose based on its elution position and reported presence in beer (56). The concentrations of maltose, dextrose,

Figure VII-9. Chromatographic analysis of human urine

Separation achieved with the Dionex column

Peaks:

D. dextrose
X. xylose
A. arabinose
G. glycerol
U. urea

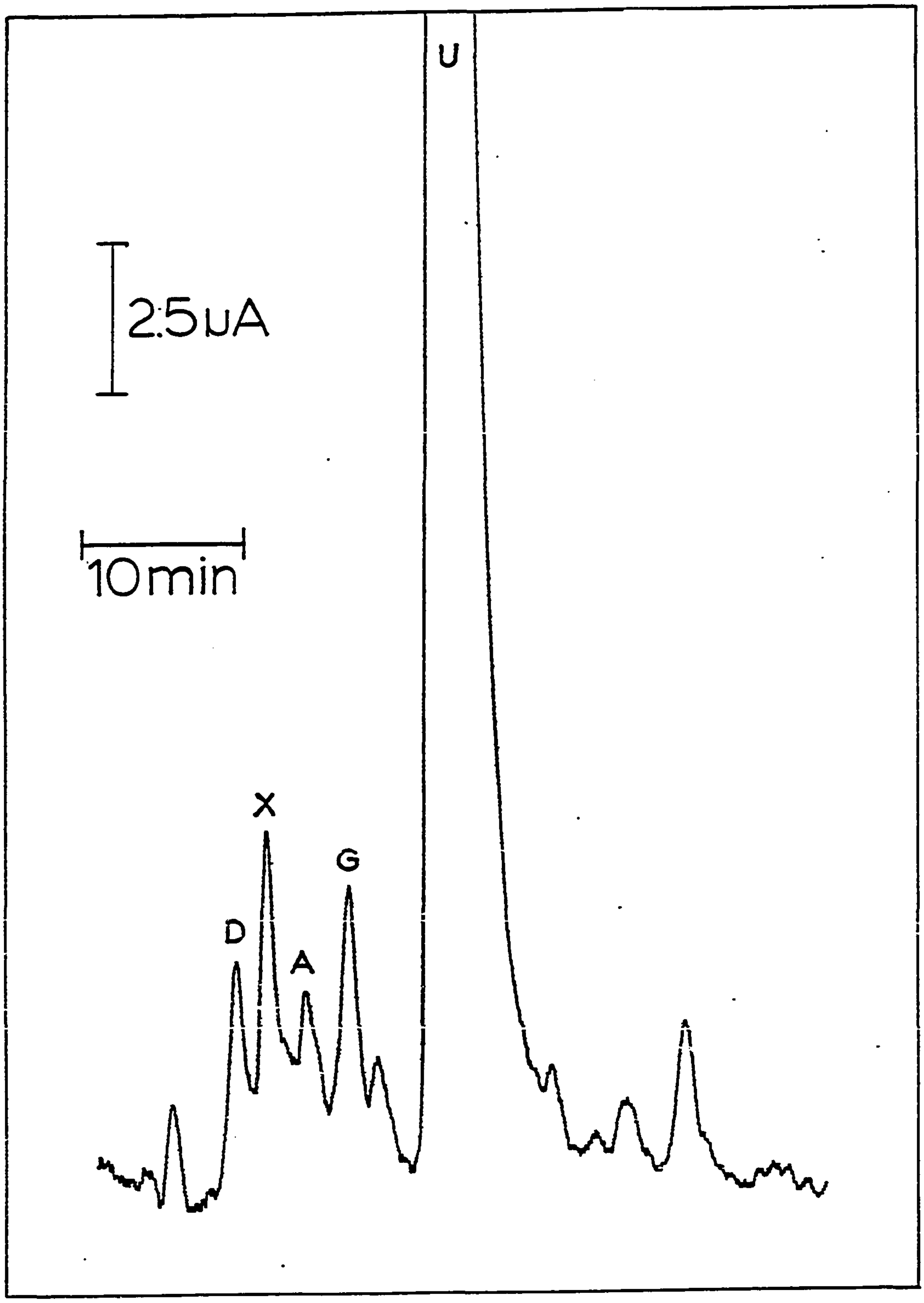
U
2.5 μA
10 min
X
G
D
A

Figure VII-10. Chromatographic analysis with Hamilton column

I. Miller Lite beer
II. Coors beer

Peaks:

m3.	maltotriose
m.	maltose
d.	dextrose
x.	xylose
a.	arabinose
g.	glycerol
e.	ethanol
s'.	sorbitol

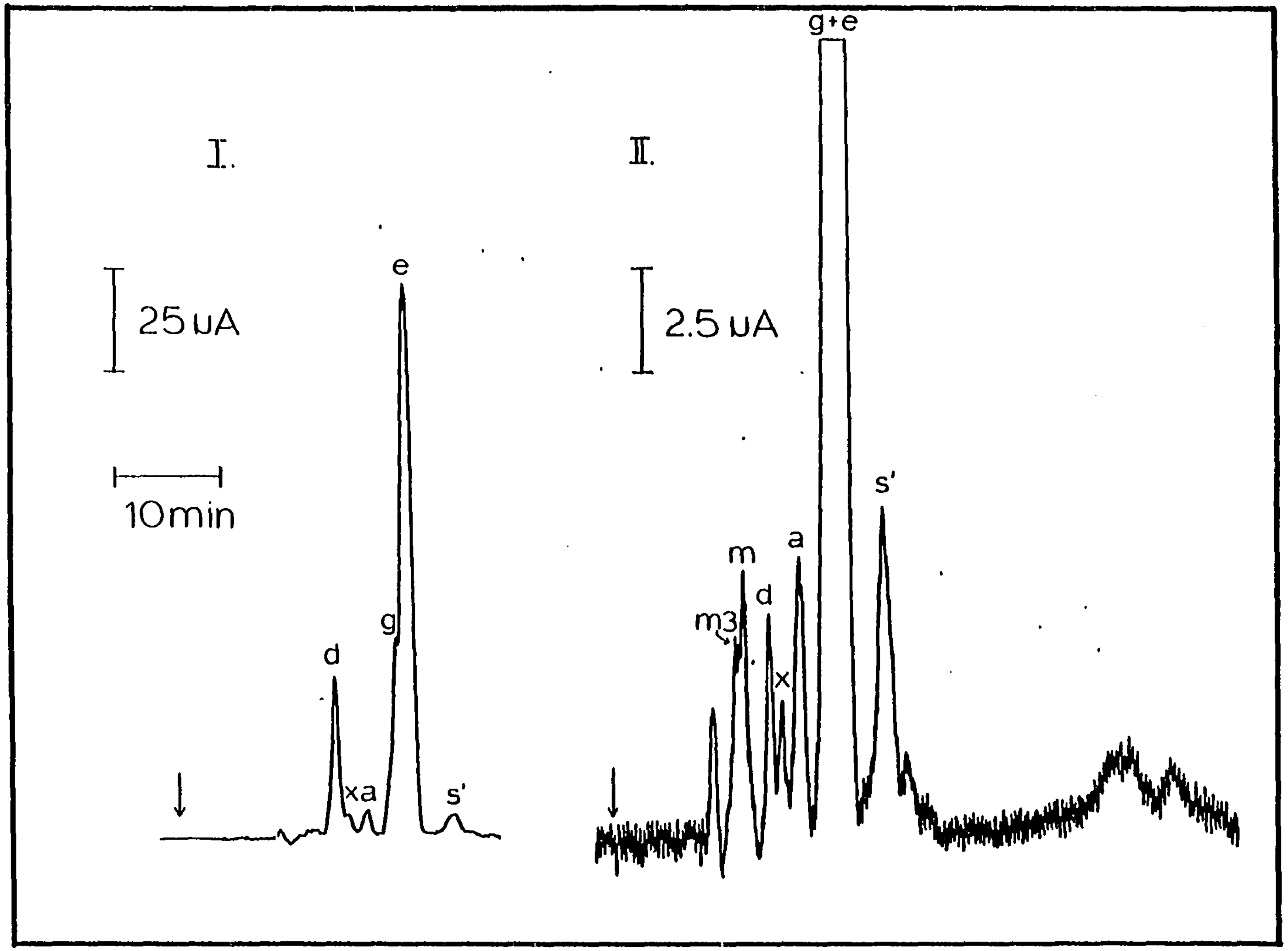
I.
25 µA
10 min
d
x a
g
e
s'
II.
2.5 µA
m3
m
d
x
a
g+e
s'

xylose, arabinose and sorbitol were determined for a variety of brands of beer. A calibration curve was made for each carbohydrate. The concentration of the carbohydrates in the beer varieties are listed in Table VII-4.

Table VII-4. Concentration of carbohydrates in beer varieties

	μg ml^{-1}				
Brand	maltose	dextrose	xylose	arabinose	sorbitol
Miller lite	65±9	844±106	51±7	56±5	51±8
Pabst Blue Ribbon	37±3	14±1	28±2	68±9	62±12
Pabst Extra Light	37±3	13±1	32±3	59±7	36±4
Coors	108±26	55±7	33±3	74±11	40±5
Coors Light	93±19	499±34	45±5	102±21	32±3

Chromatograms are shown in Figure VII-11 for three varieties of wine; a "sweet" white wine, a "dry" red and a "light" Burgundy. Peaks were observed for dextrose, fructose, glycerol and ethanol. A calibration curve was made for each of these compounds. The concentration of these compounds in the wine varieties is given in Table VII-5. Even though many other carbohydrates than detected here are found in grapes, they are broken down in the fermentation process and, therefore, are not observed in the

Table VII-5. Analytical results of wine analysis

		mg ml^{-1}			% by vol.
Brand	Type	Dextrose	Fructose	Glycerol	Ethanol
Grey Goose	Liefraulmilch-"sweet" white	5.6±0.7	14±2	5.3±0.6	9.4±0.9
Fetzer	Premium Red-"dry" red	0.50±0.06	1.3±0.2	7.5±0.9	12±1
Villa Sorrento	Light Burgundy-"sweet" red	7.6±0.9	10±2	6.3±0.7	5.9±0.6

Figure VII-11, Chromatographic analysis of wine using the Dionex column

I, Grey Goose
II, Fetzer
III, Villa Sorrento

Peaks:

D, dextrose
F, fructose
G, glycerol
E, ethanol

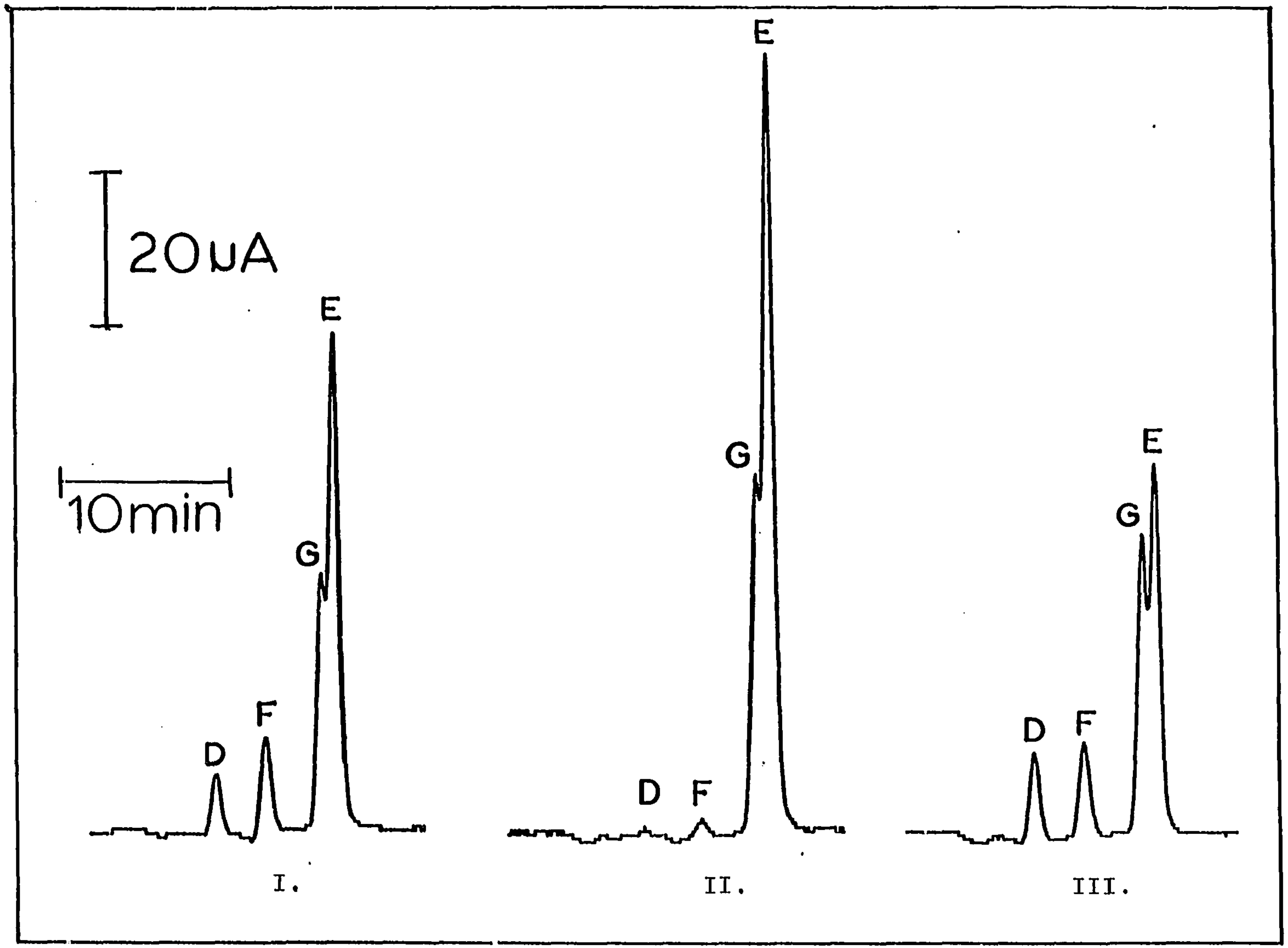
20µA
10min
D
F
G
E
I.
D
F
G
E
II.
D
F
G
E
III.

final product (4). The absence of a peak for sorbitol is consistent with the fact that this carbohydrate, though commonly found in many fruits, is not observed in grapes. The presence of sorbitol in wines has been used to indicate adulteration of the grape wine with fermentation products of other fruits (4).

The sweetness of a wine is a function of the carbohydrate concentration. This fact is readily observed by an examination of Table VII-7 with the dry, unsweet wine (Fetzer) having very low dextrose and fructose concentrations compared to the sweet liefraumilch (Grey Goose). The light Burgundy (Villa Sorrento) is marketed as a diet wine, lower in calories than regular wines. The results of the analysis indicate that the caloric savings are not due to the lowering of carbohydrates but to the reduction of the ethanol content of the product.

Extensive taste studies were performed to attempt a correlation between the calculated carbohydrate concentration and the sensory response of this author. Due to interference from the ethanol present in the samples, it was determined that more studies are necessary before a conclusion can be remembered.

D. Summary

The application of TPA for detection of carbohydrates and alcohols in HPLC has been demonstrated. Linear calibration curves were obtained for plots of $-1/I_p$ vs. $1/C$. Because of the inverse nature of the calibration curve, the variance of estimates made from the curve increased greatly with increasing concentration. The detection limit was determined to be approximately 4.6 $\mu g\ ml^{-1}$ for dextrose at a detector temperature of 60° C. This is more than 100x lower than that reported for refractive index detection (45). Detection current was found to increase with increasing detector temperature. The technique was successfully applied to the analysis of a variety of "real" samples including beer, wine and urine.

VIII. SUMMARY

The development of a platinum electrochemical detector using the technique of triple pulse amperometry was described for the detection of alcohols and carbohydrates separated by HPLC. The electrochemical oxidation of most organic compounds on platinum electrodes is characterized by a large anodic current which decays to a negligible value within a few seconds. The mechanism for the oxidation is believed to involve adsorption of the organic molecule onto the electrode, followed by surface-catalyzed dehydrogenation of the adsorbed molecule and subsequent oxidation of the resulting adsorbed hydrogen. The hydrocarbon products of the dehydrogenation remain adsorbed on the electrode surface, thereby inhibiting adsorption of unreacted molecules and the resulting anodic current. At sufficiently positive electrode potentials, these adsorbed hydrocarbons are oxidatively removed from the electrode as CO_2 with the concomitant formation of platinum oxide. Reduction of the surface platinum oxide results in a "reactivated" electrode which is again capable of adsorbing organic molecules from solution.

The properties of the oxidation of organic compounds on platinum were utilized to design a potential waveform which can "continuously" reactivate a platinum electrode involved in the oxidation of organic molecules. The resulting waveform consists of three potentials. The faradaic signal is determined at a potential, E1, for oxidation of the adsorbed compounds without formation of PtO. The charging current associated with a potential step to E1 decreases rapidly (< 100 ms) and the faradaic signal is measured after substantial decay of charging current but before significant loss of electrode activity has occurred. The faradaic signal is retained in the potentiostat by a sample-hold circuit until updated following the next repetition of the waveform. The surface of the platinum electrode is then cleaned of the adsorbed organic residue by stepping the applied potential to the positive limit, E2, accessible for the solvent, at which value the adsorbed organic material is believed to be oxidatively desorbed as CO_2 simultaneously with formation of PtO. The potential is then stepped to a value E3 near the negative limit for the solvent where PtO is reduced and adsorption of the analyte can occur. Because of the use of a three potential waveform with the measurement of the faradaic current at a single potential (E1), the technique has been termed "triple pulse amperometry" (TPA). The result of the TPA technique is the maintenance of a high and uniform electrode activity making possible the reproducible anodic detection of many organic compounds.

The faradaic signal obtained by TPA was determined to be proportional to the equilibrium surface coverage of the electrode by the adsorbed organic molecules. For low analyte concentrations, the adsorption was found to be described by the Langmuir isotherm with the I vs. C response described by

$$-I = \frac{C}{B + AC}$$

where A and B are the intercept and slope respectively of the linear regression line obtained for plots of -1/I vs. 1/C. Due to the form of the I-C equation, the relative variances of concentrations determined from a calibration curve increase as the square of the concentration. This necessitates the dilution of samples with high concentration to minimize the relative variance of the determined concentration.

The TPA technique was applied to the detection of carbohydrates and alcohols separated by HPLC. The system utilized a cation-exchange column with water as the eluent for the separation of the carbohydrates and alcohols. Concentrated NaOH was introduced in the effluent stream at a low flow rate between the column and the wire-tip platinum detector to achieve a detector concentration of 0.10 M NaOH required for the TPA detection. Detection limits for dextrose were approximately 4.6 $\mu g\ ml^{-1}$ which is more than 100x lower than the limit reported for refractive index detection. The analyses of several "real" samples were reported including beer, wine and urine.

IX. SUGGESTIONS FOR FUTURE WORK

The limit of detection of carbohydrates with the TPA detector described results mainly from the uncertainty of the baseline, caused by the fluctuation in the flow rate of the peristaltic pump, which produces a changing NaOH concentration in the detector. A reduction of the uncertainty would lead to lower detection limits. The application of a moving average algorithm to the detector current by the computer data acquisition system significantly reduced the "high" frequency oscillation (~4 hz), but was ineffective for the lower frequency changes. The ultimate solution is to eliminate the differential flow by the use of a pump capable of a more ideal pulseless output for the low rate of flow required (0.01 ml min^{-1}). A syringe pump capable of head pressures above that of the detector (15 psi) would meet these requirements.

The response of the technique for the detection of other analytes, such as polyalcohols, aldehydes and ketones should be investigated.

The use of the TPA waveform with electrode materials other than platinum is a promising avenue for future work. Solid electrodes are plagued with the problem of loss of activity due to adsorption of impurities from solution (22).

A possible example of this is the oxidation of dextrose on gold electrodes. Although under amperometric conditions the anodic current is not as transitory as for oxidation on platinum, the current of the gold electrode does steadily decrease with time (23), making its use inadequate for an analytical response. It is possible that with the use of TPA the surface impurities could be oxidatively removed, establishing a stable electrode activity.

X. BIBLIOGRAPHY

1. Lehninger, A. L. "Biochemistry", 2nd ed.; Worth; New York, 1975; Chapter 10.
2. Tietz, N. W. "Fundamentals of Clinical Chemistry"; W. B. Saunders Co.: New York, 1970.
3. Touster, O.; Shaw D. R. D. Physiological Rewiews 1962, 42, 181.
4. Gallander, J. F. In "Chemistry of Winemaking"; Webb, A. D., Ed.; American Chemical Society: Washington, D.C., 1974, Chapter 2.
5. Shaw, P. E.; Wilson, C. W.,III; Knight, R. J.,Jr. J. Agr. Food Chem. 1980, 28, 379.
6. Palmer, J. K.; Brandes, W. B. J. Agr. Food Chem. 1974, 22, 709.
7. Fried, I. "The Chemistry of Electrode Processes"; Acedemic: New York, 1973.
8. Breiter, M. W.; Gilman, S. J. Electrochem. Soc. 1962, 109, 622.
9. Damaskin, B. B.; Petrii, O. A.; Batrakov, V. V. "Adsorption of Organic Compounds on Electrodes"; Plenum: New York, 1971.
10. Bagotzky, V. S.; Vassiliev, Y. B. Electrochim. Acta 1966, 11, 1439.
11. Breiter, M. W.; Gilman, S. J. Electrochem. Soc. 1962, 109, 1099.
12. Breiter, M. W. Electrochim. Acta 1963, 8, 447.
13. Breiter, M. W. Electrochim. Acta 1963, 8, 457.
14. Rao, M. L. B.; Drake, R. F. J. Electrochem. Soc. 1969, 116, 334.

15. Ernst, S.; Heitbaum, J.; Hamann, C. H. *Ber. Bunsenges. Phys. Chem.* 1980, 84, 50.

16. Ernst, S.; Heitbaum, J.; Hamann, C. H. *J. Electroanal. Chem.* 1979, 100, 173.

17. Skou, E. *Electrochim. Acta* 1977, 22, 313.

18. Attwood, P. A.; McNicol, B. D.; Short, R. T. *J. Appl. Electrochem.* 1980, 10, 213.

19. Breiter, M. W. *J. Electroanal. Chem.* 1967, 14, 407.

20. Breiter, M. W. *J. Electroanal. Chem.* 1967, 15, 221.

21. Gough, D. A.; Anderson, F. L.; Ginger, J.; Colton, C. K.; Soeldner, J. S., *Anal. Chem.* 1978, 50, 941.

22. Adams, R. "Electrochemistry at Solid Electrodes"; Marcel Dekker: New York, 1969.

23. Tsang, R. W. Ph.D. Dissertation, Iowa State University, Ames, Iowa, 1981.

24. Nadebaum, P. R.; Fahidy, T. Z. *Electrochim. Acta*, 1975, 20, 715.

25. Nadebaum, P. R.; Fahidy, T. Z. *Electrochim. Acta*, 1975, 20, 721.

26. Farooque, M.; Fahidy, T. Z. *Electrochim. Acta*, 1979, 24, 547.

27. Marincic, L.; Soeldner, J. S.; Colton, C. K.; Giner, J.; Morris, S. *J. Electrochem. Soc.* 1979, 126, 43.

28. Lerner, H.; Giner, J.; Soeldner, J. S.; Colton, C. K. *J. Electrochem. Soc.* 1979, 126, 237.

29. Marincic, L.; Soeldner, J. S.; Giner, J.; Colton, C. K. *J. Electrochem. Soc.* 1979, 126, 1687.

30. Giner J.; Marincic, L.; Soeldner, J. S.; Colton, C. K. *J. Electrochem. Soc.* 1981, 128, 2106.

31. Pomeranz, Y.; Meloan, C. E. "Food Analysis: Theory and Practice", Revised ed.; AVI: Westport, CT., 1978, Chapter 35.

32. Katz, S.; Dinsmore, S. R.; Pitt, W. W., Jr. *Clin. Chem.* 1971, 17, 731.

33. Morrison, R. T.; Boyd, R. N. "Organic Chemistry", 3rd ed.; Allyn and Bacon; Boston, MA., 1973, Chapter 34.

34. Buckee, G. K.; Hargitt, R. *J. Inst. Brew.* 1977, 83, 275.

35. Dische, Z. In "Methods in Carbohydrate Chemistry", Whistter, R. L.; Wolfrom, M. L., Editors; "Color Reactions of Carbohydrates"; Academic; New York, 1962.

36. Salomon, L. L.; Johnson, J. E. *Anal. Chem.* 1959, 31, 453.

37. "AACC Approved Methods", 7th ed.; American Association of Cereal Chemists: St. Paul MN., 1969, Method 80-10.

38. Elvidge, J. A.; Sammes, P. G. "A Course in Modern Techniques of Organic Chemistry", 2nd ed.; Butterworths: London, 1966.

39. Dickes, G. J.; Nicholas, P. V. "Gas Chromatography in Food Analysis"; Butterworths: London, 1976, Chapters 8 & 15.

40. Wrolstad, R. E.; Culbertson, J. D.; Nagaki, D. A.; Madero, C. F. *J. Agr. Food Chem.* 1980, 28, 553.

41. Jamieson, A. M. *ASBC Journal* 1976, 34, 44.

42. Laker, M. F. *J. Chrom.* 1980, 184, 457.

43. Siebert, K. J. *Masters Brewers Association of the Americas Technical Quarterly* 1972, 9, 205.

44. Linden, J. C.; Lawhead, C. L. *J. Chrom.* 1975, 105,125.

45. Johncock, S. I. M.; Wagstaffe, P. J. Analyst 1980, 105, 581.

46. Aitzetmuller, K. J. Chrom. 1978, 156, 354.

47. Wilson, A. M.; Work, T. M.; Bushway, A. A.; Bushway, R. J. J. Food Sci. 1981, 46,300.

48. Conrad, E. C.; Palmer, J. K. Food Tech. 1976, Oct., 84.

49. Verhaar, L. A.; Kuster, B. F. M. J. Chrom. 1981, 220, 313.

50. Kuo, J. C.; Yeung, E. S. J. Chrom. 1981, 223, 321.

51. Jolley, R. L.; Freeman, M. L. Clin. Chem. 1968, 14, 538.

52. Mopper, K. Anal. Biochem. 1978, 87, 162.

53. Hobbs, J. S.; Lawrence, J. G. J. Chrom. 1978, 72, 311.

54. Martinson, E.; Samuelson, O. J. Chrom. 1970, 50, 429.

55. Jandera, P.; Churacek, J. J. Chrom. 1974, 98, 55.

56. Havlicek, J.; Samuelson, O. J. Inst. Brew. 1975, 81, 466.

57. Scobell, H. D.; Brobst, K. M.; Steele, E. M. Cereal Chem. 1977, 54, 905.

58. Binder, H. J. Chrom. 1980, 189, 414.

59. D'Amboise, M.; Noël, D.; Hanai, T. Carbohyd. Res. 1980, 79, 1.

60. Jennings, W. "Gas Chromatography with Glass Capillary Columns", 2nd ed.; Acedemic: New York, 1980, Chapter 1.

61. Waters Technical Bulletin "Carbohydrates"; Waters Associates: Milford, MA., 1981.

62. Hodgin, J. C. Liquid Chromatography News 1981, 3, 8.

63. Yeung, E. S.; Steenhoek, L. E.; Woodruff, S. D.; Kuo, J. C. Anal. Chem. 1980, 52, 1399.

64. Lindstrom, T. R. Ph.D. Dissertation, Iowa State University, Ames, Iowa, 1980.

65. Yamada, J.; Mastuda, H. J. Electroanal. Chem. Interfacial Electrochem. 1973, 44, 189.

66. Fleet, B.; Little, C. F. J. Chrom. Sci., 1974, 12, 747.

67. Pratt, K. W. Ph.D. Dissertation, Iowa State University, Ames, Iowa, 1981.

68. Larochelle, J. H. Ph.D. Dissertation, Iowa State University, Ames, Iowa, 1977.

69. Meschi, P. L. Ph.D. Dissertation, Iowa State University, Ames, Iowa, 1981.

70. Albery, W. J.; Hitchman, M. L. "Ring-disc Electrodes"; Clarendon: Oxford, 1971.

71. Meschi, P. L.; Johnson, D. C. Anal. Chim. Acta 1981, 124, 303.

72. Khomchenko, I. G.; Zelinskii, A. G.; Petrii, O. A. Soviet Electrochem. 1981, 17, 109.

XI. ACKNOWLEDGEMENTS

I would like to thank Dennis Johnson for his extensive help and guidance throughout this research project. His technical expertise as well as his unique teaching abilities are greatly appreciated.

The financial support from the Utopia Instrument Co. and the Dionex Corp. are gratefully acknowledged.

I thank the soybean group of the Food Technology Dept. for the use of their water bath.

Much gratitude goes to Larry Meschi for designing and constructing the timing circuit which made this project possible. To my labmates, Deb Austin, Tim Cabelka and Ron Tsang, I extend my thanks for their continuous support and welcomed diversions.

I would like to thank Phil Stewart (Arro Laboratories, Inc.) for teaching me how to design efficient experiments which expedite research. This project would not have proceeded so quickly without these skills.

My education from Beloit College, in general, and my chemistry education from Brock Spencer, Mike Flood and Bern Saxe, in particular, are extremely appreciated. Their teaching the process of thinking rather than the reiteration of facts has enabled me to quickly learn new areas of expertise with relative ease.

I owe great appreciation to my mother, Fay Hughes, for convincing me to pursue graduate study and for the love and affection she showed me throughout her life.

I thank my father, David Hughes, for giving me my arrogance and for teaching me many basic skills including the courage to aggressively attack any problem and that failure is not an end but merely a turning point.

Lastly, to my partner Sandy, I give a very special thanks. The extensive sharing of ideas has been both technically productive as well as intellectually and emotionally stimulating. Sandy has been a great asset throughout this project and I look foward to our joint participation in future endeavors.

XII. APPENDIX

This appendix contains printouts of the data acquisition computer programs used with the HPLC system. The first program, "CHROMATOGRAPHIC DATA ACQUISITION", described in Sec. III-D-3, has the function of collecting and manipulating the data from the TPA detector. The second program, "RE-EVAL" (page 189), can be called by the first program to redisplay current-time chromatograms, from data retained in memory from the first program or read from previously recorded data tapes, on the CRT, printer or external X-Y recorder.

```
 10 ! CHROMATOGRAPHIC
 15 ! DATA ACQUISITION PROGRAM
 20 ! COPYRIGHT 1981
 25 ! BY SCOTT HUGHES
 30 CONTROL 4,6 ; 1 ! STROBE TIM
    E
 40 CONTROL 4,4 ; 160 ! STROBE B
     TO R
 50 CONTROL 4,3 ; 3 ! INVERT CTL
    A AND CTL0
 60 OPTION BASE 1
 70 COM SHORT A,A1(20),B2,D1,F1,
    I(4200),P9,R(20),T1,T5,T9,S1
     ,INTEGER E(20),I,I1,I2,M(20
    ),N,P(20),R
 80 SHORT A(102),B,B1,C9,E,S,S2,
    S3,S4,S5,T,K,O,T6,T7,V3,V2,S
    6,P7,T3,D4,T8,D5
 90 INTEGER C7,C8,D2,F,F2,M,P,Q,
    Q1,R7,R8,R9,V,V8,V9,W,W2,X,X
    2,Z7,Z8,N1,K1,C6
100 DIM R$[10],K$[174]
110 K$=""
120 FOR I2=0 TO 173
130 K$=K$&CHR$(I2)
140 NEXT I2
150 K$=K$[1,142]&K$[144,158]&K$[
    161,174]
160 COM N$[96],F$[6]
170 N=30 @ T5=1 @ T6=1000 @ V3,V
    2=2.5 @ S6,S1=100 @ T7,T8,T9
    =0 @ P9=.075 @ P7,P8=.75 @ D
    3=1 @ D1$,D2$="T" @ T2=1
180 T3,T1=30 @ D4,D5=4 @ N,N1=30
     @ T7=0 @ T4=1
190 D3$,D4$="A"
200 V8,S2,S3,S4,S5,W2,W,X2,V,V9,
    M,F2,I1,I2,D2,F,S,I,A(101)=0
210 P,R,A(102)=1
220 CLEAR @ DISP "ENTER SAMPLE I
    DENTIFICATION";@ LINPUT N$
230 GOSUB 240 @ GOTO 400
240 CLEAR
250 DISP USING "6X,25A" ; "RUN P
    ARAMETERS  OLD   NEW"
260 DISP USING "19A,4X,A,5X,A" ;
     "DATA I"&CHR$(206)&"PUT:TIM
    E/INT",D1$,D2$
270 DISP USING "19A,3X,3D,3X,3D"
     ; "# OF PTS TO "&CHR$(193)&
    "VERAGE";N1,N
280 DISP USING "19A,4X,A,5X,A" ;
     CHR$(194)&"ASELINE:AVE OR R
    EG";D3$,D4$
290 DISP USING "15A,8X,D.D,3X,D.
    D" ; CHR$(195)&"YCLE TIME(SE
    C)",T4,T5
```

```
300 DISP USING "19A,3X,2D.D,2X,2
    D.D" ; "DISPLAY "&CHR$(211)&
    "EN.(µA/in)",V3,V2
310 DISP USING "17A,4X,3D.D,X,3D
    .D" ; CHR$(208)&"OTEN. SEN.(
    µA/V)",S6,S1
320 DISP USING "13A,9X,D.2D,2X,D
    .2D" ; CHR$(212)&"HRESHOLD(µ
    A)",T7,T8
330 DISP USING "13A,9X,D.2D,2X,D
    .2D" ; CHR$(201)&"p REJECT(µ
    A)",P7,P8
340 DISP USING "13A,9X,2D.D,2X,2
    D.D" ; CHR$(210)&"UN TIME(MI
    N)",T3,T1
350 DISP USING "15A,7X,2D.D,2X,2
    D.D" ; CHR$(196)&"ELAY TIME(
    MIN)",D4,D5
360 DISP CHR$(207)&"K - START"
370 DISP
380 DISP "PRESS "&HGL$("UNDERLIN
    ED")&" LETTER TO      CHANGE
     PARAMETER"
390 RETURN
400 ON KYBD K1,K$ GOTO 420
410 GOTO 410
420 I$=CHR$(K1)
430 IF I$="N" THEN GOSUB 550
440 IF I$="A" THEN GOSUB 630
450 IF I$="B" THEN GOSUB 690
460 IF I$="C" THEN GOSUB 750
470 IF I$="S" THEN GOSUB 800
480 IF I$="P" THEN GOSUB 830
490 IF I$="T" THEN GOSUB 870
500 IF I$="I" THEN GOSUB 910
510 IF I$="R" THEN GOSUB 950
520 IF I$="D" THEN GOSUB 990
530 IF I$="O" THEN GOSUB 1020
540 GOTO 410
550 D1$=D2$
560 DISP "TAKE DATA ON INTERUPT
    OR TIME   INTERVAL:I/T";@ IN
    PUT R$
570 D2$=UPC$(R$[1,1])
580 IF UPC$(R$[1,1])="T" THEN 61
    0
590 IF UPC$(R$[1,1])#"I" THEN 56
    0
600 T2=0 @ GOTO 620
610 T2=1
620 GOSUB 240 @ RETURN
630 N1=N
640 DISP "# OF PTS. IN RUNNING A
    VERAGE";
650 INPUT N
```

```
660 IF N>100 THEN 670 ELSE 680
670 DISP "MAXIMUM # OF AVERAGE P
    TS IS 100" @ GOTO 640
680 GOSUB 240 @ RETURN
690 D3$=D4$
700 DISP "AVERAGED OR REGRESSION
              BASELINE:A/R";@ IN
    PUT R$@ D4$=UPC$(R$[1,1])
710 IF UPC$(R$[1,1])="A" THEN 74
    0
720 IF UPC$(R$[1,1])#"R" THEN 70
    0
730 D3=0 @ GOSUB 240 @ RETURN
740 D3=1 @ GOSUB 240 @ RETURN
750 DISP @ DISP "ENTER CYCLE TIM
    E IN SECONDS";
760 T4=T5
770 INPUT T5
780 T6=T5*1000
790 GOSUB 240 @ RETURN
800 V3=V2
810 DISP "DISPLAY SENSITIVITY(μA
    /IN)";@ INPUT V2
820 GOSUB 240 @ RETURN
830 DISP @ DISP "POTENTIOSTAT SE
    NSITIVITY(μA/V)";
840 S6=S1
850 INPUT S1
860 GOSUB 240 @ RETURN
870 DISP @ DISP "ENTER THRESHOLD
     VALUE ABOVE     BASELINE FO
    R INTEGRATION START  (μA)";
880 T7=T8
890 INPUT T8
900 GOSUB 240 @ RETURN
910 DISP @ DISP "Ip REJECT (μA)"
    ;
920 P7=P8
930 INPUT P8
940 GOSUB 240 @ RETURN
950 DISP @ DISP "ENTER TIME(MIN)
    OF RUN";
960 T3=T1
970 INPUT T1
980 GOSUB 240 @ RETURN
990 D4=D5
1000 DISP @ DISP "MINUTES DELAY
     BEFORE TAKING DATAAFTER INJ
     ECTION";@ INPUT D5
1010 GOSUB 240 @ RETURN
1020 Q=INT(T1*60/T5)
1030 C9=60*3.75/(T5*Q)
1040 T9=T8/S1
1050 P9=P8/S1
1060 D1=D5*60
```

```
1070 Q1=INT((T1-D5)*60/T5)
1080 IF Q1>4500 THEN 1090 ELSE 1
     110
1090 DISP @ DISP "NET TIME OF RU
     N EXCEEDS MEMORY  MAXIMUM N
     ET TIME(RUN-DELAY TIME)";
1100 DISP "IS ";4200*T5/60;" MIN
     UTES" @ DISP "PLEASE REENTE
     R" @ WAIT 6000 @ GOTO 240
1110 IF D5>T1 THEN 1120 ELSE 113
     0
1120 DISP @ DISP "DELAY TIME CAN
     NOT BE > RUN TIME" @ DISP "
     PLEASE REENTER" @ WAIT 6000
      @ GOTO 240
1130 IF D1=0 THEN D2=1
1140 OFF KYBD K$
1150 CLEAR
1160 DISP "PLEASE STAND BY" @ DI
     SP "LOADING DATA BUNCH"
1170 IF NOT T2 THEN 1210
1180 ON TIMER# 1,T6 GOSUB 1280
1190 SETTIME 0,0
1200 GOTO 1200
1210 ON INTR 4 GOSUB 1250
1220 SETTIME 0,0
1230 ENABLE INTR 4;32 ! FLGB INT
     ERRUPT
1240 GOTO 1240
1250 STATUS 4,1 ; X
1260 STATUS 4,2 ; X
1270 IF BIT(X,5) THEN 1250
1280 A(101)=A(101)+1
1290 GOSUB 2110 ! INPUT
1300 S=S+A(A(101))
1310 IF A(101)=N THEN 1350
1320 IF NOT T2 THEN 1340
1330 RETURN
1340 ENABLE INTR 4;32 @ RETURN
1350 IF NOT T2 THEN 1370
1360 OFF TIMER# 1 @ GOTO 1390
1370 OFF INTR 4
1380 T5=TIME/N
1390 B=S/N @ A(101)=N+1
1400 GCLEAR @ X2=0 @ PENUP
1410 B1=B-V2/S1 @ F1=B1+V2/S1*2.
     874
1420 SCALE 0,0,B1,F1
1430 XAXIS F1-.75*(F1-B1),300/T5
1440 MOVE 4*Q/256,F1-.95*(F1-B1)
1450 LDIR 0 @ LABEL "START"
1460 MOVE 10,F1-.05*(F1-B1)
1470 LABEL "PRESS START KEY TO B
     EGIN"
1480 MOVE 10,F1-.1*(F1-B1)
```

```
1490 LABEL "I WILL TAKE DATA AFT
     ER 5 BEEPS"
1500 IF NOT T2 THEN 1530
1510 ON TIMER# 1,T6 GOSUB 1600
1520 GOTO 1550
1530 ON INTR 4 GOSUB 1570
1540 ENABLE INTR 4;32 ! FLGB
1550 IF NOT F THEN 2200
1560 GOTO 1560
1570 STATUS 4,1 ; X
1580 STATUS 4,2 ; X
1590 IF BIT(X,5) THEN 1570
1600 GOSUB 2110 ! INPUT A(A(101)
     )
1610 S=S-A(A(102))+A(A(101))
1620 E=S/N
1630 IF NOT F THEN 2010
1640 IF D2 THEN A=B @ B2=0
1650 IF D1<TIME THEN 1730
1660 I1=I1+1
1670 S2=S2+I1
1680 S3=S3+E
1690 S4=S4+I1*I1
1700 S5=S5+E*I1
1710 PLOT I1,E
1720 GOTO 2040
1730 IF F2 THEN 1800 ELSE F2=1
1740 IF D2 THEN 1800
1750 IF D3 THEN A=S3/I1 ELSE 178
     0
1760 B2=0
1770 GOTO 1800
1780 B2=(S5-S2*S3/I1)/(S4-S2*S2/
     I1)
1790 A=S3/I1-B2*S2/I1
1800 I=I+1
1810 I(I)=E
1820 IF I=1 THEN 1990
1830 IF NOT P THEN 1870
1840 IF I(I)>T9+FNB(I) THEN W=W+
     1 ELSE W=0
1850 IF W=1 THEN P(R)=I-1
1860 IF W=6 THEN GOSUB 2480
1870 IF NOT M THEN 1910
1880 IF I(I)<I(I-1) THEN W=W+1 E
     LSE W=0
1890 IF W=1 THEN R(R)=TIME @ M(R
     )=I-1
1900 IF W=6 THEN GOSUB 2550
1910 IF NOT V THEN 1980
1920 IF I(I)>I(I-1) THEN W=W+1 E
     LSE W=0
1930 IF W=1 THEN E(R)=I-1
1940 IF W=6 THEN GOTO 2770
1950 IF I(I)<FNB(I)+T9 THEN W2=W
     2+1 ELSE W2=0
```

```
1960 IF W2=1 THEN E(R)=I
1970 IF W2=6 THEN GOTO 2900
1980 IF I=Q1 THEN 3010
1990 PLOT I+I1,E
2000 GOTO 2040
2010 X2=X2+1
2020 PLOT X2,E
2030 IF X2=Q THEN 1400
2040 IF A(101)=100 THEN A(101)=1
2050 A(101)=A(101)+1
2060 IF A(102)=100 THEN A(102)=1
2070 A(102)=A(102)+1
2080 IF NOT T2 THEN 2100
2090 RETURN
2100 ENABLE INTR 4;32 @ RETURN
2110 ENTER 408 USING "#,W" ; T
2120 T=BINAND(T,4095)
2130 IF BIT(T,11) THEN 2160 ! CH
     ECK IF POS
2140 T=-(5*(1-T/2048))
2150 GOTO 2180
2160 T=BINAND(T,2047)
2170 T=5*(T/2048)
2180 A(A(101))=INT(T*1000+.5)/10
     00
2190 RETURN
2200 ON KEY# 1,"START" GOTO 2220
2210 GOTO 2210
2220 B=E
2230 IF NOT T2 THEN 2250
2240 OFF TIMER# 1 @ GOTO 2260
2250 OFF INTR 4
2260 ON KEY# 1,"STOP" GOTO 3010
2270 FOR Z7=1 TO 5
2280 BEEP @ WAIT 1000
2290 NEXT Z7
2300 SETTIME 0,0
2310 GCLEAR
2320 B1=B-.375*V2/S1 @ F1=B1+V2/
     S1*2.874
2330 SCALE 0,Q,B1,F1
2340 XAXIS F1-.95*(F1-B1),300/T5
2350 PENUP
2360 MOVE 4*Q/256,F1-.995*(F1-B1
     )
2370 LDIR 0 @ LABEL "STOP"
2380 PENUP
2390 F=1
2400 GOTO 1500
2410 DEF FNR
2420 IF NOT LEN(R$) THEN K=1 @ G
     OTO 2440
2430 K=POS("YN",UPC$(R$[1,1]))+1
2440 IF K=1 THEN BEEP
2450 FNR=K
```

```
2460 FN END
2470 DEF FNB(O) = A+B2*(O+I1)
2480 MOVE I1+P(R),I(P(R))-2*((F1
     -B1)/192) ! PK START
2490 DRAW I1+P(R),I(P(R))-.05*(F
     1-B1)
2500 PENUP
2510 BEEP 500,20
2520 W,P=0
2530 M=1
2540 RETURN
2550 IF I(M(R))-FNB(M(R))>P9 THE
     N 2650
2560 IF V8 THEN 2620
2570 PEN -1
2580 MOVE I1+P(R),I(P(R))-2*((F1
     -B1)/192)
2590 DRAW I1+P(R),I(P(R))-.05*(F
     1-B1)
2600 PEN 1
2610 PENUP
2620 V,V9=1 ! V9 FLAG REJECT
2630 W,M,V8=0
2640 RETURN
2650 MOVE I1+M(R)+Q/256*4,F1-.2*
     (F1-B1)
2660 T$=VAL$(INT(R(R)/60)) @ T1$
     =VAL$(FP(R(R)/60)*60+.5)
2670 IF T1$[2,2]="." OR T1$[1,1]
     ="." THEN 2680 ELSE 2700
2680 IF T1$[1,1]="." THEN T1$="0
     0" ELSE T1$="0"&T1$[1,1]
2690 GOTO 2710
2700 T1$=T1$[1,2] ,
2710 LDIR 45 @ LABEL T$&":"&T1$
2720 PENUP
2730 BEEP 200,20
2740 W,M,V8=0
2750 V=1
2760 RETURN
2770 MOVE I1+E(R),I(E(R)) ! PEAK
      VALLEY
2780 DRAW I1+E(R),I(E(R))-.05*(F
     1-B1)
2790 PENUP
2800 BEEP 50,20
2810 IF NOT V9 THEN 2850
2820 P(R)=E(R)
2830 V9=0
2840 GOTO 2870
2850 P(R+1)=E(R) @ V8=1 ! FLG NO
     T TO ERASE TIC IF NEXT PK I
     S NOISE
2860 R=R+1
2870 W2,W,V=0
```

```
2880 M=1
2890 GOTO 1980
2900 IF NOT V9 THEN 2920 ! PK EN
     D
2910 GOTO 2960
2920 MOVE I1+E(R),I(E(R))
2930 DRAW I1+E(R),I(E(R))-.05*(F
     1-B1)
2940 PENUP
2950 BEEP 50,20
2960 W2,W,V=0
2970 P=1
2980 IF NOT V9 THEN R=R+1
2990 V9=0
3000 GOTO 1980
3010 IF NOT T2 THEN 3030 ! FROM
     STOP
3020 OFF TIMER# 1 @ GOTO 3040
3030 OFF INTR 4
3040 BEEP 50,200
3050 CLEAR @ DISP "COMPUTING DAT
     A--PLEASE STAND BY"
3060 IF R#1 THEN 3090
3070 PRINT @ PRINT @ PRINT N$ @
     PRINT @ PRINT "NO PEAKS DET
     ECTED"
3080 GOTO 3490
3090 IF P THEN 3130
3100 IF V AND NOT V9 THEN E(R)=I
      ELSE 3240
3110 R=R+1
3120 IF D2 THEN 3240
3130 FOR Z7=E(R-1) TO I
3140 S2=S2+Z7+I1
3150 I2=I2+1
3160 S3=S3+I(Z7)
3170 S4=S4+(Z7+I1)^2
3180 S5=S5+I(Z7)*(Z7+I1)
3190 NEXT Z7
3200 IF D3 THEN A=S3/(I1+I2) ELS
     E 3220
3210 GOTO 3240
3220 B2=(S5-S2*S3/(I2+I1))/(S4-S
     2*S2/(I2+I1))
3230 A=S3/(I2+I1)-B2*S2/(I2+I1)
3240 FOR Z7=1 TO R-1
3250 A1(Z7)=0 @ NEXT Z7
3260 FOR Z7=1 TO R-1
3270 FOR Z8=P(Z7) TO E(Z7)
3280 A1(Z7)=A1(Z7)+I(Z8)-FNB(Z8)
3290 NEXT Z8
3300 NEXT Z7
3310 MOVE 4*Q/256,F1-.995*(F1-B1
     )
3320 PEN -1 @ LDIR 0
```

```
3330 LABEL "STOP" @ PEN 1
3340 PRINT @ GRAPH @ COPY
3350 PRINT @ PRINT @ PRINT
3360 PRINT N$ @ PRINT
3370 PRINT "Pk# RT(m:s)  Ip(μA)
      Area(μCoul)"
3380 IMAGE 2D,X,7A,2X,3DZ.2D,X,6
     DZ.2D
3390 PRINT
3400 FOR Z7=1 TO R-1
3410 T$=VAL$(INT(R(Z7)/60)) @ T1
     $=VAL$(FP(R(Z7)/60)*60+.005
     )
3420 IF T1$[2,2]="." OR T1$[1,1]
     ="." THEN 3430 ELSE 3450
3430 IF T1$[1,1]="." THEN T1$="0
     0"&T1$[1,3] ELSE T1$="0"&T1
     $[1,4]
3440 GOTO 3460
3450 T1$=T1$[1,5]
3460 T$=T$&":"&T1$
3470 PRINT USING 3380 ; Z7,T$,(I
     (M(Z7))-FNB(M(Z7)))*S1,A1(Z
     7)*T5*S1
3480 NEXT Z7
3490 ALPHA @ CLEAR @ KEY LABEL
3500 ON KEY# 1,"REPLOT" GOTO 392
     0
3510 ON KEY# 2,"B.LINE" GOSUB 37
     20
3520 ON KEY# 3,"REPORT" GOTO 375
     0
3530 ON KEY# 4,"STORE" GOTO 3590
3540 ON KEY# 5,"NEW" GOTO 200
3550 ON KEY# 6,"EXIT" GOTO 3910
3560 ON KEY# 7,"RE-EVAL" GOTO 45
     60
3570 CLEAR @ KEY LABEL
3580 GOTO 3580
3590 DISP "NAME OF FILE";
3600 INPUT F$
3610 DISP "CREATE FILE:Y/N"
3620 INPUT R$
3630 ON FNR GOTO 3610,3640,3650
3640 CREATE F$,150
3650 ASSIGN# 1 TO F$
3660 CRT OFF
3670 PRINT# 1 ; N$,R,A,B2,S1,T5,
     Q,Q1,P(),M(),R(),E(),A1(),I
     ()
3680 ASSIGN# 1 TO *
3690 CRT ON
3700 BEEP 50,200
3710 GOTO 3570
3720 MOVE 1,FNB(1-I1)
```

```
3730 DRAW I+I1,FNB(J)
3740 RETURN
3750 DISP "DISP. PARAMETERS:Y/N"
     ;
3760 INPUT R$
3770 ON FNR GOTO 3750,3780,3890
3780 CLEAR
3790 DISP N$ @ DISP
3800 DISP "# OF POINTS IN RUNNIN
     G AVE..";N
3810 DISP "SENSITIVITY(μA/IN)...
     ....";V2
3820 DISP "BASELINE THRESHOLD(μA
     ).....";T9*S1
3830 DISP "Ip REJECT(μA)........
     ......";P9*S1
3840 DISP "RUN TIME (MIN).......
     ......";T1
3850 DISP "DELAY TIME (MIN).....
     ......";INT(D1/60*1000)/100
     0
3860 DISP USING "26A,D.3D" ; "CH
     ART SPEED (IN/MIN)......",C
     9
3870 DISP "DATA INTERVAL(SEC)...
     ";T5
3880 DISP @ DISP "PRINT RESULTS:
     Y/N";
3890 INPUT R$
3900 ON FNR GOTO 3880,3350,3570
3910 END
3920 DISP "Y-AXIS SELECT OPTION"
3930 DISP "1...SELECT NEW SENSIT
     IVITY."
3940 DISP "2....SCALE TO LARGEST
      PEAK"
3950 DISP "3....AS IS"
3960 DISP @ DISP "INPUT #";
3970 INPUT R8
3980 IF R8#1 AND R8#2 AND R8#3 T
     HEN 3920
3990 ON R8 GOTO 4060,4000,4070
4000 F1=0
4010 FOR Z7=1 TO R-1
4020 IF F1<I(M(Z7)) THEN F1=I(M(
     Z7))
4030 NEXT Z7
4040 V2=(F1-B1)*S1/2.874
4050 GOTO 4070
4060 DISP "SENSITIVITY(μA/IN)";@
      INPUT V2
4070 CLEAR @ DISP "SELECT OPTION
     "
4080 DISP @ DISP "1....RETENTION
      TIMES PRINTED"
```

```
4090 DISP "2....NO RETENTION TIM
     ES PRINTED"
4100 DISP "3....REFLECT OFFSCALE
      PEAKS"
4110 DISP @ DISP "INPUT #";
4120 INPUT R7
4130 IF R7#1 AND R7#2 AND R7#3 T
     HEN 4070
4140 CLEAR
4150 DISP "PRESENT CHART SPEED I
     S " @ DISP C9;" IN/MIN" @ D
     ISP
4160 DISP "INPUT CHART SPEED";@
     INPUT C9
4170 DISP "DRAW BASELINE:Y/N";@
     INPUT R$
4180 ON FNR GOTO 4170,4190,4200
4190 SFLAG 1 @ GOTO 4210
4200 CFLAG 1
4210 C8,C6=60*3.75/(T5*C9)
4220 B1=B-.375*V2/S1 @ F1=B1+V2/
     S1*2.874 @ GCLEAR @ C7=1
4230 SCALE 0,C6,B1,F1
4240 XAXIS F1-.95*(F1-B1),300/T5
4250 PENUP @ IF C8>I THEN C8=I
4260 FOR Z7=C7 TO C8
4270 IF I(Z7)>F1 AND R7=3 THEN 4
     280 ELSE 4300
4280 PLOT Z7,2*F1-I(Z7)
4290 GOTO 4310
4300 PLOT Z7,I(Z7)
4310 NEXT Z7
4320 FOR Z8=1 TO R-1
4330 MOVE P(Z8),I(P(Z8))-2*((F1-
     B1)/192)
4340 DRAW P(Z8),I(P(Z8))-.05*(F1
     -B1)
4350 MOVE E(Z8),I(E(Z8))-2*((F1-
     B1)/192)
4360 DRAW E(Z8),I(E(Z8))-.05*(F1
     -B1)
4370 IF R7#1 THEN 4450
4380 MOVE M(Z8)+(C8-C7)/256*4,F1
     -.2*(F1-B1)
4390 T$=VAL$(INT(R(Z8)/60)) @ T1
     $=VAL$(FP(R(Z8)/60)*60+.5)
4400 IF T1$[2,2]="." OR T1$[1,1]
     ="." THEN 4410 ELSE 4430
4410 IF T1$[1,1]="." THEN T1$="0
     " ELSE T1$="0"&T1$[1,1]
4420 GOTO 4440
4430 T1$=T1$[1,2]
4440 LDIR 45 @ LABEL T$&":"&T1$
4450 NEXT Z8
4460 IF FLAG(1) THEN GOSUB 3720
```

```
4470 IF C8<I THEN 4480 ELSE 4520
4480 C7=C8 @ C8=C8+C6 @ COPY
4490 GCLEAR @ SCALE C7,C8,B1,F1
4500 SFLAG 2
4510 GOTO 4240
4520 IF FLAG(2) THEN COPY
4530 CFLAG 2
4540 BEEP 50,500
4550 GOTO 3570
4560 CHAIN "RE-EVAL"
```

```
 10 ! RE-EVAL ROUTINE
 20 ! COPYRIGHT 1982
 25 ! BY SCOTT HUGHES
 30 CONTROL 4,6 ; 1 ! STROBE TIM
    E
 40 CONTROL 4,4 ; 160 ! STROBE B
     TO R
 50 CONTROL 4,3 ; 3 ! INVERT CTL
    A AND CTL0
 60 OPTION BASE 1
 70 COM SHORT A,A1(20),B2,D1,F1,
    I(4200),P9,R(20),T1,T5,T9,S1
     ,INTEGER E(20),I,I1,I2,M(20
    ),N,P(20),R
 80 COM N$[96],F$[6]
 90 GOTO 630
100 DISP "FILE NAME";
110 INPUT F$
120 ASSIGN# 1 TO F$
130 CRT OFF
140 READ# 1 ; N$,R,A,B2,S1,T5,Q,
    Q1,P(),M(),R(),E(),A1(),I()
150 ASSIGN# 1 TO *
160 CLEAR @ CRT ON
170 DISP "PLEASE STAND BY"
180 C9=.125 @ V2=2.5
190 ON ERROR GOTO 290
200 DEFAULT OFF
210 FOR Z8=E(R-1) TO 4200
220 Z9=I(Z8)
230 IF Z9>5 THEN 340
240 NEXT Z8
250 OFF ERROR
260 DEFAULT ON
270 I=4200
280 GOTO 370
290 IF ERRL=280 AND ERRN=7 THEN
    340
300 DISP "ERROR ";ERRN;" @ LINE
    ";ERRL @ BEEP
310 DEFAULT ON
320 OFF ERROR
330 PAUSE
340 I=Z8-1
350 DEFAULT ON
360 OFF ERROR
370 I1=Q-Q1
380 D1=T5*I1
390 T1=(I+I1)*T5/60
400 D1=D1/1000
410 B=INF
420 FOR Z8=1 TO I
430 B=MIN(B,I(Z8))
440 NEXT Z8
450 B=.99*B
```

```
460 B1=B-.375*V2/S1
470 BEEP 50,200
480 GOTO 720
490 PRINT @ PRINT @ PRINT
500 PRINT N$ @ PRINT
510 PRINT "Pk# RT(m:s)  Ip(μA)
    Area(μCoul)"
520 IMAGE 2D,X,7A,2X,3DZ.2D,X,6D
    Z.2D
530 PRINT
540 FOR Z7=1 TO R-1
550 T$=VAL$(INT(R(Z7)/60)) @ T1$
    =VAL$(FP(R(Z7)/60)*60+.005)
560 IF T1$[2,2]="." OR T1$[1,1]=
    "." THEN 570 ELSE 590
570 IF T1$[1,1]="." THEN T1$="00
    "&T1$[1,3] ELSE T1$="0"&T1$[
    1,4]
580 GOTO 600
590 T1$=T1$[1,5]
600 T$=T$&":"&T1$
610 PRINT USING 520 ; Z7,T$,(I(M
    (Z7))-FNB(M(Z7)))*S1,A1(Z7)*
    T5*S1
620 NEXT Z7
630 ALPHA @ CLEAR @ KEY LABEL
640 ON KEY# 1,"REPLOT" GOTO 910
650 ON KEY# 2,"B.LINE" GOSUB 740
660 ON KEY# 3,"REPORT" GOTO 770
670 ON KEY# 4,"ENTER" GOTO 100
680 ON KEY# 5,"OUTPUT" GOTO 1560
690 ON KEY# 6,"EXIT" GOTO 900
700 ON KEY# 7,"RETURN" GOTO 1550
710 ON KEY# 8,"CAT" GOTO 1960
720 CLEAR @ KEY LABEL
730 GOTO 730
740 MOVE 1,FNB(1-I1)
750 DRAW I+I1,FNB(I)
760 RETURN
770 DISP "DISP. PARAMETERS:Y/N";
780 INPUT R$
790 ON FNR GOTO 770,800,880
800 CLEAR
810 DISP N$ @ DISP
820 DISP "SENSITIVITY..........
    ";V2
830 DISP "RUN TIME (MIN)........
    .....";T1
840 DISP "DELAY TIME (MIN)......
    .....";INT(D1/60*1000)
850 DISP USING "26A,D.3D" ; "CHA
    RT SPEED (IN/MIN)......",CS
860 DISP "DATA INTERVAL(SEC)..."
    ;T5
870 DISP @ DISP "PRINT RESULTS:Y
    /N";
```

```
880 INPUT R$
890 ON FNR GOTO 870,490,720
900 END
910 DISP "Y-AXIS SELECT OPTION"
920 DISP "1...SELECT NEW SENSITI
    VITY."
930 DISP "2....SCALE TO LARGEST
    PEAK"
940 DISP "3....AS IS"
950 DISP @ DISP "INPUT #";
960 INPUT R8
970 IF R8#1 AND R8#2 AND R8#3 TH
    EN 910
980 ON R8 GOTO 1050,990,1060
990 F1=0
1000 FOR Z7=1 TO R-1
1010 IF F1<I(M(Z7)) THEN F1=I(M(
     Z7))
1020 NEXT Z7
1030 V2=(F1-B1)*S1/2.874
1040 GOTO 1060
1050 DISP "SENSITIVITY(μA/IN)";@
      INPUT V2
1060 CLEAR @ DISP "SELECT OPTION
     "
1070 DISP @ DISP "1....RETENTION
      TIMES PRINTED"
1080 DISP "2....NO RETENTION TIM
     ES PRINTED"
1090 DISP "3....REFLECT OFFSCALE
      PEAKS"
1100 DISP @ DISP "INPUT #";
1110 INPUT R7
1120 IF R7#1 AND R7#2 AND R7#3 T
     HEN 1060
1130 CLEAR
1140 DISP "PRESENT CHART SPEED I
     S " @ DISP C9;" IN/MIN" @ D
     ISP
1150 DISP "INPUT CHART SPEED";@
     INPUT C9
1160 DISP "DRAW BASELINE:Y/N";@
     INPUT R$
1170 ON FNR GOTO 1160,1180,1190
1180 SFLAG 1 @ GOTO 1200
1190 CFLAG 1
1200 C8,C6=60*3.75/(T5*C9)
1210 B1=B-.375*V2/S1 @ F1=B1+V2/
     S1*2.874 @ GCLEAR @ C7=1
1220 SCALE 0,C8,B1,F1
1230 XAXIS F1-.95*(F1-B1),300/T5
1240 PENUP @ IF C8>I THEN C8=I
1250 FOR Z7=C7 TO C8
1260 IF I(Z7)>F1 AND R7=3 THEN 1
     270 ELSE 1290
```

```
1270 PLOT Z7,2*F1-I(Z7)
1280 GOTO 1300
1290 PLOT Z7,I(Z7)
1300 NEXT Z7
1310 FOR Z8=1 TO R-1
1320 MOVE P(Z8),I(P(Z8))-2*((F1-
     B1)/192)
1330 DRAW P(Z8),I(P(Z8))-.05*(F1
     -B1)
1340 MOVE E(Z8),I(E(Z8))-2*((F1-
     B1)/192)
1350 DRAW E(Z8),I(E(Z8))-.05*(F1
     -B1)
1360 IF R7#1 THEN 1440
1370 MOVE M(Z8)+(C8-C7)/256*4,F1
     -.2*(F1-B1)
1380 T$=VAL$(INT(R(Z8)/60)) @ T1
     $=VAL$(FP(R(Z8)/60)*60+.5)
1390 IF T1$[2,2]="." OR T1$[1,1]
     ="." THEN 1400 ELSE 1420
1400 IF T1$[1,1]="." THEN T1$="0
     " ELSE T1$="0"&T1$[1,1]
1410 GOTO 1430
1420 T1$=T1$[1,2]
1430 LDIR 45 @ LABEL T$&":"&T1$
1440 NEXT Z8
1450 IF FLAG(1) THEN GOSUB 740
1460 IF C8<I THEN 1470 ELSE 1510
1470 C7=C8 @ C8=C8+C6 @ COPY
1480 GCLEAR @ SCALE C7,C8,B1,F1
1490 SFLAG 2
1500 GOTO 1230
1510 IF FLAG(2) THEN COPY
1520 CFLAG 2
1530 BEEP 50,500
1540 GOTO 720
1550 CHAIN "CHROM2"
1560 DISP "STRIP CHART RECORDER
     SENSITIVITY(V/IN)";
1570 INPUT S9
1580 DISP "INPUT REQUIRED DATA S
     ENSITIVITY (µA/IN)";
1590 INPUT V2
1600 S8=S1*S9/V2
1610 M1=-INF
1620 FOR Z8=1 TO R
1630 M1=MAX(M1,I(M(Z8)))
1640 NEXT Z8
1650 IF M1*S8<5 THEN 1700
1660 DISP "OUT OF DAC RANGE"
1670 DISP "STRIP CHART SENSITIVI
     TY NEEDS TOBE ";5*V2/(M1*S1
     );" V/IN"
1680 DISP "FOR CURRENT SENSITIVI
     TY OF      ";V2;" µA/IN"
```

```
1690 GOTO 1560
1700 DISP "PRESS CONT WHEN READY
     "
1710 PAUSE
1720 FOR Z8=1 TO I
1730 E=I(Z8)*S8
1740 IF E<0 THEN 1780
1750 E1=INT(E*2048/5+.5)
1760 E1=BINIOR(E1,2048)
1770 GOTO 1790
1780 E1=INT(2048*(E/5+1)+.5)
1790 L=BINAND(E1,15)
1800 B$=DTB$(E1)
1810 M=BTD(B$[9,12])
1820 M=BINIOR(M,64)
1830 H=BTD(B$[5,8])
1840 H=BINIOR(H,128)
1850 OUTPUT 404 USING "#,B" ; L,
     M,H,192
1860 NEXT Z8
1870 BEEP 50,200
1880 GOTO 720
1890 DEF FNR
1900 IF NOT LEN(R$) THEN K=1 @ G
     OTO 1920
1910 K=POS("YN",UPC$(R$[1,1]))+1
1920 IF K=1 THEN BEEP
1930 FNR=K
1940 FN END
1950 DEF FNB(O) = A+B2*(O+I1)
1960 CAT
1970 GOTO 730
```